

# Air-Sea Interaction in Biophysical Modeling

With focus on Northeast Arctic Cod

---

Kjersti Opstad Strand

Thesis for the Degree of Philosophiae Doctor (PhD)  
University of Bergen, Norway  
2019

UNIVERSITY OF BERGEN



# **Air-Sea Interaction in Biophysical Modeling**

With focus on Northeast Arctic Cod

Kjersti Opstad Strand



Thesis for the Degree of Philosophiae Doctor (PhD)  
at the University of Bergen

Date of defence: 15.02 2019

© Copyright Kjersti Opstad Strand

The material in this publication is covered by the provisions of the Copyright Act.

Year: 2019

Title: Air-Sea Interaction  
in Biophysical Modeling

Name: Kjersti Opstad Strand

Print: Skipnes Kommunikasjon / University of Bergen

## Scientific environment

This PhD study has been conducted at the Institute of Marine Research (IMR) in the research group Oceanography and Climate, in collaboration with the Division of Oceanography and Marine Meteorology at the Norwegian Meteorological Institute (MET), both situated in Bergen, Norway. The formal educational institution has been the Geophysical Institute, University of Bergen. The work has been funded by the Norwegian Research Council through grant number 244262 (RETROSPECT). The RETROSPECT project is a collaboration between IMR, the Division of Ocean and Ice at MET and the Nansen Environmental and Remote Sensing Center (NERSC). In addition, I have been associated with the Research school on changing climates in the coupled earth system (CHESS) and the Bjerknes Centre for Climate Research. I spent ten weeks of 2017 at the Department of Oceanography, University of Hawai'i at Mañoa visiting Associate professor Anna B. Neuheimer.



Norwegian  
Meteorological  
Institute



# Acknowledgements

First and foremost, I would like to thank my great team of supervisors (Øyvind, Frode and Svein) for guiding me through the tough PhD path. You have taught me so much, from how to write articles to how to manage a tight researcher-schedule. Your knowledge, enthusiasm and expertise is truly appreciated. Frode, Øyvind and Svein thank you for always finding time to respond to my questions, and for me being able to ask all kinds of questions and related concerns. Frode, your ability to focus and structure the research effort is encouraging. Øyvind, thank you for keeping me on-track in an efficient way. Svein, thank you for all your knowledge you have shared with me.

I would also thank IMR and all my wonderful colleagues at the Oceanography and Climate department, my colleagues at the communication department and my football-colleagues making my days more enjoyable. A special thank you to Ingrid for being my everyday mentor, and Marcos, Håvard and Sebastian for being a super Bergen-PhD team. Thank you NFR for funding (RETROSPECT, grant number 244262). Thank you GFI (UIB) for providing the framework around this education. Anna, thank you for hosting me at the University of Hawai'i and for broaden my scientific view to other areas of the world. Thank you MET for giving me the possibility to take a PhD-leave, while still collaborate through the RETROSPECT project. Thank you to all institutions that have provided accessible data (LoVe-Observatory (through IMR and Equinor), ECMWF (Jean-Raymond Bidlot), MET and IMR). Thank you Johannes for recommending this PhD project.

My family and friends also deserves a big thank you for always believing in me. I am lucky that there are too many of you to mention all by names. Magnus, thank you for always encouraging me. Patrik and Lisbeth, thank you so much for the help during the last crucial formatting stage of the thesis.

This journey has been wonderful thanks to all of you.



# Abstract

The focus of this thesis is on upper ocean dynamics and the interactions between the atmosphere and the oceans in relation to early life stages of Northeast Arctic cod. The main spawning sites of Northeast Arctic cod are along the Norwegian coast with positively buoyant eggs being transported towards the nursery grounds of the Barents Sea by the prevailing ocean currents. The physical processes investigated are the role of the wind-driven transport, cross-shelf exchange, vertical current shear, stratification and mixing processes affecting dispersal of the early life stages of cod.

The first main finding is a modeled potential connectivity route of Northeast Arctic cod due to wind-driven transport and cross-shelf exchange towards the Northeast Greenland shelf. This modeled transport route is supported by observations of cod at the Northeast Greenland shelf as well as a surface drifter trajectory. Northeasterly winds over several days during spring cause higher occurrences of cross-shelf transport of cod, while southwesterly winds are maintaining the prevailing path towards the Barents Sea. The spawning ground close to the Norwegian continental shelf edge has the highest probability for cross-shelf transport. The second main finding is the role of vertical current shear causing deviations in vertical cod egg concentrations from the diffusion-buoyancy equation within a limited spawning ground. Since cod eggs are positively buoyant, the concentrations are expected to increase towards the surface. By investigating the occasionally observed sub-surface maxima in NEA cod egg concentrations the importance of variable current forcing in the vertical and spatially limited spawning grounds are identified as necessary conditions. The third main finding is the importance of correct representation of ocean stratification. A shallow surface layer will be more dynamically responsive to wind forcing, and effort should be made to ensure correct representation of stratification in physical-biological modeling. Here, this is addressed by comparing ocean model forcing with and without data assimilation. The latter demonstrated improved stratification as compared to in situ observation. The final main finding is related to resolving upper ocean mixing by breaking waves. A relationship between observed bubble depth and modeled turbulent kinetic energy flux is found similar to the relationship between the flux and wind. The bubble depth is also found to be highly correlated with wind speed and wave height. Wind sea height shows the highest correlation against air-bubble depth, and the summertime mixed layer depth is not limiting the breaking waves. All findings are relevant for understanding processes affecting dispersal of early life stages of Northeast Arctic cod, as well as for plankton and other buoyant particles (such as plastic and oil droplets) in general.



# List of papers

1. **Strand, K. O., Sundby, S., Albretsen, J. and Vikebø, F. B. (2017):** *The Northeast Greenland Shelf as a Potential Habitat for the Northeast Arctic Cod*, *Frontiers in Marine Science* **4**, 304.
2. **Strand, K. O., Vikebø, F. B., Sundby, S., Sperrevik, A.K. and Breivik, Ø.:** *Sub-surface maxima in buoyant fish eggs indicate vertical velocity shear and spatially limited spawning grounds*, accepted for publication in *Limnology and Oceanography*.
3. **Strand, K. O., Breivik, Ø., Pedersen G., Vikebø F. B. and Sundby, S.:** *Long-term Statistics of Bubble Depth and the Energy Flux from Breaking Waves*, submitted for publication in *Geophysical Research Letters*.

*Paper 1 is published with the Creative Commons (CC-BY) licence. Reprint of paper 2 was made with permission from the publisher of the Association for the Sciences of Limnology and Oceanography (in partnership with John Wiley and Sons).*



# Contents

<b>Scientific environment</b>	<b>i</b>
<b>Acknowledgements</b>	<b>iii</b>
<b>Abstract</b>	<b>v</b>
<b>List of papers</b>	<b>vii</b>
<b>1 Introduction</b>	<b>1</b>
1.1 Objectives . . . . .	2
<b>2 Scientific background</b>	<b>3</b>
2.1 Study area - The northeastern North Atlantic . . . . .	3
2.2 Methodological approaches . . . . .	8
2.2.1 The biophysical particle tracking model . . . . .	8
2.2.2 Ocean, wind and wave hindcast archives . . . . .	9
2.2.3 Observations . . . . .	10
<b>3 Summary of papers</b>	<b>13</b>
<b>4 Discussion</b>	<b>15</b>
4.1 Physical perspective . . . . .	15
4.2 Biological perspective . . . . .	16
4.3 Societal perspective . . . . .	18
<b>5 Scientific results</b>	<b>29</b>
5.1 The Northeast Greenland Shelf as a Potential Habitat for the Northeast Arctic Cod . . . . .	31
5.2 Sub-surface maxima in buoyant fish eggs indicate vertical velocity shear and spatially limited spawning grounds . . . . .	49
5.3 Long-term Statistics of Bubble Depth and the Energy Flux from Breaking Waves . . . . .	79



# Chapter 1

## Introduction

The coastal ocean, and in particular the upper mixed layer, is the basis for marine life and the most productive and dynamic part of the world oceans. It provides opportunities for harvesting and services for humans to an increasing degree, but new knowledge is needed to secure sustainability. Quantitative assessment of human pressures often includes ocean models describing coastal circulation with high resolution and dispersal of species and stages vulnerable to human-induced stressors such as climate change, plastics and petroleum spill. Understanding anthropogenic impacts require detailed knowledge of exposure duration, doses and effect thresholds.

Successful growth and dispersal of early life stages of fish require an environment with sufficient and suitable prey and transport to favorable nursery grounds [29]. Northeast Arctic (NEA) cod start its life floating in the upper ocean as a buoyant egg [55] originating from the many spawning grounds along the Norwegian coast [71]. A successful cod egg will drift pelagically in the mixed layer from the surface down to about 50 m with the prevailing currents as part of the Norwegian coastal current (NCC) and the Norwegian Atlantic Slope Current (NwASC) towards the nursery areas of the Barents Sea [85, 86]. Here, the pelagic juveniles settle at deeper layers close to the bottom and attain a more stationary distribution, thus being defined as a demersal (near-bottom) fish species [90]. But first, it must survive the pelagic drift phase lasting around 6-8 months [45].

During the drift phase the individual cod trajectories are affected by the upper ocean dynamics, largely by the air-sea interaction which vary greatly from daily variations in passing weather systems, shaped by seasonal to interannual and decadal scale variability [85]. It has been known since the early work by Johan Hjort [29] that the year-class strength of the NEA cod stock will be affected by the variability during its early life stages. The recruitment hypotheses of Hjort's seminal work have been subjected to testing for 100 years. The major issue is the sampling frequency needed to resolve the small-scale and short-time processes relevant for testing the hypotheses (e.g. ecosystem patchiness, ecological processes and mixing-layer dynamics).

Today's ocean models coupled to individual-based biophysical models have enabled quantification of the key issues raised by Hjort [29]. Together with observations, both in laboratory and field studies, this represents a powerful tool to test hypotheses. Understanding the air-sea interaction and the upper ocean dynamics affecting the advection of early life stages is one piece of the puzzle that may eventually allow identification and prediction of key processes and pressures during the early life stages ultimately affect-

ing the spawning stock biomass [45]. Increased knowledge on upper ocean dynamics affecting NEA cod eggs may also help improving our understanding of dispersal of buoyant particles in general, such as oil droplets, small plastic litter and search and rescue operations. This thesis is therefore an interdisciplinary work including physical oceanography, meteorology, ecology and marine biology using advanced numerical tools and statistical analysis providing a framework for addressing upper ocean dispersal in general of great importance to society.

## 1.1 Objectives

The objective of my work has been to study air-sea interactions and the consequences for early life stages of NEA cod through upper ocean dynamics. As the PhD work progressed, the research questions were refined in accordance with findings of relevant spatial and time scales, as well as key processes and parameters:

- Paper 1, horizontal distribution: What is the daily to interannual variability in advection off favorable drift routes along the shelf and into the Norwegian Sea? What are the mechanisms behind this cross-shelf transport? What is the fate of the pelagic juveniles apparently lost at sea? How do these processes contribute to understand interaction between neighboring populations in the ocean?
- Paper 2, vertical distribution: What causes the hourly to daily variability in vertical profiles of Northeast Arctic cod eggs across a spawning ground? How does this relate to different atmospheric forcing? What are the consequences for dispersal?
- Paper 3, wave-breaking and distribution of buoyant particles: What can we learn about the parameterization of turbulent energy flux from breaking waves by measuring air bubbles with bottom-mounted echo-sounders? How may this be included in biophysical models used to study dispersal of plankton?

A biophysical particle-tracking model coupled with a high-resolution ocean model along with extensive in-situ measurements describing plankton distribution is used to answer the research questions of Paper 1 and 2. In Paper 1 the interannual dispersal trajectories are compared to observations of pelagic juveniles to study processes regulating the chance of successfully reaching the Barents Sea. In Paper 2, a similar biophysical model setup as Paper 1 is used but now including data assimilation to improve in particular the upper ocean stratification in the model. The model performance is compared against observational data from a scientific cruise at a key spawning ground during the egg stage. The main purpose was to study the counter-intuitive occurrences of sub-surface maxima in buoyant fish eggs by improving the representation of upper ocean structures for plankton dispersal. Paper 3 used air-bubble depth observations from a bottom-mounted echo sounder to evaluate a parameterization of turbulent kinetic energy from breaking waves. This was related to observed wind and modeled wind and waves. The area investigated is in the main advection route of most NEA cod eggs and larvae, and thus revealing important physical processes not usually included in biophysical models used in studies on plankton dispersals.

# Chapter 2

## Scientific background

### 2.1 Study area - The northeastern North Atlantic

The area addressed in the thesis is the northeastern North Atlantic (south of the Arctic Ocean) including the Norwegian Sea, the Barents Sea and partly the Greenland Sea (Figure 1). The area is enclosed by shallow shelves, including the northeastern Greenland shelf, the Barents Sea shelf and the Norwegian continental shelf. Here the particular focus is on the shelf areas around Lofoten.

**The ocean circulation** in the focus area can roughly be divided into the northward flowing Atlantic water, the northward flowing coastal water (along the Norwegian coast) and the southward flowing Arctic water (along the Greenland shelf edge), see Figure 2.1. The northward flowing warm and saline Atlantic water enters the Nordic Seas across the Faroe-Shetland Channel where it splits into two branches, one flowing along the shelf break of the Norwegian continental shelf, (the Norwegian Atlantic Slope Current, NwASC), and the second part farther off the shelf in the Norwegian Sea [24, 43]. As the NwASC flows farther north, the current again splits, where one branch flows into the Barents Sea [43], and the other continues to the west of Svalbard either recirculating in the Fram Strait [26] or flowing eastward north of Svalbard [5]. Cold and fresh Arctic water, named the East Greenland Current, flows southward through the Fram Strait following the shelf edge of the northeastern Greenland continental shelf [19, 89]. The warm northward flowing Atlantic waters interact with the cold southward flowing Arctic waters at the northern limb of the Atlantic Meridional Overturning Circulation [14]. Along the Norwegian coast, the fresher Norwegian Coastal Current (NCC) transport fresher water from the Baltic Sea as well as river runoff from the Norwegian mainland northward [39, 53, 57]. All three current systems are forced by atmospheric and thermohaline drivers together with the Earth's rotation and topographic steering. These currents also exhibit a general weaker cross-shelf component dominating the exchange of nutrients and marine organisms between the continental shelf and the deep ocean basin [10, 52, 61], as discussed in Paper 1.

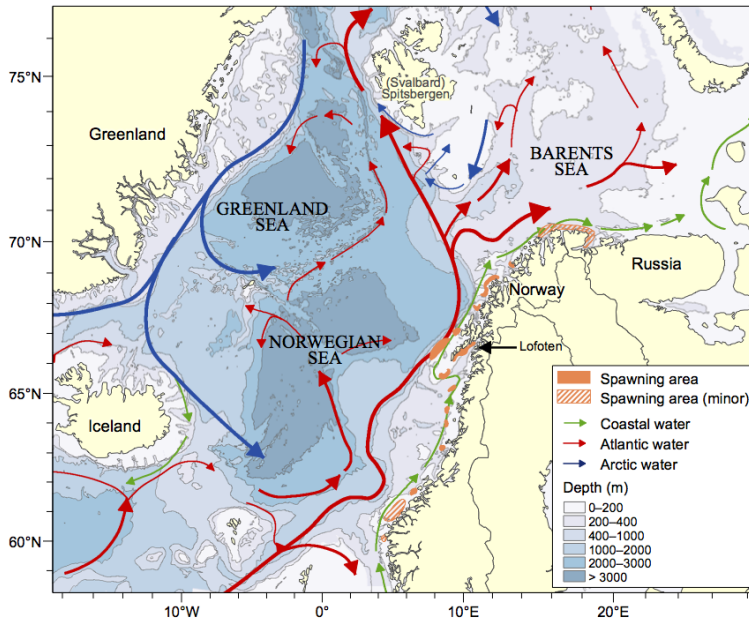


Figure 2.1: Overview of the study area with dominating ocean current systems. The bathymetry contours are given in blue shading. The main spawning areas of Northeast Arctic cod are marked with orange areas, where striped orange indicate minor spawning areas. The labeled Lofoten area is the main spawning area. By courtesy of Karen Gjertsen, Institute of Marine Research.

**The climate and weather** in the northeastern North Atlantic are controlled by the heat transported by the ocean currents into the area [50] and the formation and movement of low pressure systems often steered by the jet stream, an upper atmospheric region with high wind speeds due to the temperature gradient between the Arctic and the Tropics [51]. The area is thus highly dynamic with high fluxes between the atmosphere and ocean. The weather is dominated by low pressure systems forming when colder air meets warmer waters in areas with potential vorticity present in the atmosphere, moving eastward with a cyclonic circulation around its center [6, 13]. Daily variability in weather will affect the upper ocean currents and consequently the distribution of particles (Paper 1 and 2). There is also monthly to interannual variability such as the North Atlantic Oscillation (NAO), which is simply defined as the pressure difference between Iceland and the Azores [31]. The NAO is positive when there is located a low pressure system over Iceland and a high pressure system over the Azores. This is considered as the more frequent state. A strong positive NAO leads to a narrow and deep NwASC [7]. The NAO becomes negative if there is higher pressure over Iceland than over the Azores with shifts in the weather (wind, precipitation and temperature) patterns and consequently upper ocean properties. A "longer time" variability is the Atlantic mul-

tidecadal Oscillation (AMO), on decadal-to-multidecadal time scales, defined as a sea surface temperature anomaly in the North Atlantic [33, 84]. The north-south extension of the spawning areas of NEA cod along the Norwegian coast are affected by this AMO variability [71] where spawning occurs further north in warm years relatively to colder years along the Norwegian coast.

*Climate is what on average we may expect, weather is what we actually get*  
– Andrew John Herbertson [27]

**Air-sea interactions** affect the fluxes of heat, gases and momentum between the ocean and atmosphere (Figure 2.2). Heat exchange and freshwater fluxes will alter the air and sea water properties, and thus the buoyancy. Heating of surface waters are important for storing excess heat from the atmosphere. Cooling of surface waters release heat to the atmosphere leading to denser water forming and potential for downward convection ventilating the deep ocean [38]. Wind stress forces the upper ocean currents directly through Ekman transport and shear-induced vertical mixing [10]. Wind also generates waves, and the breaking of waves cause direct injection of air from the atmosphere to the ocean [79], discussed in Paper 3.

All the aforementioned processes are important for the formation of the ocean mixed layer, defined as a region with homogenous vertical density properties; a region important for marine life [76]. To understand the transport routes of planktonic organisms in the mixed layer it is necessary to know the vertical distribution [85, 86]. Progress were made in the 1980s to mathematically describe this by the buoyancy-diffusion balance [64]. Here it is interesting to note the similarities in mathematical approaches on vertical distribution of fish eggs [64] and of air bubbles [78], the focus of Paper 2 and 3, respectively. Recently, there has been focus on distinguishing between the mixed layer depth and the mixing layer depth, the region of active mixing [73].

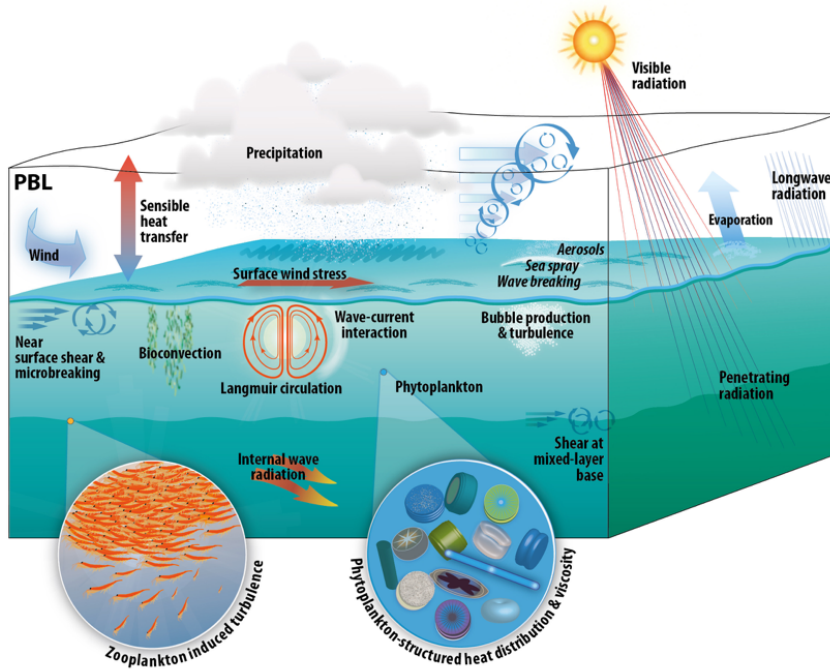


Figure 2.2: Illustration of typical upper ocean processes related to air-sea interactions (Institute of Marine Research).

**The ecosystem** in the North Atlantic consists of relatively few species with high abundance (Figure 2.3). Here, the main spawning grounds of the world's largest cod stock, the Northeast Arctic (NEA) cod, is located along the Norwegian coast [45]. The NEA cod has been important to Norway for a millennium and a large research effort has gone into investigating the species. Mature NEA cod (older than around 7 years) undertake a yearly migration distance up to 1500 km from the Barents Sea to the Norwegian coast to spawn [45]. I focus on the physical environment affecting the NEA cod (text in bold). The maturation and growth depend on food availability and **temperature** conditions [44]. The eggs are released in the **thermocline** (between coastal and Atlantic water masses) in a temperature range of 4 – 6 °C, usually at depths between 50 – 200 m [15]. The depth of this thermocline varies according to the **freshwater runoff** and **wind-driven (Ekman) transport and upwelling** of the Atlantic layer below [23]. The spawning grounds stretch from Møre in the south to Finnmark in the north, and varies latitudinally due to **longer-term temperature changes** [71]. The main spawning ground is located in Lofoten. The ecosystem of the Norwegian coast is defined as a spring-bloom system, where spawning occurs during springtime, for NEA cod mainly from March through April, with peak spawning April 1<sup>st</sup> [17]. The onset of the spring-bloom (and thus phytoplankton bloom) is regulated by the **mixed layer depth**, **light availability** and nutrient availability [76]. The timing of the spawning coincides

with the increased food availability during the bloom and the inflow of zooplankton ascending from overwintering in the deep Norwegian Sea [66]. The eggs are **advected by the prevailing currents** along the Norwegian coast, affected by the interaction between the atmosphere and ocean [85]. The NEA cod eggs are homohaline, meaning that they keep constant internal **salinity** by osmoregulation [70, 72]. The buoyancy of the eggs thus depends on the ambient seawater salinity, and not temperature. During the drift phase the eggs hatch after around 2 – 3 weeks and the cod larvae start a diurnal vertical migration following the daily light availability in a trade-off between eating zooplankton and avoid being eaten by visual predators [16, 35]. At around 3 months the larvae go through metamorphosis and gets its fish appearance [45]. As the cod grows, the fish will start seeking towards the bottom layers for larger prey [90]. At this point, most of the NEA cod has died, either by starvation, predation, malformation, diseases or through advection to unsuitable areas [67]. But the successful survivors have reached the Barents Sea. Even though most die, the total amount of eggs released in the upper water columns is so enormous (of the order of  $10^{13}$  eggs in the Lofoten area [68]) that the small fraction of survivors may still produce a large year class. At age 3 years the cod is considered to be recruited to the fishery.

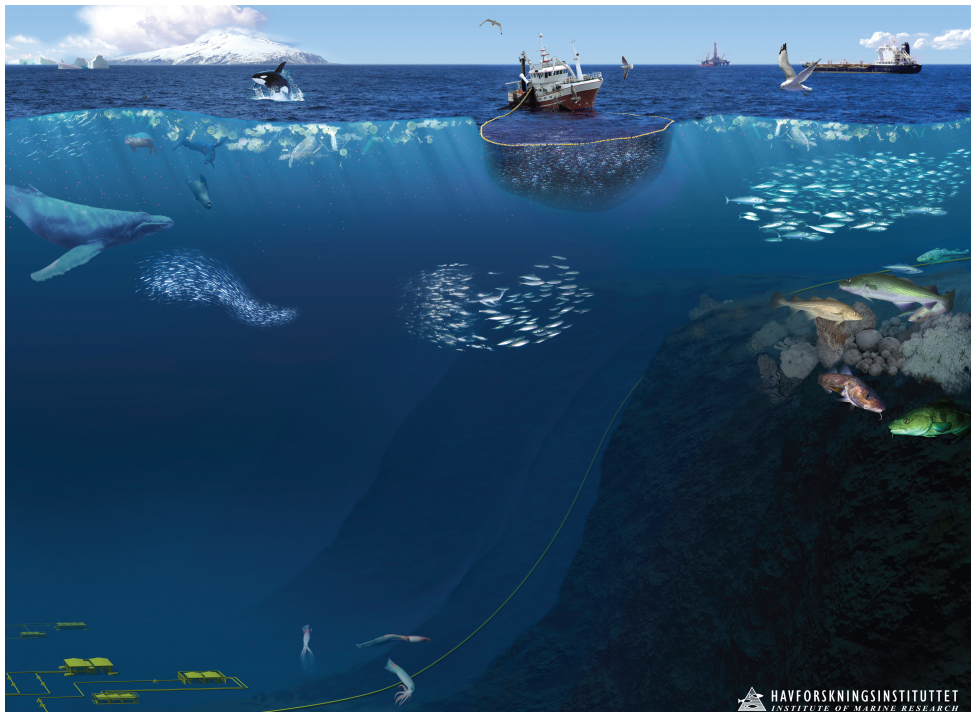


Figure 2.3: Illustration of the ecosystem on the shelf areas of the Norwegian Sea (Institute of Marine Research).

## 2.2 Methodological approaches

To investigate the different research questions related to the objective of air-sea interactions and early life stages of NEA cod I have used a wide range of different methodological approaches. This is necessary because of the general undersampling of the ocean. Papers 1 and 2 include a biophysical particle tracking model (2.2.1) forced by different three-dimensional dynamical ocean model hindcast archives (2.2.2). Different observations are used to evaluate the model performance including observed early life stages of NEA cod and oceanographic and meteorological observations (2.2.3). A parameterization of upper ocean turbulent mixing from breaking waves from a wave hindcast (2.2.2) is evaluated in Paper 3 against echo sounder observations of down-mixed air bubbles (2.2.3), a process not usually parameterized in the biophysical particle tracking model to date. A brief summary of the different models and data sets is presented below.

### 2.2.1 The biophysical particle tracking model

The biophysical model is an individual-based lagrangian particle tracking model named the ‘‘Lagrangian Diffusion Model’’ (LADIM) [1]. The vertical distribution of NEA cod eggs,  $C(z)$ , is determined by a known concentration  $C_a$  at depth  $a$ , the individual egg densities (buoyancy) through their vertical rising speed,  $w$ . This equation is determined by the vertical diffusion-buoyancy balance equation by Sundby [64] modified by modeled ocean density and turbulence (through the vertical eddy diffusion coefficient,  $K$ ) at the individual time-varying location of each egg:

$$C(z) = C_a e^{-w(a-z)/K} \quad (2.1)$$

The vertical dynamical positioning of eggs is calculated in the model based on the numerical scheme by Thygesen and Ådlandsvik [80]. The particles are moved horizontally with a 4<sup>th</sup> order Runge-Kutta advection scheme and a sub-module handling the eggs’ response to environmental forcing. When the particles are advected near land, they are only moved by the direction of the offshore velocity component to avoid artificial stranding. The particle-tracking model utilize three-dimensional ocean currents and vertical turbulent mixing from different ocean hindcast archives (2.2.2). The model parameters are tri-linearly interpolated to the location of each egg. In Paper 1, to compensate for unresolved mesoscale processes, a horizontal eddy turbulent diffusion coefficient of  $K = 1 \text{ m}^2\text{s}^{-1}$  is included. The sub-module handling eggs includes a temperature-dependent growth according to equation by Folkvord [20, 21]. Once the eggs hatch, the vertical migration by larvae and pelagic juvenile is controlled by a diurnal migration which depends on light conditions and swimming capabilities according to equation by Opdal et al. [42]. The larvae will move between 5 – 30 m during night and 10 – 40 m during day in a trade-off between eating and avoid being eaten.

Release locations follow from observations of the well-known spawning grounds, in addition to observations from post-larvae surveys (2.2.3). The eggs are released continuously at regular grids (in Paper 1; 200 eggs per day from 1978-2015, and in Paper 2; 25 eggs four times per day at 66 grid cells defined as one spawning ground in 1984)

during the spawning season (March through April, in total of 61 days). In Paper 1 a second setup was performed with 500 eggs released at year-specific observation locations from the post larvae surveys from 1978-1991. The model is run for 200 days (first part, Paper 1), run for 120 days (second part Paper 1) or run for 80 days (Paper 2). Particle positions are stored every 24 (Paper 1) or every 3 hours (Paper 2).

### 2.2.2 Ocean, wind and wave hindcast archives

The different dynamical ocean model hindcast archives are a configuration of the Regional Ocean Modeling System (ROMS) with different resolutions and domains. ROMS is a free-surface, primitive equation ocean model with terrain-following sigma-coordinates [56]. The equations are solved using hydrostatic and boussinesq assumptions on an Arakawa C-grid. For all three configurations vertical eddy diffusivity terms from the local turbulent closure scheme with  $k - \omega$  setup were used [81, 82]. One configuration also included four-dimensional variational data assimilation improving in particular the stratification and consequently the oceanic response to wind forcing (Paper 2). In addition to the ocean model hindcasts, wave hindcast archives (EC-WAM and NORA10) are evaluated to investigate turbulent kinetic energy flux from breaking waves (Paper 3). The wind from NORA10 is also used directly in Paper 1 and 2.

#### SVIM (4 km)

This ROMS (ocean) hindcast archive has six-hourly three-dimensional currents fields and a 4 by 4 km horizontal resolution covering the Nordic Seas and the Barents Sea [37]. The model has 32 vertical sigma layers and are available for the period 1958-2015 forced on the lateral boundaries by the Simple Ocean Data Assimilation data set [11] as well as the regional European Centre for Medium-range Weather Forecasts (ECMWF) reanalysis including previous prognostic runs downscaled to a grid of 10 by 10 km (NORA10, see below) on the ocean surface. This ocean model hindcast reproduces many oceanographic features, but due to the resolution of 4 by 4 km this model does not resolve processes related to the first baroclinic Rossby radius [62] such as mesoscale eddies [32] and a hindcast archive of higher resolution is examined, see NorKyst-800.

#### NorKyst-800 (800 m)

To investigate mesoscale eddies, a downscaled version of SVIM to 800 by 800 m and 35 sigma layers covering the Norwegian coast from the northern North Sea to the Barents Sea extending off the shelf edge [2] covering 2005-2015 is used. This resolution is considered as eddy-resolving for the area, including the most parts of the Norwegian continental shelf.

#### SVIM-4DVAR (2.4 km)

SVIM-4DVAR is SVIM downscaled to a resolution of 2.4 by 2.4 km covering Vestfjorden out to the shelf edge with 35 sigma layers. This resolution is considered as eddy-permitting for the area [62]. The model hindcast is set up for 1984 with the use

of four-dimensional variational (4D-Var) data assimilation improving the stratification in the Vestfjorden [62].

### NORA10

NORA10 is a three-hourly atmosphere and wave hindcast archive including model fields of waves, temperature, pressure, humidity, cloud cover and precipitation forced with down-scaled wind from a regional European Centre of Medium Range Weather Forecasting (ECMWF) reanalysis including previous prognostic runs downscaled to a grid of 10 by 10 km [48]. The wind from this hindcast archive was used in Paper 1 and 2 (prepared as six-hourly fields in Paper 1).

In addition, a new setup with hourly model fields forced with down-scaled ERA-Interim wind from ECMWF (NORA10EI) is investigated in Supplementary material of Paper 3. The standard bias is improved from the original NORA10.

### EC-WAM

Hourly wind and wave fields from the EC-WAM hindcast archive from ECMWF forced with ERA-Interim wind [9] is used in Paper 3. The model resolution is 0.36 degrees (approximately 40 by 40 km) and includes the turbulent kinetic energy flux from breaking waves,  $\Phi_{oc}$ , evaluated by echo sounder observations (2.2.3):

$$\Phi_{oc} = -\rho_w g \int_0^{2\pi} \int_0^{\infty} S_{ds} d\omega d\theta \propto u_*^3 \quad (2.2)$$

Here  $\rho_w$  is the density of water,  $g$  is the gravitational acceleration,  $S_{ds}$  is the dissipation source term of the energy balance equation integrated over all frequencies ( $\omega$ ) and directions ( $\theta$ ) and  $u_*$  is the water-side friction velocity.

## 2.2.3 Observations

Observations span from positional information of early life stages of NEA cod, meteorological and oceanographic data to echo sounder data of down-mixed air bubbles from breaking waves.

### Historical observations of Northeast Arctic cod

Scientific cruises mapping spawning grounds are performed every year during March and April by the Institute of Marine Research. In the first part of Paper 1 data from 1978-2015 are used as release points in the biophysical model (see references to cruises 1978-2004 in Appendix of Paper 1 and data from IMR's fish database for cruises 2005-2015). The focus has been on the 10 main spawning grounds from Møre to Finnmark. During the investigated period there has been an observed northward shift in spawning grounds [71] with only occasional occurrence of a spawning ground outside of Vestfjorden. The particle concentration at each spawning ground was weighted according to these observations, in addition to a Gaussian spawning intensity with peak April 1<sup>st</sup> [68].

Positional information from post-larvae surveys from 1978-1991 during June and July by the Institute of Marine Research mapping the condition of young pelagic juveniles drifting on its way towards the Barents Sea [74] is used as release points in the biophysical tracking model (second part of Paper 1). In Paper 2 detailed positional information from one spawning ground in 1984 (see Sundby and Bratland [68]) is used to investigate the particle transport by SVIM-4DVAR set up for 1984 (see Supplementary material of Paper 2).

### **Scientific cruise 2016**

In Paper 2, observations from a scientific cruise with R/V Johan Hjort in Vestfjorden are used. The cruise was conducted April 4-7<sup>th</sup> 2016. Observations include vertical pump profiles of NEA cod eggs, net hauls of egg concentrations, CTD profiles, wind observations from MET's Skrova weather station (WMO st. no. 01160) together with ship wind and two moored ADCP instruments measuring ocean currents.

### **Meteorological and oceanographic data**

In Paper 1, a drifter trajectory from the Global Drifter Program (id = 78758) was compared to the transport patterns of NEA cod juveniles towards the northeastern Greenland shelf investigating connectivity routes.

In Paper 3, wind from MET's weather stations Andøya (WMO st. no. 01010) and Røst (WMO st. no. 01107) and hydrographic data from IMR's Eggum station were used to compare with acoustic observations in the same area, see below.

### **LoVe-Observatory**

Acoustic echo sounder data from a bottom-installed cabled stationary underwater observatory were used in Paper 3 to investigate depth of down-mixed air bubbles. These observations were used to evaluate the parameterization of turbulent kinetic energy flux from breaking waves described above. The echo sounder is an upward looking scientific narrow band split-beam echo sounder with one frequency (70 kHz) and beamwidth of 7°. The instrument is standing at a depth of 258 m giving a detection diameter of approximately 31 m at the surface. The backscatter intensity was sampled at 0.25 Hz with vertical sample interval of 0.191 m.



# Chapter 3

## Summary of papers

**Paper 1:** *The Northeast Greenland Shelf as a Potential Habitat for the Northeast Arctic Cod*

Paper 1 is a connectivity study of NEA cod with focus on wind-driven transport and cross-shelf exchange. We based our research question on observed distributions of pelagic juveniles off the continental shelf, in the Lofoten Basin (in the Norwegian Sea). Suthers and Sundby [74] found that these individuals were in better conditions than those at the same age onto the continental shelf. We challenged Johan Hjort's [29] assumptions that the ones off the shelf will (most probably) die. We first examined mechanisms causing off-shelf transport of young NEA cod, then we examined potential transport routes back onto a shelf using the biophysical model (2.2.1) with two different hindcast archives (2.2.2) together with observations (2.2.3). Our results show that the total off-shelf transport is highly variable caused by episodic events with varying frequency and dates for each year. The spawning ground close to the shelf edge has the highest probability for cross-shelf transport. The cross-shelf events are positively correlated with northeasterly wind 3-7 days before the event, while negatively correlated with southwesterly wind being consistent with wind-driven Ekman transport. There are three routes for offspring off the shelf edge; back onto the Norwegian shelf and into the Barents Sea, recirculating within the Lofoten Basin or drifting northwest towards the northeast Greenland shelf. The latter route is consistent with recent observations of NEA cod indicating potential for survival.

**Paper 2:** *Sub-surface maxima in buoyant fish eggs indicate vertical velocity shear and spatially limited spawning grounds*

Paper 2 investigates the occasionally observed deviation from the diffusion-buoyancy equation (Eq. 2.1) of vertical NEA cod egg concentrations. Cod eggs are buoyant and concentrations are expected to increase towards the surface. However, from time to time a sub-surface maximum in NEA cod egg concentrations is observed. We used the biophysical model (2.2.1) with hindcast archive including data assimilation (2.2.2) and compared model results against observations from a scientific cruise with observed vertical profiles of NEA cod eggs and concurrent environmental conditions (2.2.3). Our results show that vertical ocean current shear and spatially limited spawning grounds

are the two most important factors creating observed transient sub-surface maxima in NEA cod egg concentrations. By this we demonstrate the importance of resolving small-scale dynamics in the upper ocean as well as representing spawning grounds with realistic patchiness in biophysical models. We also demonstrate the importance of improved stratification by data assimilation for buoyant particle drift.

**Paper 3:** *Long-term Statistics of Bubble Depth and the Energy Flux from Breaking Waves*

Paper 3 is concerned with resolving processes related to upper ocean mixing due to breaking waves relevant for dispersal of plankton. The flux (Eq. 2.2) of turbulent kinetic energy (TKE) from breaking waves was compared against observations of down-mixed air bubbles (2.2.3) over a year (November 2014 to November 2015). The area investigated is in the hotspot of the drift route of NEA cod. First we evaluated the down-mixed air bubbles against wind and waves and found that these are highly correlated, in accordance with previous studies. We investigated both hourly mean and maximum values of air-bubble depth. Wind sea shows the highest correlation against air-bubble depth, both for mean and maximum depth values. The summertime mixed layer depth is not limiting the breaking waves. We proceeded by evaluating the variability in the TKE flux from breaking waves. Rank correlation coefficients showed a higher correlation than linear correlation coefficients between bubble depth and TKE flux. A relationship between bubble depth and TKE flux is found similar to the relationship between TKE flux and wind. At last we considered a parameterization of TKE flux from breaking waves based on wind speed. There was no distinct difference between the modeled and parameterized TKE flux and we conclude that both are representing the upper ocean mixing due to breaking waves adequately at least in open-ocean conditions with waves being close to full development. Especially the parameterization based on wind speed can easily be incorporated in biophysical models if a wave model is not available.

# Chapter 4

## Discussion

### 4.1 Physical perspective

This thesis has used model output together with a wide range of observations to study physical processes affecting early life stages of NEA cod. The inclusion of models compensates for the generally under-sampled oceans while observations represent the ground truth and initialization of the models.

In Paper 1 the spatial transport routes of young NEA cod larvae were linked to variability in cross-shelf exchange caused by variability in wind forcing. A second important process for cross-shelf exchange is mesoscale eddies [10]. As a consequence, efforts were made in Paper 1 on discussing ROMS's ability to resolve eddies along the continental shelf break. Since ROMS is a hydrostatic model with a terrain-following sigma-coordinate system this results in an erroneous strong pressure gradient force along steep topography. This is limiting off-shelf flow. Isachsen et al. [32] showed that mesoscale eddies across the continental shelf slope is underestimated in the ROMS model with horizontal resolution of 4 km in the Lofoten area due to strong topographic steering. To (partly) compensate for this, we added a constant horizontal diffusive term to increase the horizontal particle spreading, in addition to investigating a model with 800 by 800 m resolution. For future improvements it would be wise to include a horizontally varying eddy diffusivity from observations, e.g. Kozalka et al. [34]. The first baroclinic Rossby radius (the length scale where rotational motions become important) is around 2.4 for the Lofoten area. In order to permit eddies in ocean models set up for the area, the resolution should therefore be at least 2.4 by 2.4 km. To be sure the mesoscale eddies are fully resolved, the grid size should be 1200 by 1200 m or smaller (small enough so that the length of two grid cells is smaller than the Rossby radius). Interestingly, In Paper 1 when we investigated a ROMS's model setup with resolution of 800 by 800 m, this reduced the off-shelf transport, contrary to what was expected. This is most likely caused by the strong horizontal gradients along the shelf break from SVIM (4 km) affecting the higher-resolution model (800 m) at the boundaries. In contrast to our findings, Hatterman et al. [26] showed that a ROMS setup of 800 by 800 m was capable of resolving eddy shedding across the Fram Strait (between Svalbard and Greenland). This strengthens our suspicion that the model boundaries in our domain are too close to the shelf break and are not able to fully resolve the processes occurring in this highly dynamic area.

A ROMS model setup with improved stratification should increase the accuracy of the upper ocean drift. This latter is illustrated in Paper 2 making the upper layer more responsive to wind forcing. The stratification was improved by adding four-dimensional variational data assimilation into the model. During the investigations of variability on shorter time scales (hours to days), another physical model question arises: How well is the parameterization of turbulent mixing in ROMS for short time scale variability used in particle tracking models? In this thesis the Generic length Scale with  $k - \omega$  setup is used in both Paper 1 and Paper 2. From our sensitivity model run in Paper 2 running both with and without turbulent dynamical vertical positioning of eggs, the effect of vertical mixing on small time scales is revealed. Care should be taken interpreting the results if there are small amounts of particles in the model sample.

Measurements of upper ocean processes for validating parameterizations of vertical mixing and buoyant particle dynamics are usually sparse. Especially capturing variability in both time and space (horizontal and vertical) is challenging. In Paper 3 this is solved by evaluating a parameterization of turbulent kinetic energy flux from breaking waves against echo sounder observations of down-mixed air bubbles. Upward-looking echo sounder data provide a valuable opportunity to measure the upper ocean continuously over long periods. In the context of upper ocean biophysical particle tracking wave-breaking is a process that requires additional improvements. This may be incorporated into biophysical models either by including wave parameterizations from wind or by including coupled wind-ocean-wave models as forcing. Such knowledge may help improving our understanding of dispersal of buoyant particles in general, not only fish eggs and air bubbles.

### Recommendations for future work

- Improve ocean models with respect to representation of mesoscale eddies and cross-shelf exchange.
- Improve modeled stratification by assimilating CTD data into ocean models.
- Compare with a model that do not have sigma-coordinates
- Test horizontally varying eddy diffusivity
- Include turbulent mixing due to breaking waves in biophysical particle tracking models

## 4.2 Biological perspective

Enough prey is crucial for survival of NEA cod. Prey availability was discussed in Paper 1. In short, across the Fram Strait en route towards the Northeast Greenland shelf, there are high numbers of zooplankton during summer [59] and early autumn [75] in addition to the larger krill species [30] identified as main food sources for growing cod juveniles [65, 77]. In the Norwegian Sea, it makes sense to assume that the cod transported off-shelf is accompanied by other planktonic species following the same water

masses. This knowledge together with the recent observed and predicted northward shift in species [18, 22] and the newly observed 2-year old NEA cod specimen along the Northeast Greenland shelf [12] support the suggested transport route of NEA cod to the Northeast Greenland shelf described in Paper 1. In the light of the recent northward shift, it is worth to note the first successful fishing in modern times after cod (and halibut) around Jan Mayen was reported this year on November 12<sup>th</sup>, 2018 [41]. However, not all species are predicted to shift northward; only the species able to adapt to winter-darkness by storing lipids may be the winners of the north [69].

Including modeled prey availability evaluated against in-situ observations together with predator pressure would improve the precision of the horizontal distribution of pelagic juveniles, as illustrated in relation to oil spill effects and the resulting patchiness in mortality [36]. Prey and predator distributions may be predicted by ecosystem models of various complexity [25, 28, 58]. Recent work on changes in primary production in the Nordic Seas and Arctic Ocean [3, 8, 49] may give a heads up on what to expect in the future. Studies show a general increase and northward expansion the last decade, but a decline in the Greenland sector [3, 49]. It should be noted though that the sector division of both studies [3, 49] are quite coarse and that the Greenland shelf area is highly variable, with small patches of increased primary production. More detailed investigations in relation to the “Northeast Water” Polynya [46, 60] would be interesting. Børsheim [8] divided his study into smaller sectors and reported an increased primary production close to the East Greenland Current along the shelf break in the same area where Christiansen et al. [12] found healthy cod. The Northeast Greenland shelf may thus be a quite rough nursery ground where only a limited amount of NEA cod would be able to settle, but it will be exciting to see how this might develop in the future.

In addition, horizontal swimming behavior of the NEA cod juveniles lost at sea in the Norwegian Sea should be considered since this may change the transport routes; are there cues that may lead them back to favorable nursery grounds in the Barents Sea and do they have the capability of doing so (e.g. see Staaterman and Paris [63])?

The spawning behavior of NEA cod is well-known and follows the thermocline between the coastal and Atlantic water masses [15]. In Paper 1 and 2 a fixed spawning depth of 50 m was assumed. A variable spawning depth following the thermocline depth may alter the drift of cod eggs due to the effect of vertical current shear (before the eggs have reached the ocean surface layers).

### Recommendations for future work

- Investigate interannual variability in connectivity routes towards Jan Mayen
- Include prey and predators to resolve patchiness in relation to mortality
- Further develop studies of the “Northeast Water” Polynya with respect to food availability
- Investigate how horizontal swimming behavior may change dispersal
- Include temperature-dependent spawning depth in relation to the thermocline

### 4.3 Societal perspective

First, biophysical models have the ability to predict dispersal of both buoyant marine plankton and human stressors. In this way there is a potential to quantify the contact rate between marine plankton and human stressors [87, 88] as well as the potential to predict consequences of temperature increase on marine populations [4]. Such information would assist in predicting when doses are lethal or when ambient temperatures become unfavorable for survival. Understanding the impact of these human stressors requires detailed knowledge of exposure duration, doses and effect thresholds together with the metabolic response of the different marine species. This can effectively be accomplished through targeted observations supplemented by the inclusion of data assimilation to improve the ocean models and thereby drift trajectories and individual exposure rates.

Second, forecasting early life stages of marine organisms is predicted to have a flourishing future by Payne et al. [47]. As I see it, it is the next level of marine weather prediction focusing on fish stock recruitment aiming for end-users such as marine scientists involved in stock assessment and politicians planning for future marine harvest. An analogue example from Norway is the newly established operational salmon lice forecasting system for fish farms along the coast [40, 54]. This system is adopted by the Norwegian government for monitoring and managing risk and sustainability in aquaculture. If the increased need for food production for a growing population is going to come from the oceans, a growth should be environmentally sustainable and careful management is needed (UN's goal number 14 – “Life below water” [83]).

#### Recommendations for future work

- Develop methods to estimate contact rate between plankton and pollution
- Further develop marine forecasting systems similar to weather forecasting.
- Develop risk assessments and integrated ecosystem assessment for selected species, stages and stressors.

# Bibliography

- [1] ADLANDSVIK, B., AND SUNDBY, S. Modelling the transport of cod larvae from the Lofoten area. In *ICES Marine Science Symposia* (1994), vol. 198, Copenhagen, Denmark: International Council for the Exploration of the Sea, 1991-, pp. 379–392. [2.2.1](#)
- [2] ALBRETSEN, J. NorKyst-800 report no. 1: User manual and technical descriptions. *Fisken og havet* (2011). [2.2.2](#)
- [3] ARRIGO, K. R., AND VAN DIJKEN, G. L. Continued increases in Arctic Ocean primary production. *Progress in Oceanography* 136 (2015), 60–70, doi: [10.1016/j.pocean.2015.05.002](https://doi.org/10.1016/j.pocean.2015.05.002). [4.2](#)
- [4] ÅRTHUN, M., BOGSTAD, B., DAEWEL, U., KEENLYSIDE, N. S., SANDØ, A. B., SCHRUM, C., AND OTTERSEN, G. Climate based multi-year predictions of the Barents Sea cod stock. *PloS one* 13, 10 (2018), e0206319, doi: [10.1371/journal.pone.0206319](https://doi.org/10.1371/journal.pone.0206319). [4.3](#)
- [5] BESZCZYNSKA-MÖLLER, A., FAHRBACH, E., SCHAUER, U., AND HANSEN, E. Variability in Atlantic water temperature and transport at the entrance to the Arctic Ocean, 1997–2010. *ICES Journal of Marine Science* 69, 5 (2012), 852–863, doi: [10.1093/icesjms/fss056](https://doi.org/10.1093/icesjms/fss056). [2.1](#)
- [6] BJERKNES, J. On the structure of moving cyclones. *Monthly Weather Review* 47, 2 (1919), 95–99, doi: [10.1175/1520-0493\(1919\)47<95:OTSOMC>2.0.CO;2](https://doi.org/10.1175/1520-0493(1919)47<95:OTSOMC>2.0.CO;2). [2.1](#)
- [7] BLINDHEIM, J., BOROVKOV, V., HANSEN, B., MALMBERG, S.-A., TURRELL, W., AND ØSTERHUS, S. Upper layer cooling and freshening in the Norwegian Sea in relation to atmospheric forcing. *Deep Sea Research Part I: Oceanographic Research Papers* 47, 4 (2000), 655–680, doi: [10.1016/S0967-0637\(99\)00070-9](https://doi.org/10.1016/S0967-0637(99)00070-9). [2.1](#)
- [8] BØRSHEIM, K. Y. Bacterial and primary production in the Greenland Sea. *Journal of Marine Systems* 176 (2017), 54–63, doi: [10.1016/j.jmarsys.2017.08.003](https://doi.org/10.1016/j.jmarsys.2017.08.003). [4.2](#)
- [9] BREIVIK, Ø., MOGENSEN, K., BIDLOT, J.-R., BALMASEDA, M. A., AND JANSSEN, P. A. Surface wave effects in the NEMO ocean model: Forced and coupled experiments. *Journal of Geophysical Research: Oceans* 120, 4 (2015), 2973–2992, doi: [10.1002/2014JC010565](https://doi.org/10.1002/2014JC010565). [2.2.2](#)

- [10] BRINK, K. H. Cross-shelf exchange. *Annual review of marine science* 8 (2016), 59–78, doi: [10.1146/annurev-marine-010814-015717](https://doi.org/10.1146/annurev-marine-010814-015717). 2.1, 2.1, 4.1
- [11] CARTON, J. A., AND GIESE, B. S. A reanalysis of ocean climate using Simple Ocean Data Assimilation (SODA). *Monthly Weather Review* 136, 8 (2008), 2999–3017, doi: [10.1175/2007MWR1978.1](https://doi.org/10.1175/2007MWR1978.1). 2.2.2
- [12] CHRISTIANSEN, J. S., BONSDORFF, E., BYRKJEDAL, I., FEVOLDEN, S.-E., KARAMUSHKO, O. V., LYNHAMMAR, A., MECKLENBURG, C. W., MØLLER, P. D., NIELSEN, J., NORDSTRÖM, M. C., ET AL. Novel biodiversity baselines outpace models of fish distribution in Arctic waters. *The Science of Nature* 103, 1-2 (2016), 8, doi: [10.1007/s00114-016-1332-9](https://doi.org/10.1007/s00114-016-1332-9). 4.2
- [13] DAVIS, C. A., AND EMANUEL, K. A. Potential vorticity diagnostics of cyclogenesis. *Monthly weather review* 119, 8 (1991), 1929–1953, doi: [10.1175/1520-0493\(1991\)119<1929:PVDOC>2.0.CO;2](https://doi.org/10.1175/1520-0493(1991)119<1929:PVDOC>2.0.CO;2). 2.1
- [14] ELDEVIK, T., NILSEN, J. E. Ø., IOVINO, D., OLSSON, K. A., SANDØ, A. B., AND DRANGE, H. Observed sources and variability of Nordic seas overflow. *Nature Geoscience* 2, 6 (2009), 406, doi: [10.1038/NGEO518](https://doi.org/10.1038/NGEO518). 2.1
- [15] ELLERTSEN, B. Influence of wind induced currents on the distribution of cod eggs and zooplankton in Vestfjorden. In *Proc. Norwegian Coastal Current Symp. Geilo, 9-12 September 1980* (1981), University of Bergen. 2.1, 4.2
- [16] ELLERTSEN, B. A case study on the distribution of cod larvae and availability of prey organisms in relation to physical processes in Lofoten. *The propagation of cod Gadus morhua L. Flodevigen rapportser 1* (1984), 453–478. 2.1
- [17] ELLERTSEN, B. Relation between temperature and survival of eggs and first feeding larvae of the North-East Arctic cod (*Gadus morhua*). *Rapp. P.-V. Reun. Cons. Int. Explor. Mer.* 191 (1989), 209–219. 2.1
- [18] ELLINGSEN, I. H., DALPADADO, P., SLAGSTAD, D., AND LOENG, H. Impact of climatic change on the biological production in the Barents Sea. *Climatic change* 87, 1-2 (2008), 155–175, doi: [10.1007/s10584-007-9369-6](https://doi.org/10.1007/s10584-007-9369-6). 4.2
- [19] FOLDVIK, A., AAGAARD, K., AND TØRRESEN, T. On the velocity field of the East Greenland Current. *Deep Sea Research Part A. Oceanographic Research Papers* 35, 8 (1988), 1335–1354, doi: [10.1016/0198-0149\(88\)90086-6](https://doi.org/10.1016/0198-0149(88)90086-6). 2.1
- [20] FOLKVORD, A. Comparison of size-at-age of larval Atlantic cod (*Gadus morhua*) from different populations based on size-and temperature-dependent growth models. *Canadian Journal of Fisheries and Aquatic Sciences* 62, 5 (2005), 1037–1052, doi: [10.1139/f05-008](https://doi.org/10.1139/f05-008). 2.2.1
- [21] FOLKVORD, A. Erratum: Comparison of size-at-age of larval Atlantic cod (*Gadus morhua*) from different populations based on size-and temperature-dependent growth models. *Canadian Journal of Fisheries and Aquatic Sciences* 64, 3 (2007), 583–585, doi: [10.1139/f07-045](https://doi.org/10.1139/f07-045). 2.2.1

- [22] FOSSHEIM, M., PRIMICERIO, R., JOHANNESSEN, E., INGVALDSEN, R. B., ASCHAN, M. M., AND DOLGOV, A. V. Recent warming leads to a rapid borealization of fish communities in the Arctic. *Nature Climate Change* 5, 7 (2015), 673, doi: [10.1038/NCLIMATE2647](https://doi.org/10.1038/NCLIMATE2647). 4.2
- [23] FURNES, G., AND SUNDBY, S. Upwelling and wind induced circulation in Vestfjorden. *The Norwegian Coastal Current. R. Saetre and M. Mork (eds.) 1* (1981), 152–177. 2.1
- [24] HANSEN, B., AND ØSTERHUS, S. Faroe bank channel overflow 1995–2005. *Progress in Oceanography* 75, 4 (2007), 817–856, doi: [10.1016/j.pocean.2007.09.004](https://doi.org/10.1016/j.pocean.2007.09.004). 2.1
- [25] HANSEN, C., SKERN-MAURITZEN, M., VAN DER MEEREN, G., JÄHKEL, A., AND DRINKWATER, K. Set-up of the Nordic and Barents Seas (NoBa) Atlantis Model. *Fisken og Havet* (2016). 4.2
- [26] HATTERMANN, T., ISACHSEN, P. E., VON APPEN, W.-J., ALBRETSSEN, J., AND SUNDFJORD, A. Eddy-driven recirculation of Atlantic Water in Fram Strait. *Geophysical Research Letters* 43, 7 (2016), 3406–3414, doi: [10.1002/2016GL068323](https://doi.org/10.1002/2016GL068323). 2.1, 4.1
- [27] HERBERTSON, A. J. *Outlines of Physiography: An Introduction to the Study of the Earth*. Arnold, 1908. 2.1
- [28] HJØLLO, S. S., HUSE, G., SKOGEN, M. D., AND MELLE, W. Modelling secondary production in the Norwegian Sea with a fully coupled physical/primary production/individual-based Calanus finmarchicus model system. *Marine Biology Research* 8, 5-6 (2012), 508–526, doi: [10.1080/17451000.2011.642805](https://doi.org/10.1080/17451000.2011.642805). 4.2
- [29] HJORT, J. Fluctuations in the great fisheries of northern Europe viewed in the light of biological research. In *Rapports et Procès-Verbeaux* (1914), vol. 20, Réunion Conseil Permanent International Pour l'Exploration de la Mer, pp. 1–228. 1, 3
- [30] HOP, H., FALK-PETERSEN, S., SVENDSEN, H., KWASNIEWSKI, S., PAVLOV, V., PAVLOVA, O., AND SØREIDE, J. E. Physical and biological characteristics of the pelagic system across Fram Strait to Kongsfjorden. *Progress in Oceanography* 71, 2-4 (2006), 182–231, doi: [10.1016/j.pocean.2006.09.007](https://doi.org/10.1016/j.pocean.2006.09.007). 4.2
- [31] HURRELL, J. W., KUSHNIR, Y., OTTERSEN, G., AND VISBECK, M. *An overview of the North Atlantic oscillation*, vol. 134. Wiley Online Library, 2003, pp. 1–35. 2.1
- [32] ISACHSEN, P., KOSZALKA, I., AND LACASCE, J. Observed and modeled surface eddy heat fluxes in the eastern Nordic Seas. *Journal of Geophysical Research: Oceans* 117, C8 (2012), doi: [10.1029/2012JC007935](https://doi.org/10.1029/2012JC007935). 2.2.2, 4.1
- [33] KERR, R. A. A North Atlantic climate pacemaker for the centuries. *Science* 288, 5473 (2000), 1984–1985, doi: [10.1126/science.288.5473.1984](https://doi.org/10.1126/science.288.5473.1984). 2.1

- [34] KOSZALKA, I., LACASCE, J., ANDERSSON, M., ORVIK, K., AND MAURITZEN, C. Surface circulation in the Nordic Seas from clustered drifters. *Deep Sea Research Part I: Oceanographic Research Papers* 58, 4 (2011), 468–485, doi: [10.1016/j.dsr.2011.01.007](https://doi.org/10.1016/j.dsr.2011.01.007). 4.1
- [35] KRISTIANSEN, T., VOLLSET, K., SUNDBY, S., AND VIKEBØ, F. Turbulence enhances feeding of larval cod at low prey densities. *ICES Journal of Marine Science* 71, 9 (2014), 2515–2529, doi: [10.1093/icesjms/fsu051](https://doi.org/10.1093/icesjms/fsu051). 2.1
- [36] LANGANGEN, Ø., OLSEN, E., STIGE, L. C., OHLBERGER, J., YARAGINA, N. A., VIKEBØ, F. B., BOGSTAD, B., STENSETH, N. C., AND HJERMANN, D. Ø. The effects of oil spills on marine fish: Implications of spatial variation in natural mortality. *Marine pollution bulletin* 119, 1 (2017), 102–109, doi: [10.1016/j.marpolbul.2017.03.037](https://doi.org/10.1016/j.marpolbul.2017.03.037). 4.2
- [37] LIEN, V. S., GUSDAL, Y., AND VIKEBØ, F. B. Along-shelf hydrographic anomalies in the Nordic Seas (1960–2011): locally generated or advective signals? *Ocean Dynamics* 64, 7 (2014), 1047–1059, doi: [10.1007/s10236-014-0736-3](https://doi.org/10.1007/s10236-014-0736-3). 2.2.2
- [38] MARSHALL, J., AND SCHOTT, F. Open-ocean convection: Observations, theory, and models. *Reviews of Geophysics* 37, 1 (1999), 1–64, doi: [10.1029/98RG02739](https://doi.org/10.1029/98RG02739). 2.1
- [39] MORK, M. Circulation phenomena and frontal dynamics of the Norwegian Coastal Current. *Phil. Trans. R. Soc. Lond. A* 302, 1472 (1981), 635–647, doi: [10.1098/rsta.1981.0188](https://doi.org/10.1098/rsta.1981.0188). 2.1
- [40] MYKSVOLL, M. S., SANDVIK, A. D., ALBRETSEN, J., ASPLIN, L., JOHNSEN, I. A., KARLSEN, Ø., KRISTENSEN, N. M., MELSOM, A., SKARDHAMAR, J., AND ÅDLANDSVIK, B. Evaluation of a national operational salmon lice monitoring system—From physics to fish. *PloS one* 13, 7 (2018), e0201338, doi: [10.1371/journal.pone.0201338](https://doi.org/10.1371/journal.pone.0201338). 4.3
- [41] NTB. Lønnsomt torskefiske ved jan mayen for første gang i nyere tid [press release]. <https://www.ntbinfo.no/pressemelding/spennende-fiskeri-ved-jan-mayen?publisherId=14516866&releaseId=17856586>, 2018. 4.2
- [42] OPDAL, A. F., VIKEBØ, F. B., AND FIKSEN, Ø. Parental migration, climate and thermal exposure of larvae: spawning in southern regions gives Northeast Arctic cod a warm start. *Marine Ecology Progress Series* 439 (2011), 255–262, doi: [10.3354/meps09335](https://doi.org/10.3354/meps09335). 2.2.1
- [43] ORVIK, K. A., AND NILER, P. Major pathways of Atlantic water in the northern North Atlantic and Nordic Seas toward Arctic. *Geophysical Research Letters* 29, 19 (2002), 2–1, doi: [10.1029/2002GL015002](https://doi.org/10.1029/2002GL015002). 2.1
- [44] OTTERLEI, E., NYHAMMER, G., FOLKVORD, A., AND STEFANSSON, S. O. Temperature- and size-dependent growth of larval and early juvenile Atlantic cod

- (*Gadus morhua*): a comparative study of Norwegian coastal cod and northeast Arctic cod. *Canadian Journal of Fisheries and Aquatic Sciences* 56, 11 (1999), 2099–2111, doi: [10.1139/f99-168](https://doi.org/10.1139/f99-168). 2.1
- [45] OTTERSEN, G., BOGSTAD, B., YARAGINA, N. A., STIGE, L. C., VIKEBØ, F. B., AND DALPADADO, P. A review of early life history dynamics of Barents Sea cod (*Gadus morhua*). *ICES Journal of Marine Science* 71, 8 (2014), 2064–2087, doi: [10.1093/icesjms/fsu037](https://doi.org/10.1093/icesjms/fsu037). 1, 2.1
- [46] PARKINSON, C. L., COMISO, J. C., ZWALLY, H. J., CAVALIERI, D. J., GLOERSEN, P., AND CAMPBELL, W. J. Arctic sea ice, 1973-1976: Satellite passive-microwave observations. Tech. rep., NASA, Washington, DC, 1987. 4.2
- [47] PAYNE, M. R., HOBDA, A. J., MACKENZIE, B. R., TOMMASI, D., DEMPSEY, D. P., FÄSSLER, S. M., HAYNIE, A. C., JI, R., LIU, G., LYNCH, P. D., ET AL. Lessons from the first generation of marine ecological forecast products. *Frontiers in Marine Science* 4 (2017), 289, doi: [10.3389/fmars.2017.00289](https://doi.org/10.3389/fmars.2017.00289). 4.3
- [48] REISTAD, M., BREIVIK, Ø., HAAKENSTAD, H., AARNES, O. J., FUREVIK, B. R., AND BIDLOT, J.-R. A high-resolution hindcast of wind and waves for the North Sea, the Norwegian Sea, and the Barents Sea. *Journal of Geophysical Research: Oceans* 116, C5 (2011), doi: [10.1029/2010JC006402](https://doi.org/10.1029/2010JC006402). 2.2.2
- [49] RENAUT, S., DEVRED, E., AND BABIN, M. Northward Expansion and Intensification of Phytoplankton Growth During the Early Ice-Free Season in Arctic. *Geophysical Research Letters* (2018), doi: [10.1029/2018GL078995](https://doi.org/10.1029/2018GL078995). 4.2
- [50] RHINES, P., HÄKKINEN, S., AND JOSEY, S. A. Is oceanic heat transport significant in the climate system? In *Arctic–subarctic ocean fluxes*. Springer, 2008, pp. 87–109. 2.1
- [51] RIEHL, H., ALAKA, M., JORDAN, C., AND RENARD, R. The jet stream in relation to middle latitude cyclones. In *The Jet Stream*. Springer, 1954, pp. 38–47. 2.1
- [52] ROSSBY, T., OZHIGIN, V., IVSHIN, V., AND BACON, S. An isopycnal view of the Nordic Seas hydrography with focus on properties of the Lofoten Basin. *Deep Sea Research Part I: Oceanographic Research Papers* 56, 11 (2009), 1955–1971, doi: [10.1016/j.dsr.2009.07.005](https://doi.org/10.1016/j.dsr.2009.07.005). 2.1
- [53] SÆTRE, R., AND LJØEN, R. *The Norwegian Coastal Current*. The Technical University of Norway, 1972. 2.1
- [54] SANDVIK, A. D., BJØRN, P. A., ÅDLANDSVIK, B., ASPLIN, L., SKARÐHAMAR, J., JOHNSEN, I. A., MYKSVOLL, M., AND SKOGEN, M. D. Toward a model-based prediction system for salmon lice infestation pressure. *Aquaculture Environment Interactions* 8 (2016), 527–542, doi: [10.3354/aei00193](https://doi.org/10.3354/aei00193). 4.3

- [55] SARS, G. *Indberetning til Departementet for det Indre fra Professor Dr. G. O. Sars om de af ham i Aarene 1864-1878 anstillende undersøgelser angaaende saltvandsfiskeriene*. Christiania, 1879. 1
- [56] SHCHEPETKIN, A. F., AND MCWILLIAMS, J. C. The regional oceanic modeling system (ROMS): a split-explicit, free-surface, topography-following-coordinate oceanic model. *Ocean modelling* 9, 4 (2005), 347–404, doi: [10.1016/j.ocemod.2004.08.002](https://doi.org/10.1016/j.ocemod.2004.08.002). 2.2.2
- [57] SKAGSETH, Ø., DRINKWATER, K. F., AND TERRILE, E. Wind-and buoyancy-induced transport of the Norwegian Coastal Current in the Barents Sea. *Journal of Geophysical Research: Oceans* 116, C8 (2011), doi: [10.1029/2011JC006996](https://doi.org/10.1029/2011JC006996). 2.1
- [58] SKOGEN, M. D., AND SØILAND, H. A user’s guide to NORVECOM V2. 0. the norwegian ecological model system. Tech. rep., Havforskningsinstituttet, Bergen, 1998. 4.2
- [59] SMITH, S. L. Copepods in Fram Strait in summer: distribution, feeding and metabolism. *Journal of Marine Research* 46, 1 (1988), 145–181, doi: [10.1357/002224088785113720](https://doi.org/10.1357/002224088785113720). 4.2
- [60] SMITH JR, W. O. Primary productivity and new production in the Northeast Water (Greenland) Polynya during summer 1992. *Journal of Geophysical Research: Oceans* 100, C3 (1995), 4357–4370, doi: [10.1029/94JC02764](https://doi.org/10.1029/94JC02764). 4.2
- [61] SØILAND, H., CHAFIK, L., AND ROSSBY, T. On the long-term stability of the Lofoten Basin Eddy. *Journal of Geophysical Research: Oceans* 121, 7 (2016), 4438–4449, doi: [10.1002/2016JC011726](https://doi.org/10.1002/2016JC011726). 2.1
- [62] SPERREVIK, A. K., RÖHRS, J., AND CHRISTENSEN, K. H. Impact of data assimilation on Eulerian versus Lagrangian estimates of upper ocean transport. *Journal of Geophysical Research: Oceans* 122, 7 (2017), 5445–5457, doi: [10.1002/2016JC012640](https://doi.org/10.1002/2016JC012640). 2.2.2, 2.2.2
- [63] STAATERMAN, E., AND PARIS, C. B. Modelling larval fish navigation: the way forward. *ICES Journal of Marine Science* 71, 4 (2013), 918–924, doi: [10.1093/icesjms/fst103](https://doi.org/10.1093/icesjms/fst103). 4.2
- [64] SUNDBY, S. A one-dimensional model for the vertical distribution of pelagic fish eggs in the mixed layer. *Deep Sea Research Part A. Oceanographic Research Papers* 30, 6 (1983), 645–661, doi: [10.1016/0198-0149\(83\)90042-0](https://doi.org/10.1016/0198-0149(83)90042-0). 2.1, 2.2.1
- [65] SUNDBY, S. Wind climate and foraging of larval and juvenile Arcto-Norwegian cod (*Gadus morhua*). In *Climate Change and Northern Fish Populations*. Canadian Special Publication of Fisheries and Aquatic Sciences, 1995, pp. 405–415. 4.2
- [66] SUNDBY, S. Recruitment of Atlantic cod stocks in relation to temperature and advection of copepod populations. *Sarsia* 85, 4 (2000), 277–298, doi: [10.1080/00364827.2000.10414580](https://doi.org/10.1080/00364827.2000.10414580). 2.1

- [67] SUNDBY, S., BJØRKE, H., SOLDAL, A., AND OLSEN, S. Mortality rates during the early life stages and year class strength of the Arcto-Norwegian cod (*Gadus morhua* L.). *Rapp. P.-V. Reun. Cons. Int. Explor. Mer* 191 (1989), 351–358. [2.1](#)
- [68] SUNDBY, S., AND BRATLAND, P. Kartlegging av gytefeltene for norsk-arktisk torsk i Nord-Norge og beregning av eggproduksjonen i årene 1983-1985. *Fisken og Havet* (1987). [2.1](#), [2.2.3](#)
- [69] SUNDBY, S., DRINKWATER, K. F., AND KJESBU, O. S. The North Atlantic spring-bloom system—Where the changing climate meets the winter dark. *Frontiers in Marine Science* 3 (2016), 28, [doi: 10.3389/fmars.2016.00028](#). [4.2](#)
- [70] SUNDBY, S., AND KRISTIENSEN, T. The principles of buoyancy in marine fish eggs and their vertical distributions across the world oceans. *PloS one* 10, 10 (2015), e0138821, [doi: 10.1371/journal.pone.0138821](#). [2.1](#)
- [71] SUNDBY, S., AND NAKKEN, O. Spatial shifts in spawning habitats of Arcto-Norwegian cod related to multidecadal climate oscillations and climate change. *ICES Journal of Marine Science* 65, 6 (2008), 953–962, [doi: 10.1093/icesjms/fsn085](#). [1](#), [2.1](#), [2.1](#), [2.2.3](#)
- [72] SUNDNES, G., LEIVESTAD, H., AND IVERSEN, O. Buoyancy determination of eggs from the cod (*Gadus morhua* L.). *ICES Journal of Marine Science* 29, 3 (1965), 249–252, [doi: 10.1093/icesjms/29.3.249](#). [2.1](#)
- [73] SUTHERLAND, G., REVERDIN, G., MARIÉ, L., AND WARD, B. Mixed and mixing layer depths in the ocean surface boundary layer under conditions of diurnal stratification. *Geophysical Research Letters* 41, 23 (2014), 8469–8476, [doi: 10.1002/2014GL061939](#). [2.1](#)
- [74] SUTHERS, I. M., AND SUNDBY, S. Dispersal and growth of pelagic juvenile Arcto—Norwegian cod (*Gadus morhua*), inferred from otolith microstructure and water temperature. *ICES Journal of Marine Science* 50, 3 (1993), 261–270, [doi: 10.1006/jmsc.1993.1028](#). [2.2.3](#), [3](#)
- [75] SVENSEN, C., SEUTHE, L., VASILYEVA, Y., PASTERNAK, A., AND HANSEN, E. Zooplankton distribution across Fram Strait in autumn: Are small copepods and protozooplankton important? *Progress in oceanography* 91, 4 (2011), 534–544, [doi: 10.1016/j.pocean.2011.08.001](#). [4.2](#)
- [76] SVERDRUP, H. On conditions for the vernal blooming of phytoplankton. *ICES Journal of Marine Science* 18, 3 (1953), 287–295, [doi: 10.1093/icesjms/18.3.287](#). [2.1](#), [2.1](#)
- [77] SYSOEVA, T. The relation between the feeding of cod larvae and pelagic fry and the distribution and abundance of their principal food organisms. *International Commission of the Northwest Atlantic Fisheries Special Publication* 6 (1965), 411–416. [4.2](#)

- [78] THORPE, S. On the determination of  $K_v$  in the near-surface ocean from acoustic measurements of bubbles. *Journal of Physical Oceanography* 14, 5 (1984), 855–863, doi: [10.1175/1520-0485\(1984\)014<0855:OTDOIT>2.0.CO;2](https://doi.org/10.1175/1520-0485(1984)014<0855:OTDOIT>2.0.CO;2). 2.1
- [79] THORPE, S. Bubble clouds and the dynamics of the upper ocean. *Quarterly Journal of the Royal Meteorological Society* 118, 503 (1992), 1–22, doi: [10.1002/qj.49711850302](https://doi.org/10.1002/qj.49711850302). 2.1
- [80] THYGESEN, U. H., AND ÅDLANDSVIK, B. Simulating vertical turbulent dispersal with finite volumes and binned random walks. *Marine Ecology Progress Series* 347 (2007), 145–153, doi: [10.3354/meps06975](https://doi.org/10.3354/meps06975). 2.2.1
- [81] UMLAUF, L., AND BURCHARD, H. A generic length-scale equation for geophysical turbulence models. *Journal of Marine Research* 61, 2 (2003), 235–265, doi: [10.1357/002224003322005087](https://doi.org/10.1357/002224003322005087). 2.2.2
- [82] UMLAUF, L., BURCHARD, H., AND HUTTER, K. Extending the  $k$ - $\omega$  turbulence model towards oceanic applications. *Ocean Modelling* 5, 3 (2003), 195–218, doi: [10.1016/S1463-5003\(02\)00039-2](https://doi.org/10.1016/S1463-5003(02)00039-2). 2.2.2
- [83] UN. Transforming Our World: The 2030 Agenda for Sustainable Development. Tech. rep., United Nations, New York, 2015. 4.3
- [84] VAN OLDENBORGH, G., TE RAA, L., DIJKSTRA, H., AND PHILIP, S. Frequency-or amplitude-dependent effects of the Atlantic meridional overturning on the tropical Pacific Ocean. *Ocean Science* 5, 3 (2009), 293–301, doi: [10.5194/os-5-293-2009](https://doi.org/10.5194/os-5-293-2009). 2.1
- [85] VIKEBØ, F., JØRGENSEN, C., KRISTIENSEN, T., AND FIKSEN, Ø. Drift, growth, and survival of larval Northeast Arctic cod with simple rules of behaviour. *Marine Ecology Progress Series* 347 (2007), 207–219, doi: [10.3354/meps06979](https://doi.org/10.3354/meps06979). 1, 2.1, 2.1
- [86] VIKEBØ, F., SUNDBY, S., ÅDLANDSVIK, B., AND FIKSEN, Ø. The combined effect of transport and temperature on distribution and growth of larvae and pelagic juveniles of Arcto-Norwegian cod. *ICES Journal of Marine Science* 62, 7 (2005), 1375–1386, doi: [10.1016/j.icesjms.2005.05.017](https://doi.org/10.1016/j.icesjms.2005.05.017). 1, 2.1
- [87] VIKEBØ, F. B., RØNNINGEN, P., LIEN, V. S., MEIER, S., REED, M., ÅDLANDSVIK, B., AND KRISTIENSEN, T. Spatio-temporal overlap of oil spills and early life stages of fish. *ICES Journal of Marine Science* 71, 4 (2013), 970–981, doi: [10.1093/icesjms/fst131](https://doi.org/10.1093/icesjms/fst131). 4.3
- [88] VIKEBØ, F. B., RØNNINGEN, P., MEIER, S., GRØSVIK, B. E., AND LIEN, V. S. Dispersants have limited effects on exposure rates of oil spills on fish eggs and larvae in shelf seas. *Environmental science & technology* 49, 10 (2015), 6061–6069, doi: [10.1021/acs.est.5b00016](https://doi.org/10.1021/acs.est.5b00016). 4.3
- [89] WOODGATE, R. A., FAHRBACH, E., AND ROHARDT, G. Structure and transports of the East Greenland Current at 75 N from moored current meters.

*Journal of Geophysical Research: Oceans* 104, C8 (1999), 18059–18072, doi: [10.1029/1999JC900146](https://doi.org/10.1029/1999JC900146). 2.1

- [90] YARAGINA, N. A., A. A., AND SOKOLOV, K. M. Cod. In *The Barents Sea-ecosystem, resources, management. Half a century of Russian-Norwegian cooperation*. Tapir Akademisk Forlag, 2011. 1, 2.1



## **Chapter 5**

### **Scientific results**



# Paper 1

## 5.1 The Northeast Greenland Shelf as a Potential Habitat for the Northeast Arctic Cod

Kjersti Opstad Strand, Svein Sundby, Jon Albretsen and Frode Bendiksen Vikebø

*Frontiers in Marine Science*, **4**, 304 (2017)





# The Northeast Greenland Shelf as a Potential Habitat for the Northeast Arctic Cod

Kjersti O. Strand<sup>1,2,3\*</sup>, Svein Sundby<sup>1</sup>, Jon Albretsen<sup>1</sup> and Frode B. Vikebø<sup>1,2</sup>

<sup>1</sup> Department of Oceanography and Climate, Institute of Marine Research, Bergen, Norway, <sup>2</sup> Bjerknes Center for Climate Research, Bergen, Norway, <sup>3</sup> Geophysical Institute, University of Bergen, Bergen, Norway

## OPEN ACCESS

### Edited by:

Brian R. MacKenzie,  
Technical University of Denmark,  
Denmark

### Reviewed by:

Yizhen Li,  
Woods Hole Oceanographic  
Institution, United States  
Clive Fox,  
Scottish Association For Marine  
Science, United Kingdom

### \*Correspondence:

Kjersti O. Strand  
kjersti.opstad.strand@imr.no

### Specialty section:

This article was submitted to  
Global Change and the Future Ocean,  
a section of the journal  
Frontiers in Marine Science

**Received:** 27 January 2017

**Accepted:** 04 September 2017

**Published:** 26 September 2017

### Citation:

Strand KO, Sundby S, Albretsen J  
and Vikebo FB (2017) The Northeast  
Greenland Shelf as a Potential Habitat  
for the Northeast Arctic Cod.  
Front. Mar. Sci. 4:304.  
doi: 10.3389/fmars.2017.00304

Observations (1978–1991) of distributions of pelagic juvenile Northeast Arctic cod (*Gadus morhua* L.) show that up to 1/3 of the year class are dispersed off the continental shelf and into the deep Norwegian Sea while on the way from the spring-spawning areas along the Norwegian coast to the autumn-settlement areas in the Barents Sea. The fate of this variable fraction of pelagic juveniles off-shelf has been an open question ever since Johan Hjort's (1914) seminal work. We have examined both the mechanisms causing offspring off-shelf transport, and their subsequent destiny using an individual-based biophysical model applied to quantify growth and dispersal. Our results show, consistently with the observations, that total off-shelf transport is highly variable between years and may be up to 27.4%. Offspring from spawning grounds around Lofoten have a higher chance of being displaced off the shelf. The off-shelf transport is dominated by episodic events where frequencies and dates vary between years. Northeasterly wind conditions over a 3–7-day period prior to the off-shelf events are a good proxy for dispersal of offspring off the shelf. Offspring transported into the open ocean are on average carried along three following routes: back onto the adjacent eastern shelves and into the Barents Sea (36.9%), recirculating within the Lofoten Basin (60.7%), or drifting northwest to the northeast Greenland shelf (2.4%). For the latter fraction the transport may exceed 12% depending on year. Recent investigations have discovered distributions of young cod on the northeast Greenland shelf indicating that conditions may support survival for Northeast Arctic cod offspring.

**Keywords:** connectivity, pelagic juvenile, cross-shelf, spawning ground, nursery ground, forecast, northeast arctic cod, recruitment

## INTRODUCTION

The Northeast Arctic (NEA) cod, the historically largest stock of Atlantic cod (*Gadus morhua* L.) (Yaragina et al., 2011), has its feeding area in the Barents Sea and undertakes spawning migration southwards along the Norwegian coast during winter, partly far outside its feeding habitat (Bergstad et al., 1987). After spawning in March and April (Ellertsen et al., 1989) from More (62° N) to the Finnmark coast (71° N) (Sundby and Nakken, 2008) the offspring returns to the Barents Sea by pelagic drift in the Norwegian Coastal Current (NCC) on the shelf and in part in the more offshore Norwegian Atlantic Slope Current (NASCC) that runs parallel to the NCC (Vikebø et al., 2005). En route toward the Barents Sea, they drift in the upper mixed layer where shifting winds due to passing weather systems significantly affects strength and direction of the flow, making them vulnerable to the variable meteorological conditions (Vikebø et al., 2007). By October, when the

pelagic juveniles have reached a typical length of more than 8 cm, they gradually migrate out of the pelagic layer (Yaragina et al., 2011) and become associated with depths closer to the bottom, which in the Barents Sea ranges from 150 to more than 350 m depth. From that stage, they are distributed over their natural habitat at the shelf region in the Barents Sea (Figure 1).

Similarly, cod stocks across the North Atlantic have their habitats confined to the continental shelves fringing the North Atlantic proper (Sundby, 2000). The pelagic eggs, larvae and free-drifting early juveniles that happen to become advected by variable currents out over the deep ocean have generally been considered lost for recruitment to the stock (e.g., Werner et al., 1993, 1997). This idea, i.e., that drift of pelagic offspring to unfavorable regions might cause recruitment loss, was already suggested by Hjort (1914), and later defined by Sinclair et al. (1985) as Hjort's second recruitment hypothesis.

Based on the post-larval (hereafter denoted pelagic juvenile) surveys conducted by the Institute of Marine Research (IMR) during the period 1977–1991 (sampled in June/July at an average age of ~70 days) it became evident that a variable portion, and in some years, a quite considerable one, of the new year class of cod was, indeed, found off the shelf in the Norwegian Sea (Bjørke and Sundby, 1987; Sundby et al., 1989). In the year 1988, which had the largest number of observed larvae offshore among these years, 35% of the year class of cod as pelagic juveniles was found in the deep-sea region off the shelf to the west of the NASC (Suthers and Sundby, 1993). Moreover, analysis of length, condition factor, and age (based on counts of daily otolith rings) discovered that this “stray” portion of the 1988 year-class consisted of larger individuals in better condition than the portion of the year class than was “on the right track” toward the Barents Sea. Suthers and Sundby (1993) ascribed this to higher accumulated ambient temperature, and hypothesized that higher zooplankton food abundances in the Norwegian Sea could be a second factor causing the increased growth as the Norwegian Sea proper is the core region for abundance of the main prey species *Calanus finmarchicus* (Sundby, 2000).

Similar to the off-shelf observations from pelagic juvenile surveys, the subsequent 0-group stage, observed during August and September by IMR-surveys, have years when the 0-group is partly found to the west of the shelf edge outside the natural habitat in the Barents Sea, apparently also in high concentrations (see maps of distributions in Eriksen and Prozorkevich, 2011). However, since the 0-group survey only covers a small area outside the western fringe of the Barents Sea it is not possible to quantify how large portion of the year class that exists outside the natural habitat at this stage.

Although such considerable portions of pelagic juvenile cod have repeatedly been observed off the prevailing current paths to the Barents Sea habitat, the destinies of these individuals have never been explored in further detail, most probably because the prevailing view has been dominated by Hjort's second recruitment hypothesis which posits that they might simply be lost for recruitment. However, for the NEA cod there are alternative scenarios. Johan Hjort (1914) himself pointed to one such alternative following his recruitment hypotheses: “During the first cruise of the “Michael Sars” in the Norwegian Sea,

*I encountered great numbers of young cod fry drifting in the water above the great depression in this region. It is possible that many individuals perish during such drift movements; nothing is, however, definitely known as to this. It would be especially desirable to ascertain the extent of such movement, and how far the young fry is able to return, of their own volition, to such localities as offer favorable conditions for their further growth.”* In other words, as a second alternative, if the pelagic juveniles in this western region attain a systematic and sustained swimming behavior toward the east they might return to the water masses that flow into the Barents Sea (e.g., Staaterman and Paris, 2013).

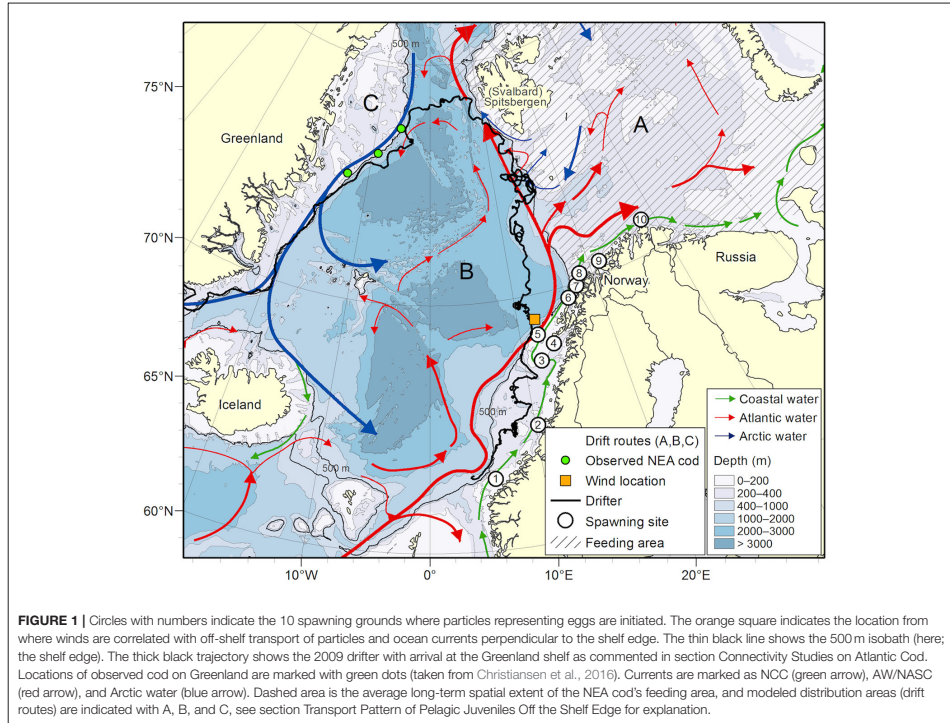
A third alternative is that the pelagic juveniles are successfully transported with the currents either back onto the eastern shelves or onto the large northeastern Greenland shelf where they might settle and grow up as a geographically separated component of NEA cod. Independent of this reasoning, a traditional folklore opinion in some Norwegian coastal fishing communities has been that Greenland cod occasionally spawn in Norwegian waters. This opinion might possibly be based on fishermen visiting Greenland waters observing specific morphometric (phenotypic) characteristics of the cod growing up in Greenland waters that they recognize in Norwegian spawning sites. In a possible support, of considering the northeastern Greenland shelf as being a distant part of NEA cod habitat, are recent findings of adult cod in the area (Christiansen et al., 2016), see Figure 1.

In this current study, we address the impacts of advection and dispersion of the offspring from the spawning area to the areas of subsequent settlement about half a year later. More specifically, we focus on the third alternative and address four main research questions related to the above outline by applying a state-of-the-art biophysical model coupled with *in-situ* data. (1) What fraction of the NEA cod spawned along the Norwegian coast is advected westward off the continental shelf, and how large is the variability in this off-shelf drift within and between years? (2) Which spawning grounds have the highest probability for off-shelf drift of cod offspring? (3) What are the mechanisms and forcing causing the off-shelf transport? (4) Where do the observed off-shelf pelagic juveniles finally end up, and what is the relative number of individuals following the alternative transport routes?

## MATERIALS AND METHODS

Firstly, we modeled transport for the years 1978–2015 with particles initiated as eggs at 10 well-known spawning sites for NEA cod along the Norwegian coast (Figure 1; Sundby and Nakken, 2008) investigating questions 1–3. Particles are being transported by an individual-based particle tracking model (IBM) utilizing daily 3D oceanic currents from an ocean model archive resulting from simulations with the Regional Ocean Modeling System (ROMS) model<sup>1</sup> (Shchepetkin and McWilliams, 2005; Lien et al., 2014, 2016). Since transportation off the shelf and shelf circulation above complex topography might be significantly influenced by small-scale dynamics, this part of the study was done with two different ocean model

<sup>1</sup>www.myroms.org



archives; both the daily mean 3D circulation archive, and an hourly mean 3D archive with an even finer grid resolution.

The weighted (see section Individual-Based Model) model distributions from known spawning grounds were evaluated against observed pelagic juveniles (see section Pelagic Juvenile Observations). For each observation location, the weighted model distribution of pelagic juveniles was summarized across the nearest four by four grid cells, still less than the distance between observations, and compared to the observations. A match is accomplished when both or neither observed and modeled pelagic juveniles are present. However, results must be interpreted with care as the biophysical model do not include natural mortality. Furthermore, the transportation of NEA cod juveniles off the shelf was correlated with NORA10 wind (see section Ocean Model and Atmospheric Forcing). In addition, we correlated the wind forcing against the modeled current component perpendicular to the shelf edge at different depth intervals in order to evaluate the potential for transportation off the shelf.

Secondly, investigating question 4, we initialized particles according to the annual observed distributions of pelagic juvenile

NEA cod off the continental shelf and followed their free pelagic drift toward nursery grounds for years with observations (1978–1991). The aim of this exercise was to investigate alternative drifts routes and new potential nursery habitats.

### Ocean Model

The main ROMS model applications used here is the 4 by 4 km resolved horizontal grid covering the Nordic Seas and the Barents Sea for the period 1958–2015 with 32 vertical sigma layers forced by the Simple Ocean Data Assimilation data set (SODA; Carton and Giese, 2008) on the lateral boundaries and regional downscaled European Centre for Medium-Range Weather Forecasts (ECMWF) re-analysis (ERA-40; Uppala et al., 2005) combined with previous prognostic runs to a grid with 10 by 10 km resolution (hereafter denoted NORA10) at the sea surface (hereafter denoted SVIM, see Lien et al., 2014). In the vertical, the spatio-temporal eddy diffusivity terms from the local turbulence closure scheme were used (a Generic Length Scale mixing scheme with  $k-\omega$  setup) in ROMS (Umhlauf and Burchard, 2003; Umhlauf et al., 2003). See Warner et al. (2005) for a thorough evaluation comparing different mixing schemes.

The ocean model archive, SVIM, has proven to reproduce many observed oceanographic features in the area (Lien et al., 2014, 2016) motivating its use for investigating intra- and inter-annual variations in drift trajectories from observed spawning grounds. In addition, we have used an 800 by 800 m horizontal resolution application with 35 sigma layers covering the entire Norwegian coast from the Skagerrak and the northern North Sea to the Barents Sea extending from the fjords out into the deep basin off the shelf edge (Albretsen et al., 2011, hereafter denoted the NorKyst800). The NorKyst800 hindcast covers the period 2005–2015 and has lateral boundary forcing from SVIM.

### Atmospheric Forcing

Atmospheric forcing for the two ROMS applications were taken from NORA10 (Reistad et al., 2011), providing 6-hourly winds, temperature, pressure, humidity, cloud cover, and accumulated precipitation, while radiative forcing is computed internally in ROMS.

### Individual-Based Model

Egg, larvae and pelagic juvenile drift are reproduced by particles advected by simulated currents in the IBM model “Lagrangian Diffusion Model” (Ådlandsvik and Sundby, 1994). The “Lagrangian Diffusion Model” is a simple particle-tracking model with a 4th order Runge-Kutta advection scheme and a sub-module handling individual physiological and behavioral responses to environmental forcing. It implies that the variable physical environment is included in the biological sub-module, but the variability in prey and predator field is uncertain and not known to a sufficient degree in relevant spatial and temporal scales to estimate the mortality and, hence, not included. Due to the horizontal resolution of the SVIM-archive (4 km), mesoscale vorticity is underestimated (Isachsen et al., 2012). Therefore, a horizontal eddy diffusive term (with turbulent diffusion coefficient  $K = 1 \text{ m}^2 \text{ s}^{-1}$ , chosen after testing different values) is included to compensate for the lack of resolving mesoscale processes. The same was included when using the NorKyst800 as forcing for particle dispersal. Vertical distribution of eggs is based on individual egg size and density (Sundby, 1983), modeled ocean densities and levels of turbulence in the water column at the individual time-varying location of each egg (based on Thygesen and Ådlandsvik, 2007; utilized in e.g., Opdal et al., 2011; Röhrs et al., 2014). The larval and juvenile growth function is taken from Folkvord (2005) and based on laboratory experiments for a range of temperatures under constant satiated feeding of the offspring. Vertical migration is included as a diel migration between upper and lower limits depending on light conditions and swimming capability (5–30 m during night and 10–40 m during day, with night defined as light levels below 1.0 micromole photons per  $\text{m}^2 \text{ s}^{-1}$ , see Opdal et al., 2011). A well-known challenge in Lagrangian particle-tracking models is the handling of particles advected near land. We tested different land-handling schemes to avoid abnormal stranding along the irregular coast. We decided to implement a solution where particles were only moved in the direction of the offshore velocity component if they were to be moved onto land in the next time step. The IBM was run with two different setups, one with particles initiated at well-known spawning grounds along the Norwegian coast for the

years 1978–2015, and another with particles initiated according to observed offshore pelagic juveniles for the years 1978–1991. For both setups, the particles are initiated at 5 m depth.

When initiating eggs at the spawning grounds, we released 200 particles at each site every day during the known spawning period from March 1st until April 30th and followed each particle for 200 days to analyze dispersal. The model results were adjusted by weighting the importance of each particle to reflect a Gaussian spawning intensity in time with peak spawning at April 1st and by considering the yearly geographical distribution across spawning grounds using observations from egg surveys (Ellertsen et al., 1987; Sundby and Bratland, 1987; Sjølingstad, 2007; Sundby and Nakken, 2008) and observations on abundance of spawning NEA cod (see the supplementary section for complete references 1978–2004, and data from IMR’s *spawning migration cruises* 2005–2015 held at IMR fish database). The particles are initiated as eggs and continue as hatched larvae after about 2–3 weeks depending on ambient temperatures.

To initiate the model with the observed distributions of pelagic juveniles we released 500 particles at each offshore station with observed NEA cod at the mid-date of the year-specific survey (Table 1) and followed each particle for 120 days until November when NEA cod reach the stage of settling to the bottom in the Barents Sea, i.e., their transition from a pelagic to a demersal habitat (Ottersen et al., 2014).

### Pelagic Juvenile Observations

During the years 1977–1991 scientific surveys<sup>2</sup> covered year-specific observational grids towing trawls of various sizes at a speed of 2–3 knots (Bjørke and Sundby, 1984, 1987; Suthers and Sundby, 1993, 1996). The number of stations, geographic coverage and duration of the surveys varied between years (Table 1). The median spatial resolution between each station was 26 km. The surveys lasted from 16 to 49 days within the period June 18th to August 5th, with mid-date for offshore stations between June 28th and July 26th. The sampling gear used started with a pelagic meshed midwater trawl with an opening of  $4 \times 10 \text{ m}$  in 1977,  $18 \times 18 \text{ m}$  from 1978 until 1984, and finally a  $29 \times 29 \text{ m}$  trawl opening from 1985 and onwards. Here, we have omitted the first year, 1977, since this is considered a test survey where the trawl used was too small. All trawls had diminishing mesh sizes toward the cod end and a 4 m long net with a mesh size of 4 mm (stretched) at the inner part of the cod end. During 1978 through 1984 two hauls were made at each station; one haul with the headline at 40 and 20 m depth, and a towing time of 15 min in each depth interval, and the second haul at the surface with five big floats on the headline and a towing time of 30 min. From 1985 through 1991 the depths were the same as the previous years, but the towing time at each depth interval was halved (Bjørke and Sundby, 1987).

### General Circulation Features

The circulation features of the northeastern North Atlantic are governed by the two-branched northward flow of warm and salty Atlantic Water (AW) across the Faeroe-Shetland Channel (Hansen and Østerhus, 2007; Eldevik et al., 2009) along the

<sup>2</sup><http://www.emodnet-biology.eu/data-catalog?module=dataset&david=4443>

TABLE 1 | NEA cod pelagic juvenile survey details between 1978 and 1991 and corresponding modeling.

Year	Observation information		Simulation information				
	Number of stations in total/offshore with/offshore without presence of juveniles	Observed mean length in total/off-shelf [mm]	Start date [dd.mm]	Particles released	Area A [%]	Area B [%]	Area C [%]
1978	120/22/34	28.7/28.8	09.07	11,000	24.7	75.3	0.0
1979	160/15/45	23.0/20.9	29.06	7,500	52.0	48.0	0.0
1980	127/1/35	20.6/22.0	28.06	500	99.0	1.0	0.0
1981	193/31/35	24.5/27.5	11.07	15,500	24.0	75.2	1.9
1982	155/8/7	27.2/33.3	21.07	4,000	35.8	63.6	0.6
1983	100/5/5	32.2/44.9	11.07	2,500	32.4	60.3	7.3
1984	145/29/3	34.4/40.0	14.07	14,500	41.4	56.6	1.9
1985	129/30/10	24.3/26.8	08.07	15,000	30.2	66.5	3.3
1986	197/16/30	27.0/29.3	13.07	8,000	21.6	66.3	12.1
1987	217/48/23	27.8/30.0	16.07	24,000	30.1	69.0	0.8
1988	242/41/57	34.8/38.5	17.07	20,500	22.1	77.8	0.1
1989	242/21/71	34.1/34.7	14.07	10,500	37.6	59.7	3.0
1990	111/35/8	47.3/57.7	26.07	17,500	35.8	64.2	0.0
1991	163/26/32	36.0/41.1	12.07	13,000	30.8	66.9	2.3

Left side: Total number of survey stations per year, number of stations offshore with and without observed presence of cod juveniles, and mean juvenile length offshore compared to all observations. Right side: Start-date for simulations, number of particles released (500 times per offshore station with observed pelagic juveniles), and the spatial distribution of juveniles per November 1st in the three areas (A–C), see explanation in text.

eastern continental slope, the NASC, and a second branch farther off the shelf. Eddy shedding brings AW off the upper shelf slope and into the Lofoten Basin (Rosby et al., 2009; Søiland et al., 2016) where it either recirculates or flows along the Mohn Ridge toward the Jan Mayen area (Isachsen and Nøst, 2012). Farther north the AW bifurcates at the entrance to the Barents Sea with one branch flowing to the northwest of Svalbard and the other entering the Barents Sea. Northwest of Svalbard AW either carries on northeast and east along the shelf north of Svalbard or eddy shedding brings it out into the Fram Strait and southwest along the Greenland Shelf (Hattermann et al., 2016). **Figure 1** shows the geographical extent of our study area including the main circulation features.

### Predominant Wind Directions and Shelf Edge Orientation

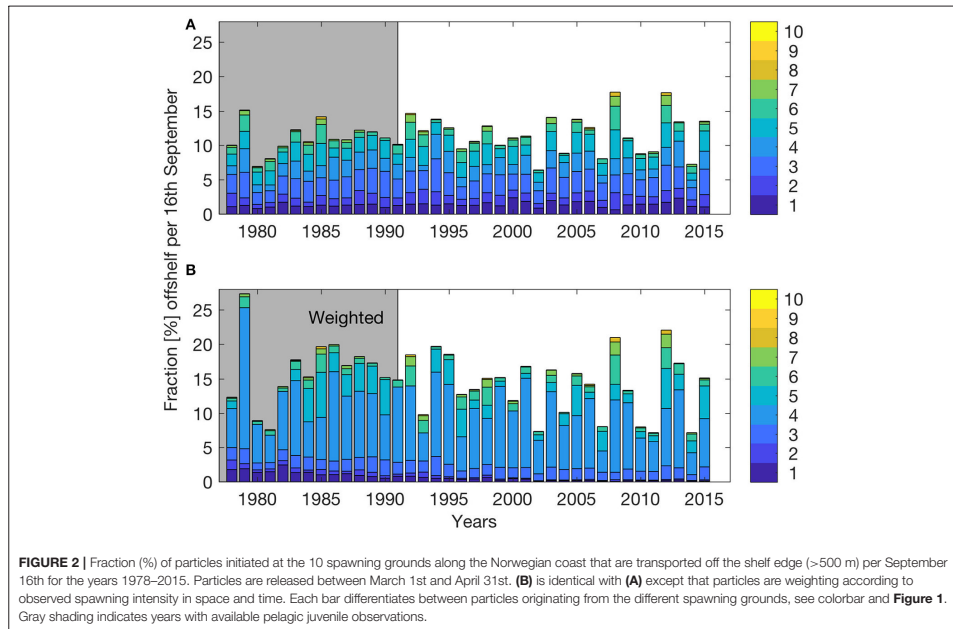
The focus area of the present study is between 67.0 and 70.0° N, where the continental shelf is largely oriented to the northeast (42° from east). Therefore, wind sectors coming from the northerly-easterly/southerly-westerly (NE/SW), within the directional sector of ± 45° of the shelf edge orientation, gives opposite wind sectors against/with the predominating currents. For NE wind, it has the potential to create instability and/or Ekman transport off the shelf edge. We have defined off-shelf areas to include waters deeper than the 500-meter isobath (here named the “shelf edge”). To investigate this further, winds are extracted from NORA10 at a point location at the shelf edge outside Lofoten (69° N, 12° E, see **Figure 1**). Directions of wind with strength <5 m/s are not considered anticipating that such wind is insufficient to cause significant perturbations to the predominant along-shelf currents. The main period chosen is

March through July since by then about 70% of the cod offspring have passed the area of interest (by then) according to the model mean.

## RESULTS

### Origin of the Pelagic Juveniles Off the Shelf Edge

**Figure 2A** shows the fractions of particles transported off the shelf by mid-September (based on SVIM) from each of the 10 spawning areas for the years 1978–2015. The mean off-shelf transport for these years is 11.5% with a minimum in 2002, and a maximum in 2008. **Figure 2B** is similar to **Figure 2A**, but here the particles are weighted according to observed spawning intensity in time and space (inter- and intra-annual, see section Individual-based Model). The mean off-shelf transport of NEA cod offspring then increases to 14.7%. The inter-annual variability also increases, reflecting the high weights added to the offspring originating from the Lofoten region (spawning sites 3–5 in **Figure 1**). In summary, **Figure 2A** illustrates the potential off-shelf transport from each spawning area, while **Figure 2B** shows the off-shelf transport based on the actual year-specific weighted spawning intensity from each spawning area. Increasing horizontal resolution in the ocean model (from SVIM to NorKyst800) for the years 2005–2015 resulted in a decreased mean off-shelf transport from 11.5 to 5.6%. However, the variations between the years have similar features between NorKyst800 and SVIM, with highest off-shelf transport in 2008 (2012) without (with) adding weights to the spawning grounds. According to Suthers and Sundby (1993), the fraction of pelagic juveniles found off shelf in mid-July 1988 was



35%. From our weighted simulations, the 1988 off-shelf transport was estimated to be 16.7%, about half of what was calculated from field observations, but close to the simulated average in our simulations. When averaged over all years, **Table 2** shows that the weighted model distributions of pelagic juveniles compare with observations in 62.4% of the observational stations, varying yearly between 40 and 79%.

### Mechanisms Causing Off-Shelf Transport

Here, we propose two major causes of off-shelf flows; (1) mesoscale eddies related to baroclinic instability of the along-shelf flow, and (2) a larger-scale interior Ekman transport related to wind forcing (Brink, 2016). Since we have used either a model with horizontal resolution of 4 by 4 km, not properly resolving mesoscale variability (Isachsen et al., 2012), or a finer-resolved grid where the lateral boundary off shelf is close to the shelf edge, we focus on the effects of periodic wind forcing.

**Figure 3** shows the number of particles (from non-weighted spawning grounds) displaced off the shelf edge per day for three sample years (1987–1989) between March 1st and July 31st. Here we have investigated the non-weighted model results since the focus is on understanding the physical forcing. The time series show that off-shelf transport is dominated by episodic events and that frequencies and timing varies significantly between years. In the area between 67 and 70° N (black line in **Figure 3**), 1987 has two main events (one late March and one mid-June; **Figure 3A**),

1988 has several events between late April to mid-June with a maximum at May 20th (**Figure 3B**), while in 1989 there are several small events from May to August (**Figure 3C**).

It seems that changing wind directions have a major impact on off-shelf transport of eggs, larvae and juveniles. Having identified off-shelf events (**Figure 3**), we correlated these events in the area between 67 and 70° N with the occurrence of two opposite wind sectors (the NE and SW sectors as described in section Predominant Wind Directions and Shelf Edge Orientation) for the period between March 1st and July 31st. Events are defined as days when the number of particles crossing the shelf edge is higher than one standard deviation of the variability for the year-specific period (see **Figure 3**). **Figure 4** shows the correlation between the frequency of such events and the NE and SW winds. There is a significant ( $p = 0.003$ ) positive (negative) correlation with NE (SW) wind sector of  $R^2 = 0.22$  (0.23).

A similar procedure is done correlating the frequency of winds directly against the modeled ocean currents at different depths. The correlation between NE (SW) wind sector and the current component perpendicular to the shelf edge (at the 500 m isobath), when the current component is above one standard deviation for the year-specific period, is  $R^2 = 0.67$  (0.45) with significance for the surface current (**Table 3**). Corresponding correlations for currents in the depth intervals 5–10 m and 5–40 m are  $R^2 = 0.48$  (0.28) and  $R^2 = 0.20$  (0.06, though not significant), respectively. These depths are relevant because

**TABLE 2** | Coinciding presence or absence of pelagic juveniles in modeled and observed data at the year-specific observation locations.

Year [19-]	78	79	80	81	82	83	84	85	86	87	88	89	90	91	Mean
Match [%]	71	58	64	68	53	40	72	73	50	49	57	75	65	79	62.4

Match (%) between the weighted model distributions and observations occur if both show presence or absence of pelagic juveniles within an area of four grid cells.

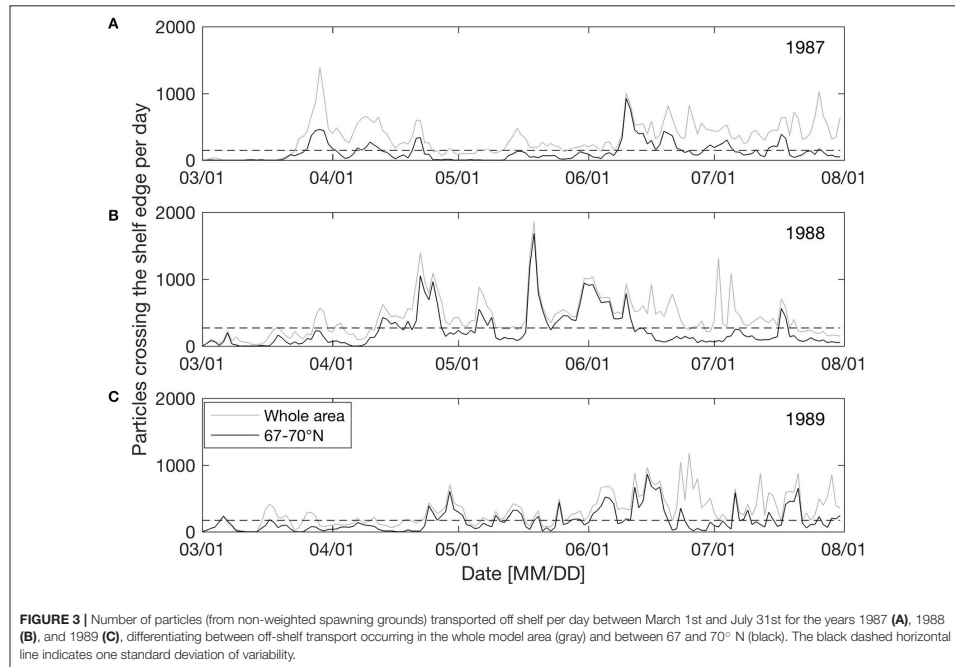


**FIGURE 3** | Number of particles (from non-weighted spawning grounds) transported off shelf per day between March 1st and July 31st for the years 1987 (A), 1988 (B), and 1989 (C), differentiating between off-shelf transport occurring in the whole model area (gray) and between 67 and 70° N (black). The black dashed horizontal line indicates one standard deviation of variability.

eggs are distributed with increasing concentrations toward the surface, while larvae avoid the surface layers and occupy the depths between 5 and 40 m (Ellertsen et al., 1984; Kristiansen et al., 2014) depending on various cues such as prey, predators, and light. Further analysis shows that 83.0% of the daily cross-shelf flow events coincides with the occurrence of NE wind (>5 m/s) during the previous 24 h. Comparing events of stronger cross-shelf currents and winds, show that NE winds above 7 m/s coincide with 90.3 or 97.6% of the cross-shelf currents above 11 or 20 cm/s.

On average for all years, 64.6% of the off-shelf (particle) events between March 1st and July 31st have mean winds coming from NE during the three prior days before each event (Figure 5). This result is even strengthened by comparing with winds preceding such events by 5–7 days (68.2–70.6% respectively). In particular, the years 1985, 1987, 1995, 2004, and 2014 have co-occurring mean 3-day NE winds in >80% of the events.

### Transport Pattern of Pelagic Juveniles Off the Shelf Edge

Observations from the pelagic juvenile surveys (1978–1991) show that pelagic juveniles are variably present all years off the shelf and that the individual juveniles are larger than those on the shelf, except for the year 1979 (Table 1). Modeled dispersal of particles representing pelagic juvenile drift from the time of observations during summer to November 1st shows large inter-annual variations in distribution, but also characteristic features that are repeated between years (Figure 6). Pelagic juveniles drift with near-surface currents largely by the following main routes: back onto the adjacent eastern shelves and into the Barents Sea (south of Svalbard and in the Bear Island Trough), to the west and north of Svalbard with a fair chance of eventually ending up in the Barents Sea, west toward Jan Mayen, northwest toward the Greenland shelf, or recirculating within the Lofoten Basin. Separating particles by their position at November 1st into three

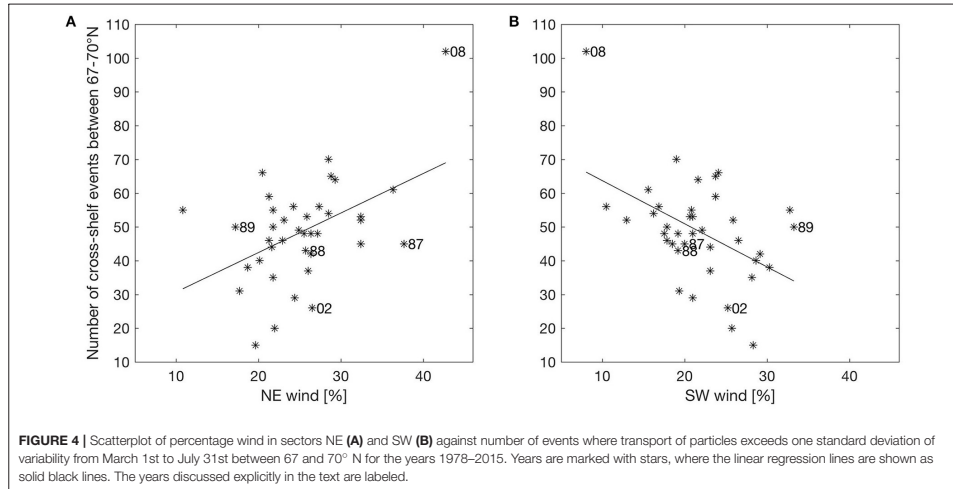


**TABLE 3** | The correlation ( $R^2$ ) and significance (P) between wind sectors (northeastern NE or southwestern SW) and current components at three different depth intervals perpendicular to the shelf edge.

Depth	$R^2/P$ (NE)	$R^2/P$ (SW)
Current at top layer (3 m)	0.67/0.000	0.45/0.000
Current between 5 and 10 m	0.48/0.000	0.28/0.001
Current at 5–40 m	0.20/0.005	0.06/0.140

(A–C) areas enables quantification of inter-annual variability in the destiny of the pelagic juveniles off-shelf (Figure 1);

- (A) The Barents Sea with depths shallower than 500 m.
- (B) Deep ocean with depths deeper than 500 m, (depth > 500 m, lon > 2°E and lat > 73.5°N) | (depth > 500 m and lat < 73.5°N).
- (C) Crossing the Fram Strait to northeastern Greenland (<2° E and >73.5° N).

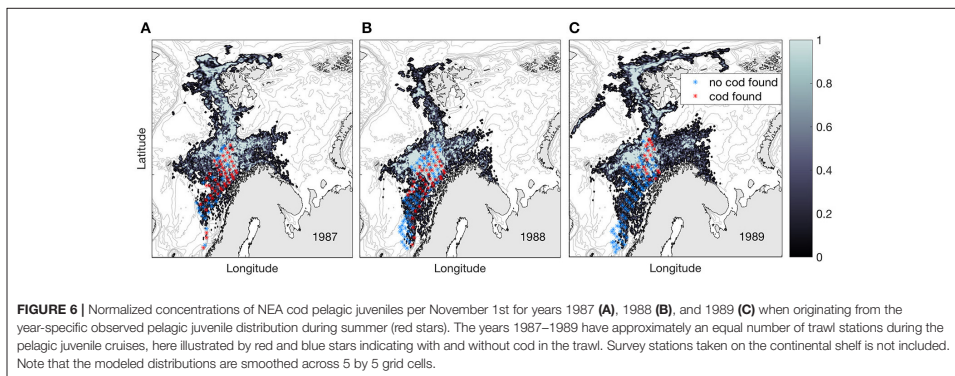
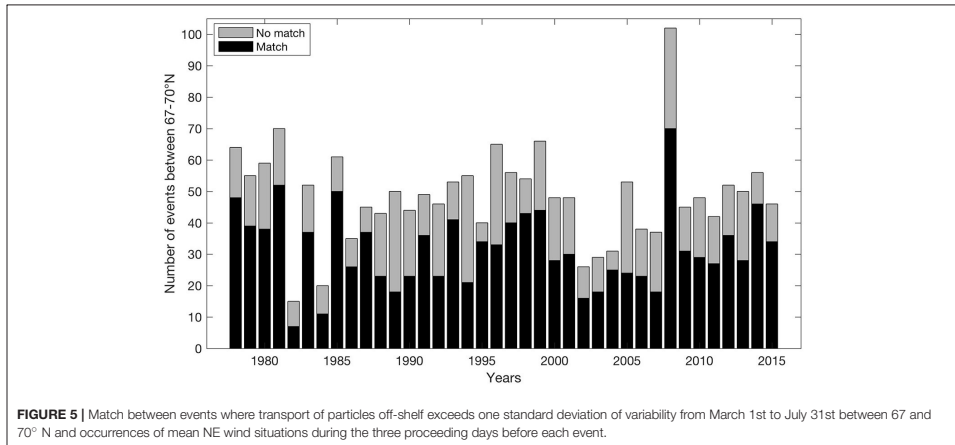
Table 1 shows that on average 36.9% of the off-shelf juveniles are advected back onto the eastern shelf into the Barents Sea habitat (A), 60.7% remain in the open ocean (B), and 2.4% head toward the northeastern Greenland shelf (C). Inter-annual variation is large, especially for area C. The fraction of pelagic juveniles transported into C varies between 0.0 and 12.1%. NEA cod offspring advected off the shelf edge have a chance of being transported back onto the shelf (A) where the main nursery grounds are located (Olsen et al., 2010) without performing directional swimming, varying between 21.6 and 52.0% (except 1980, but this year only has a single observation of pelagic juveniles off-shelf and, hence, few particles are initiated for dispersal simulation).

## DISCUSSION

A characteristic attribute of the NEA cod is that the mature part of the population migrates out of its feeding habitat in the Barents Sea to spawn along the Norwegian coast during spring. During the subsequent period from March until September, the pelagic offspring are transported northward by the NCC (and partly by the NASC) toward their feeding habitat in the Barents Sea. The present study has focused on the portion of this pelagic offspring that become advected off the shelf into the Norwegian Sea, and traditionally assumed to be lost for recruitment (defined as Hjort's 2nd hypothesis by Sinclair et al., 1985). We have investigated the origin of such juvenile loss, the driving mechanisms of this transport, and challenged Hjort's 2nd hypothesis with exploration of alternative fates of these individuals.

Our results show that off-shelf transport has strong inter-annual variations varying between 7.2 and 27.4% with an average of 14.7% during the years 1978–2015. Spawning grounds around Lofoten, especially the one located near the shelf edge (spawning site 5 in Figure 1) used by spawning cod in some years, contribute the most to off-shelf transport. The continental shelf is at its narrowest immediately downstream of this area (about 10 km wide at 69.5°N), resulting in closer dynamic interactions between the NCC and the NASC branches manifested by enhanced mixing and current instabilities.

According to field observations (Suthers and Sundby, 1993), the fraction of pelagic juveniles found off shelf in mid-July 1988 was 35%. From our weighted simulation, the 1988 off-shelf transport was estimated to be 16.7%, about half of the field observation, and close to the simulated average of 14.7%. This indicate that our estimations of off-shelf transport might be an underestimation compared to what is



transported into the Norwegian Sea each year. It should be emphasized that not only advective mechanisms may cause such differences between observed and modeled distributions. Offspring mortality differs substantially in time and space (e.g., Langangen et al., 2014) and will contribute to changes in spatial distributions. As demonstrated by Suthers and Sundby (1993) the main portion of the observed pelagic juveniles in 1988 originated from a spawning window 2 weeks after peak spawning implying an offspring mortality that differs substantially in time. Moreover, the fact that observed off-shelf juveniles in 1988 (Suthers and Sundby, 1993) were larger than those at the shelf they likely also had higher survival rates as they have outgrown some of their natural predators. Since mortality is not included in the biophysical model used here, this explains parts of the difference between modeled and observed off-shelf abundances.

Daily off-shelf advection of pelagic NEA cod offspring is dominated by episodic events where frequencies and timing varies between years. One important driving mechanism for these events are here shown to be fluctuating wind regimes, where northeasterly winds, especially winds blowing steadily over a period of several days (3–7 days), favor off-shelf transport. The correlation between NE winds and near-surface ocean currents weakens with depth down to 40 m, the depth-interval relevant for cod eggs and larvae drift, showing the importance of vertical placement of NEA cod offspring for off-shelf transport.

Based on observations of pelagic juvenile NEA cod in the Norwegian Sea we simulated the potential onward drift to explore possibilities of reaching other favorable destinations than the Barents Sea habitat, i.e., other shelf areas in the North Atlantic. An average of 36.9% are advected back onto the shelves of the Barents Sea by November 1st and thereby given the opportunity

to re-enter the NEA cod stock in its natural habitat. This includes juveniles following AW north of Svalbard. Most pelagic juveniles (average of 60.7%) remain in the deep Norwegian Sea, thus not reaching areas where it is possible to bottom-settle due to the depths (>2,000 m). Hence, this portion of the offspring is confirming the destiny suggested by Hjort's second recruitment hypothesis. However, within the investigated period up to 12.1% (average of 2.4%) heads toward the northeastern Greenland shelf, pre-conditioning bottom-settlement if the conditions are otherwise good.

### Connectivity Studies on Atlantic Cod

A recent model study (Myksovoll et al., 2014) indicates that exchange of pelagic offspring between Norwegian coastal cod and NEA cod may occur to a limited extent. However, the study indicates that exchange is dominated by export of offspring from the coastal cod populations to the NEA cod population (Myksovoll et al., 2011).

Connectivity studies over a larger geographical area were undertaken by researchers on Iceland in the 1970s (e.g., Jamieson and Jónsson, 1971). They found a West Greenland component of the spawning cod at Iceland from tagging experiments implying that connections between neighboring shelves are possible. Also here, the dominating exchange was from the Icelandic cod population to the West Greenland cod population. This is a result of the general circulation patterns where the pelagic offspring are advected downstream. Export the other way must be caused by active migration of the mature fish back to their origins of birth, i.e., natal homing.

During the previous warm period (1920s and 1930s) there was an increase of Atlantic cod in western Greenland. Cod appeared at the offshore banks and expanded their habitat northwards. This is believed to be caused by increased transport of larvae from Iceland as well as better survival due to higher abundance of zooplankton (Drinkwater, 2006).

Observational and modeling studies at Georges Bank in the northwestern Atlantic Ocean (e.g., Lough et al., 1994; Lough and O'Brien, 2012) showed that wind conditions leading to off-shelf Ekman transport is detrimental for survival in early life stages of cod. The Gulf stream is located just south of Georges Bank, and cod transported off the bank will be transported out in the large North Atlantic basin and become lost for recruitment, making this a straightforward example of Hjort's 2nd hypothesis.

Our results show similarities with the Greenland-Iceland study where most juveniles advected off-shelf are lost, but where a minor fraction may get back onto a shelf—either into the well-known nursery grounds or a new location. During the previous warm period in our focus area (the 1930s), Iversen (1934) summarized observations indicating cod could spawn as far north as west of Svalbard. If this re-occurs during the current or future warm periods, there is an even shorter distance from spawning grounds to potential nursery areas at the Greenland shelf.

From the Global Drifter Program<sup>3</sup>, one drifter (id = 78758) from 2009 showed similar transport characteristics as here shown for young NEA cod pelagic juveniles reaching the northeastern

Greenland shelf (see Figure 1). This drifter consisted of a surface buoy, a transmitter, a temperature sensor and a subsurface drogue of 15 m depth (Koszalka et al., 2011) representing a drift in the upper ocean comparable with NEA cod offspring (vertical migration between about 5 and 30 m). The drifter crossed the Norwegian continental shelf edge at February 8th 2009, and arrived at the northeastern Greenland shelf July 27th 2009, a journey of ~6 months. This is well within the period when cod should locate the seabed and become stationary (the Greenland shelf has approximately the same depth as the Barents Sea ~300 m). This observed drifter's trajectory is demonstrating the potential for drift of NEA cod pelagic juveniles to the northeastern Greenland shelf.

### Growth, Predation, and Survival Conditions

In this study, we have not investigated food availability along alternative drift routes for pelagic juveniles drifting off the shelf edge from late summer and through fall. However, zooplankton studies in the Fram Strait confirm that the region is rich in arctic and arcto-boreal copepods in summer (Smith, 1988) as well as during early autumn (Svensen et al., 2011). These copepod species have been identified as the key size groups of prey for pelagic juvenile cod during the spring and summer (Sysoeva and Degtereva, 1965; Sundby, 1995). During late summer the growing juvenile cod switches to larger prey (Sundby, 1995) such as krill. These species are also abundant in the Fram Strait region (e.g., Hop et al., 2006). Consequently, there is a good reason to assume that there are suitable and sufficient prey items for pelagic juvenile cod to survive during summer and early autumn. Hence, the recent observations of immature cod at the northeastern Greenland shelf (Christiansen et al., 2016), coinciding spatially with the present modeled entering region of pelagic juveniles, support the conclusion that cod may be transported, in good condition, from spawning areas along the coast of North Norway.

We have focused on the physical processes affecting the young NEA cod offspring, only including simple biological behavior such as a diurnal vertical migration, growth dependent only on temperature and year-specific choice of spawning grounds (both in time and space). If we also had included mortality as a function of prey and predator availability, the estimate of the percentage of off-shelf transport would likely change. e.g., if individuals located on the shelf are more subject to predation, in addition to being smaller (Suthers and Sundby, 1993), this would lead to higher mortality on-shelf than off-shelf, and the off-shelf percentage would increase. As outlined in the introduction of the Discussion above it is also possible that the larger juveniles off the shelf would be in a better situation to resist and survive potential harsh conditions on their way across the Norwegian Sea. An inclusion of mortality in the model is also expected to change the match between modeled and observed juvenile distributions (Table 2) since observations are formed by the sum of transport, dispersion and site-specific mortality.

### Homing from Northeastern Greenland to Norway?

What may happen to NEA cod arriving at the northeastern Greenland shelf? One possibility is that the shelf will function as a distant part of the NEA cod nursery habitat, while the

<sup>3</sup>[http://www.aoml.noaa.gov/envdis/gld/krig/parttrk\\_id\\_temporal.php](http://www.aoml.noaa.gov/envdis/gld/krig/parttrk_id_temporal.php)

Norwegian coast still is the preferred spawning habitat. This suggestion implies the occurrence of long-distance homing. The other possibility would be that the NEA cod settle along the eastern coast of Greenland, forming a separate sub-population. We will here focus on the first possibility, the long-distance homing strategy.

The Greenland shelf is large, with approximately the same depth as the Barents Sea (~300 m), but much of the shelf area is covered with colder water masses resulting in slower growth and possibly also being exposed to waters of less prey productivity. Keeping in mind that high latitudes have experienced recent warming, with a subsequent northward shift in boreal species (Fosshem et al., 2015), there are reasons to believe that the northeastern Greenland shelf might get increased productivity if the warming trend continues.

Tagging experiments have already shown that NEA cod tends to return to the same spawning locations along the Norwegian coast where it was tagged, and that cod from different spawning locations occupies different areas of the Barents Sea (Godø, 1984). As mentioned in the introduction, a traditional folklore opinion in some fishing communities says that Greenland cod occasionally spawn in Norwegian waters. The hypothesis is that the Norwegian fishermen are recognizing specific phenotypic traits of the cod which are characteristic for cod growing up in Greenland waters, suggesting a long-distance homing strategy. Considering distances for such a migration pattern, the cod could either take a route directly across the Norwegian Sea (~1,000 km), or crossing the Fram Strait following the continental shelf edge (against the NASC) toward Lofoten (~1,500 km). Both routes are within the distance range of observed migration from the Barents Sea to the spawning sites along the Norwegian coast (Sundby and Nakken, 2008; Yaragina et al., 2011). As mentioned in section Connectivity Studies on Atlantic Cod, Jamieson and Jónsson (1971) found that connectivity (homing) between neighboring shelves are possible, and already happening between southwestern Greenland to spawning grounds at Iceland. The difference between our suggested migration and the one described by Jamieson and Jónsson (1971) is that cod from Greenland to Norway need to migrate over deep waters (deeper than 2,000 m). To our knowledge, there is no literature describing deep ocean migration of NEA cod or other cod populations, making our suggested migration unique. A recent study, however, discusses observations of cod in deep waters of the Fram Strait feeding on a mesopelagic layer, demonstrating its highly adaptive capacity (Ingvaldsen et al., 2017).

### Model Uncertainties

In general, the ROMS model setup applied to produce the SVIM seems to overestimate topographic steering above steep slopes. Lien et al. (2014) reported extraordinary strong horizontal gradients in hydrography along the continental shelf slope and AW with a limited westward distribution as compared to observations. This is likely the reason for less stratification on the shelf and the shelf slope as compared to observations, and in turn a different vertical impact of wind stress than in reality. We believe this also affects the ability of the model to replicate eddies shedding off the shelf (Isachsen et al., 2012).

Surprisingly, a higher horizontal grid resolution in NorKyst800, a comparable ROMS setup, did not improve the off-shelf transport, but instead reduced the percentage as compared to observations. Since NorKyst800 applies SVIM-results as forcing along its open boundaries and is thus highly affected by the density field in the coarser model, our results from both model runs are thus limited by the intense horizontal gradients in hydrography. We expect that utilizing forcing fields with improved stratification would give more accurate results. In comparison, the study by Hattermann et al. (2016) successfully quantified eddy-induced westward transport of AW across the Fram Strait and emphasized the need for high horizontal resolution in the ocean model. Their model setup was comparable to the ROMS setup in NorKyst800 but limited to the western shelf of Svalbard. In light of the results by Hattermann et al. (2016), showing that ROMS is capable of replicating eddy shedding, we expect that the relative intra- and inter-annual variation reported in our study are representative for the frequency of off-shelf transport but that the strengths are underestimated as compared to reality. Furthermore, if waves were included in the ocean circulation model, the wave-induced drift could lead to higher retention toward the coast for the cod juveniles (Röhrs et al., 2014). Also looking at ocean dynamics with time scales less than daily, tides would likely change the transport pathways in Vestfjorden implying a slightly different spread of cod eggs and larvae (Lyngø et al., 2010).

If there are any errors in the setup of the biophysical model this could lead to systematic errors in the drift. For example, correlation between wind forcing and modeled ocean currents perpendicular to the shelf edge at three different depth intervals demonstrated that the vertical distribution of NEA offspring and their vertical migration affect the chance of being displaced off the shelf. The higher up in the water column, the higher chance of being transported off-shelf. We performed a sensitivity test, with particles drifting without any vertical movement but kept at fixed depths; surface, 5 and 40 m. Results from this showed that pelagic juveniles drifting close to the surface have a more dispersed horizontal distribution, while the deeper drift pattern was more trapped along topographic features following the Norwegian coast more closely. This is in accordance with Vikebo et al. (2005, 2007) and shows the importance of accurate description of the vertical placement of NEA cod to obtain correct pelagic drift pattern. Important factors to be determined are egg buoyancy (Sundby and Kristiansen, 2015), and realistic vertical migration of the larvae and juveniles (Kristiansen et al., 2014) as well as correct vertical current profile.

The number of observation sites, and observations with and without pelagic juveniles present varied a lot between years. Hence, the number of particles initiated at spawning grounds and dispersed until the time of observations should not introduce a bias in the comparison between model and observations. In contrast, if the stations were dominated by observations with (without) pelagic juveniles, a high (low) number of modeled particles would be beneficial for match. As expected, in years with a high number of observations, there is an increasing number of observations without presence of pelagic juveniles in the trawl, as the survey also covers areas beyond the extent of distribution of cod.

There are uncertainties associated with the origin of pelagic NEA cod juveniles, mainly due to observational limitations. In our study, we defined 10 different spawning grounds along the coast of Norway, and investigated dispersal of NEA cod offspring with and without weighted spawning grounds (Figure 2). The weighting is a continuation of Table 3.1 by Sjølingstad (2007) which divided NEA cod spawning into six spawning grounds. We refined these further into 10 spawning grounds and expanded the table until 2015 using available egg-survey observations (references described in Material and Methods). Four main considerations were done in accordance with Sundby and Nakken (2008); (1) spawning outside More decreases with time, (2) a northward shift in spawning locations from the early 1980s have been quantified, (3) for all years, we added highest weights to the spawning grounds around Lofoten, in accordance with well-established knowledge (Sundby and Bratland, 1987; Ottersen et al., 2014), (4) the spawning ground outside Lofoten, close to the shelf edge, only occurs occasionally (Sundby and Nakken, 2008), but increased spawning has been observed here during the recent decade, similar to the observations in the 1980s (Sundby and Bratland, 1987). The effect of weighting changed the estimated mean off-shelf amount from 11.5 to 14.7%. Any inaccurate quantification of the weighting would affect this estimation.

### Recommendations for Future Work

Both observations and a biophysical model indicate that a significant part of the NEA cod offspring may be advected off-shelf away from the typical drift routes from the spawning grounds along the Norwegian coast toward the nursery grounds in the Barents Sea. Our modeling approach focuses mainly on the physical processes, but to investigate the fate of the off-shelf drifting offspring in a more biological context, it may be necessary to explore the capability and need for horizontal swimming to re-enter the nursery areas in the Barents Sea shelf area. This may be done in a combined effort including *in-situ* observations and biophysical models (Staaterman and Paris, 2013).

Furthermore, it is essential to determine the prey availability for offspring that are advected off-shelf. Is it sufficient for survival during pelagic free drift for durations up to several months? This may be studied through combined *in-situ* observations, biophysical models and remote sensing. Egg, larval and pelagic juvenile mortality involves the enigma of the recruitment problem. The main challenge of predicting the fate of the offspring is still on larval growth and survival basically involving food abundance and the distribution of predators. Site-specific mortality will clearly contribute to the variability in distribution of offspring in addition to the physical advection.

### REFERENCES

Ådlandsvik, B., and Sundby, S. (1994). "Modelling the transport of cod larvae from the Lofoten area" in *ICES Marine Science Symposia*, Vol. 198 (Copenhagen: International Council for the Exploration of the Sea), 379–392.

A current warming trend and subsequent northward shift in boreal species (Fosshelm et al., 2015) give reasons to believe that NEA cod offspring transported off-shelf toward other shelf areas, specifically northeastern Greenland shelf, may successfully settle at the shelf. If this part of the NEA cod would be able to migrate back to its well-known habitat it will contribute to even higher recruitment to the stock if this warming trend continues. The other possibility would be that the NEA cod settle along the eastern coast of Greenland, not returning to the Norwegian coast to spawn. Observational cruises to the northeastern Greenland shelf together with tagging experiments may give better insight into this issue.

Finally, ongoing work in assimilating *in-situ* observations in local ocean model setups show promising features with respect to replicating vertical stratification of the upper ocean inhabited by NEA cod offspring (Sperrevik et al., 2017). We believe this may improve predictive capabilities for dispersal modeling of eggs, larvae and pelagic juveniles on their critical journey toward the favorable nursery grounds in the Barents Sea.

### AUTHOR CONTRIBUTIONS

All authors listed have contributed substantially, both direct and intellectually, and approved it for publication. KS, SS, and FV was responsible for formulating the hypothesis. KS performed most of the direct contribution to the work. SS and FV was responsible for synthesizing the major part of the literature. JA set up the NorKyst800 hindcast.

### FUNDING

Funding support are provided by the Research Council of Norway, through the grant RETROSPECT, project number 244262.

### ACKNOWLEDGMENTS

We thank our colleague Karen Gjertsen for all the help with Figure 1, our colleague Kjell Bakkeplass for providing us the pelagic juvenile observations, and Marta Sanchez de La lama at the University of Oslo for the help obtaining the drifter data from the Global Drifter Program. We would also like to thank the two reviewers for their constructive comments.

### SUPPLEMENTARY MATERIAL

The Supplementary Material for this article can be found online at: <http://journal.frontiersin.org/article/10.3389/fmars.2017.00304/full#supplementary-material>

Albretsen, J., Sperrevik, A. K., Staalstrøm, A., Sandvik, A. D., Vikebø, F., and Asplin, L. (2011). *NorKyst-800, Report No. 1: User Manual and Technical Descriptions*. Fiskeri og Havet, 2, 1–46.

Bergstad, O. A., Jørgensen, T., and Dragesund, O. (1987). Life history and ecology of the gadoid resources of the Barents

Sea. *Fish. Res.* 5, 119–161. doi: 10.1016/0165-7836(87)90037-3

Bjørke, H., and Sundby, S. (1984). "Distribution and abundance of post larval northeast Arctic cod and haddock," in *Proceedings of the Soviet-Norwegian Symposium on Reproduction and Recruitment of Arctic Cod*, eds O. R. Godø and S. Tilseth (Bergen: Institute of Marine Research).

Bjørke, H., and Sundby, S. (1987). "Distribution and abundance indices of postlarval and 0-group cod," in *Proceedings of the Third Soviet-Norwegian Symposium on the Effect of Oceanographic Conditions on Distribution and Population Dynamics of Commercial Fish Stocks in the Barents Sea*, ed H. Loeng (Bergen: Institute of Marine Research).

Brink, K. H. (2016). Cross-shelf exchange. *Ann. Rev. Mar. Sci.* 8, 59–78. doi: 10.1146/annurev-marine-010814-015717

Carton, J. A., and Giese, B. S. (2008). A reanalysis of ocean climate using Simple Ocean Data Assimilation (SODA). *Mon. Weather Rev.* 136, 2999–3017. doi: 10.1175/2007MWR1978.1

Christiansen, J. S., Bonsdorff, E., Byrkjedal, I., Fevolden, S. E., Karamushko, O. V., Lynghammar, A., et al. (2016). Novel biodiversity baselines outpace models of fish distribution in Arctic waters. *Sci. Nat.* 103, 1–6. doi: 10.1007/s00114-016-1332-9

Drinkwater, K. F. (2006). The regime shift of the 1920s and 1930s in the North Atlantic. *Prog. Oceanogr.* 68, 134–151. doi: 10.1016/j.pocean.2006.02.011

Eidevik, T., Nilsen, J. E. Ø., Iovino, D., Olsson, K. A., Sando, A. B., and Drange, H. (2009). Observed sources and variability of Nordic seas overflow. *Nat. Geosci.* 2, 406–410. doi: 10.1038/ngeo518

Ellertsen, B., Fossum, P., Solemdal, P., and Sundby, S. (1989). Relation between temperature and survival of eggs and first-feeding larvae of northeast Arctic cod (*Gadus morhua* L.). *Rapports et Procès-Verbaux Réunion Conseil Permanent International pour l'Exploration de la Mer*, 191, 209–219.

Ellertsen, B., Fossum, P., Solemdal, P., Sundby, S., and Tilseth, S. (1984). "A case study on the distribution of cod larvae and availability of prey organisms in relation to physical processes in Lofoten," in *The Propagation of Cod Gadus morhua* L. Flødevigen rapportserie 1-1984 (Arendal: Havforskningsinstituttet), 453–478.

Ellertsen, B., Fossum, P., Solemdal, P., Sundby, S., and Tilseth, S. (1987). "The effect of biological and physical factors on the survival of Arcto-Norwegian cod and the influence on recruitment variability," in *Proceedings of the third Soviet-Norwegian Symposium on the Effect of Oceanographic Conditions on Distribution and Population Dynamics of Commercial Fish Stocks in the Barents Sea*, ed H. Loeng (Bergen: Institute of Marine Research).

Eriksen, E., and Prozorkevich, D. (2011). "0-group survey," in *The Barents Sea Ecosystem, Resources, Management. Half a Century of Russian-Norwegian Cooperation*, eds T. Jakobsen and V. K. Ozhigin (Trondheim: Tapir Academic Press), 557–569.

Folkvord, A. (2005). Comparison of size-at-age of larval Atlantic cod (*Gadus morhua*) from different populations based on size- and temperature-dependent growth models. *Can. J. Fish. Aqu. Sci.* 62, 1037–1052. doi: 10.1139/f05-008

Fosheim, M., Primmero, R., Johannsen, E., Ingvaldsen, R. B., Aschan, M. M., and Dolgov, A. V. (2015). Recent warming leads to a rapid borealization of fish communities in the Arctic. *Nat. Clim. Chang.* 5, 673–677. doi: 10.1038/nclimate2647

Godø, O. R. (1984). "Migration, mingling and homing of north-east Arctic cod from two separated spawning grounds," in *Proceedings of the Soviet-Norwegian Symposium on Reproduction and Recruitment of Arctic Cod*, eds O. R. Godø and S. Tilseth (Bergen: Institute of Marine Research).

Hansen, B., and Østerhus, S. (2007). Faroe bank channel overflow 1995–2005. *Prog. Oceanogr.* 75, 817–856. doi: 10.1016/j.pocean.2007.09.004

Hattermann, T., Isachsen, P. E., Appen, W. J., Albretsen, J., and Sundfjord, A. (2016). Eddy-driven recirculation of Atlantic water in fram strait. *Geophys. Res. Lett.* 43, 3406–3414. doi: 10.1002/2016GL068323

Hjort, J. (1914). Fluctuations in the great fisheries of northern Europe viewed in the light of biological research. *Rapports et Procès-Verbaux Réunion Conseil Permanent International Pour l'Exploration de la Mer*, 20, 1–228.

Hop, H., Falk-Petersen, S., Svendsen, H., Kwasniewski, S., Pavlov, V., Pavlova, O., et al. (2006). Physical and biological characteristics of the pelagic system across Fram Strait to Kongsfjorden. *Prog. Oceanogr.* 71, 182–231. doi: 10.1016/j.pocean.2006.09.007

Ingvaldsen, R. B., Gjosæter, H., Ona, E., and Michalsen, K. (2017). Atlantic cod (*Gadus morhua*) feeding over deep water in the high Arctic. *Polar Biol.* doi: 10.1007/s00300-017-2115-2

Isachsen, P. E., and Nost, O. A. (2012). The air-sea transformation and residual overturning circulation within the Nordic Seas. *J. Mar. Res.* 70, 31–68. doi: 10.1357/002224012800502372

Isachsen, P. E., Koszalka, I., and LaCasce, J. H. (2012). Observed and modeled surface eddy heat fluxes in the eastern Nordic Seas. *J. Geophys. Res.* 117:C8. doi: 10.1029/2012JC007935

Iversen, T. (1934). Some observations on cod in Northern Waters. *Preliminary Report, Fiskeridirektoratets Skrifter, Serie Havundersøkelser. (Report on Norwegian Fisheries and Marine Investigations)*, Vol. 5.

Jamieson, A., and Jónsson, J. (1971). The Greenland component of spawning cod at Iceland. *J. du Conseil Int. Pour l'Explor. de la Mer* 161, 65–72.

Koszalka, I., LaCasce, J. H., Andersson, M., Orvik, K. A., and Mauritzen, C. (2011). Surface circulation in the Nordic Seas from clustered drifters. *Deep Sea Res.* 58, 468–485. doi: 10.1016/j.dsr.2011.01.007

Kristiansen, T., Vollset, K. W., Sundby, S., and Vikebø, F. (2014). Turbulence enhances feeding of larval cod at low prey densities. *ICES J. Mar. Sci.* 71, 2515–2529. doi: 10.1093/icesjms/fsu051

Langangen, Ø., Stige, L. C., Yaragina, N. A., Vikebø, F. B., Bogstad, B., and Gusdal, Y. (2014). Egg mortality of northeast Arctic cod (*Gadus morhua*) and haddock (*Melanogrammus aeglefinus*). *ICES J. Mar. Sci.* 71, 1129–1136. doi: 10.1093/icesjms/fsu007

Lien, V. S., Gusdal, Y., and Vikebø, F. B. (2014). Along-shelf hydrographic anomalies in the Nordic Seas (1960–2011): locally generated or advective signals? *Ocean Dyn.* 64, 1047–1059. doi: 10.1007/s10236-014-0736-3

Lien, V. S., Hjøllo, S. S., Skogen, M. D., Svendsen, E., Wehde, H., Bertino, L., et al. (2016). An assessment of the added value from data assimilation on modelled Nordic Seas hydrography and ocean transports. *Ocean Model.* 99, 43–59. doi: 10.1016/j.oceanmod.2015.12.010

Lough, R. G., and O'Brien, L. (2012). Life-stage recruitment models for Atlantic cod (*Gadus morhua*) and haddock (*Melanogrammus aeglefinus*) on Georges Bank. *Fish. Bull.* 110, 123–140.

Lough, R. G., Smith, W. G., Werner, F. E., Loder, J. W., Page, F. H., Hannah, C. G., et al. (1994). "Influence of wind-driven advection on interannual variability in cod egg and larval distributions on Georges Bank: 1982 vs 1985" in *ICES Marine Science Symposia*, Vol. 198 (Copenhagen: International Council for the Exploration of the Sea), 356–378.

Lyng, B. K., Berntsen, J., and Gjevik, B. (2010). Numerical studies of dispersion due to tidal flow through Moskstraumen, northern Norway. *Ocean Dyn.* 60, 907–920. doi: 10.1007/s10236-010-0309-z

Mykssvoll, M. S., Jung, K. M., Albretsen, J., and Sundby, S. (2014). Modelling dispersal of eggs and quantifying connectivity among Norwegian coastal cod subpopulations. *ICES J. Mar. Sci.* 71, 957–969. doi: 10.1093/icesjms/fts022

Mykssvoll, M. S., Sundby, S., Ådlandsvik, B., and Vikebø, F. B. (2011). Retention of coastal cod eggs in a fjord caused by interactions between egg buoyancy and circulation pattern. *Mar. Coast. Fish.* 3, 279–294. doi: 10.1080/19425120.2011.595258

Olsen, E., Aanes, S., Mehl, S., Holst, J. C., Aglen, A., and Gjosæter, H. (2010). Cod, haddock, saithe, herring, and capelin in the Barents Sea and adjacent waters: a review of the biological value of the area. *ICES J. Mar. Sci.* 67, 87–101. doi: 10.1093/icesjms/fsp229

Opdal, A. F., Vikebø, F., and Fiksen, Ø. (2011). Parental migration, climate and thermal exposure of larvae: spawning in southern regions gives Northeast Arctic cod a warm start. *Mar. Ecol. Prog. Ser.* 439, 255–262. doi: 10.3354/meps09335

Ottersen, G., Bogstad, B., Yaragina, N. A., Stige, L. C., Vikebø, F. B., and Dalpadado, P. (2014). A review of early life history dynamics of Barents Sea cod (*Gadus morhua*). *ICES J. Mar. Sci.* 71, 2064–2087. doi: 10.1093/icesjms/fsu037

Reistad, M., Breivik, Ø., Haakenstad, H., Aarnes, O. J., Furevik, B. R., and Bidlot, J. R. (2011). A high-resolution hindcast of wind and waves for the North Sea, the Norwegian Sea, and the Barents Sea. *J. Geophys. Res.* 116, C5. doi: 10.1029/2010JC006402

Röhrs, J., Christensen, K. H., Vikebø, F., Sundby, S., Saetra, Ø., and Broström, G. (2014). Wave-induced transport and vertical mixing of pelagic eggs and larvae. *Limnol. Oceanogr.* 59, 1213–1227. doi: 10.4319/lo.2014.59.4.1213

- Rossby, T., Ozhigin, V., Ivshin, V., and Bacon, S. (2009). An isopycnal view of the Nordic Seas hydrography with focus on properties of the Lofoten Basin. *Deep Sea Res.* 56, 1955–1971. doi: 10.1016/j.dsr.2009.07.005
- Shchepetkin, A. F., and McWilliams, J. C. (2005). The regional oceanic modeling system (ROMS): a split-explicit, free-surface, topography-following-coordinate oceanic model. *Ocean Model.* 9, 347–404. doi: 10.1016/j.ocemod.2004.08.002
- Sinclair, M., Tremblay, M. J., and Bernal, P. (1985). El Niño events and variability in a Pacific mackerel (*Scomber japonicus*) survival index: support for Hjort's second hypothesis. *Can. J. Fish. Aqu. Sci.* 42, 602–608. doi: 10.1139/f85-078
- Sjølingstad, B. B. (2007). *Reconstruction of UV Radiation: UV Exposure of the Arcto-Norwegian Cod Egg Population, 1957–2005*. Thesis, Bergen, Geophysical institute, University of Bergen, 1–77.
- Smith, S. L. (1988). Copepods in Fram Strait in summer: distribution, feeding and metabolism. *J. Mar. Res.* 46, 145–181. doi: 10.1357/002224088785113720
- Soiland, H., Chafik, L., and Rossby, T. (2016). On the long-term stability of the Lofoten Basin Eddy. *J. Geophys. Res.* 121, 4438–4449. doi: 10.1002/2016JC011726
- Sperrevik, A. K., Røhrs, J., and Christensen, K. H. (2017). Impact of data assimilation on Eulerian versus Lagrangian estimates of upper ocean transport. *J. Geophys. Res.* 122, 5445–5457. doi: 10.1002/2016JC012640
- Staerterman, E., and Paris, C. B. (2013). Modelling larval fish navigation: the way forward. *ICES J. Mar. Sci.* 71, 918–924. doi: 10.1093/icesjms/fst103
- Sundby, S. (1983). A one-dimensional model for the vertical distribution of pelagic fish eggs in the mixed layer. *Deep Sea Res.* 30, 645–661. doi: 10.1016/0198-0149(83)90042-0
- Sundby, S. (1995). Wind climate and foraging of larval and juvenile Arcto-Norwegian cod. *Can. Spec. Pub. Fish. Aqu. Sci.* 121, 405–415.
- Sundby, S. (2000). Recruitment of Atlantic cod stocks in relation to temperature and advection of copepod populations. *Sarsia* 85, 277–298. doi: 10.1080/00364827.2000.10414580
- Sundby, S., and Bratland, P. (1987). Kartlegging av gytefeltene for norsk-arktisk torsk i Nord-Norge og beregning av eggproduksjonen i årene 1983–1985. (Spatial distribution and production of eggs from Northeast-arctic cod at the coast of Northern Norway 1983–1985). *Fisken og Havet* 1, 1–58.
- Sundby, S., and Kristiansen, T. (2015). The principles of buoyancy in marine fish eggs and their vertical distributions across the world oceans. *PLoS ONE* 10:8821. doi: 10.1371/journal.pone.0138821
- Sundby, S., and Nakken, O. (2008). Spatial shifts in spawning habitats of Arcto-Norwegian cod related to multidecadal climate oscillations and climate change. *ICES J. Mar. Sci.* 65, 953–962. doi: 10.1093/icesjms/fsn085
- Sundby, S., Bjørke, H., Soldal, A. V., and Olsen, S. (1989). Mortality rates during the early life stages and year class strength of the Arcto-Norwegian cod (*Gadus morhua* L.). *Rapports et procès-verbaux des Réunions. Conseil permanent international pour l'Exploration de la Mer*, 191, 351–358.
- Suthers, I. M., and Sundby, S. (1993). Dispersal and growth of pelagic juvenile Arcto-Norwegian cod (*Gadus morhua*), inferred from otolith microstructure and water temperature. *ICES J. Mar. Sci.* 50, 261–270. doi: 10.1006/jmsc.1993.1028
- Suthers, I. M., and Sundby, S. (1996). Role of the midnight sun: comparative growth of pelagic juvenile cod (*Gadus morhua*) from the Arcto-Norwegian and a Nova Scotian stock. *ICES J. Mar. Sci.* 53, 827–836. doi: 10.1006/jmsc.1996.0104
- Svensen, C., Seuthe, L., Vasilyeva, Y., Pasternak, A., and Hansen, E. (2011). Zooplankton distribution across Fram Strait in autumn: are small copepods and protozooplankton important? *Prog. Oceanogr.* 91, 534–544. doi: 10.1016/j.pocean.2011.08.001
- Sysoeva, T. K., and Degtereva, A. A. (1965). The relation between feeding of cod larvae and pelagic fry and the distribution and abundance of their principal food organisms. *Int. Comm. Northwest Altan. Fish. Spec. Pub.* 6, 411–416.
- Thygesen, U. H., and Ådlandsvik, B. (2007). Simulating vertical turbulent dispersal with finite volumes and binned random walks. *Mar. Ecol. Prog. Ser.* 347, 145–153. doi: 10.3354/meps06975
- Umlauf, L., and Burchard, H. (2003). A generic length-scale equation for geophysical turbulence models. *J. Mar. Res.* 61, 235–265. doi: 10.1357/002224003322005087
- Umlauf, L., Burchard, H., and Hutter, K. (2003). Extending the k- $\omega$  turbulence model towards oceanic applications. *Ocean Model.* 5, 195–218. doi: 10.1016/S1463-5003(02)00039-2
- Uppala, S. M., Källberg, P. W., Simmons, A. J., Andrae, U., Bechtold, V. D., Fiorino, M., et al. (2005). The ERA-40 re-analysis. *Q. J. R. Meteorol. Soc.* 131, 2961–3012. doi: 10.1256/qj.04.176
- Vikebø, F., Jørgensen, C., Kristiansen, T., and Fiksen, Ø. (2007). Drift, growth, and survival of larval Northeast Arctic cod with simple rules of behaviour. *Mar. Ecol. Prog. Ser.* 347, 207–219. doi: 10.3354/meps06979
- Vikebø, F., Sundby, S., Ådlandsvik, B., and Fiksen, Ø. (2005). The combined effect of transport and temperature on distribution and growth of larvae and pelagic juveniles of Arcto-Norwegian cod. *ICES J. Mar. Sci.* 62, 1375–1386. doi: 10.1016/j.icesjms.2005.05.017
- Warner, J. C., Sherwood, C. R., Arango, H. G., and Signell, R. P. (2005). Performance of four turbulence closure models implemented using a generic length scale method. *Ocean Model.* 8, 81–113. doi: 10.1016/j.ocemod.2003.12.003
- Werner, F. E., Page, F. H., Lynch, D. R., Loder, J. W., Lough, R. G., Perry, R., et al. (1993). Influences of mean advection and simple behavior on the distribution of cod and haddock early life stages on Georges Bank. *Fish. Oceanogr.* 2, 43–64. doi: 10.1111/j.1365-2419.1993.tb00120.x
- Werner, F. E., Quinlan, J. A., Blanton, B. O., and Luettich, R. A. (1997). The role of hydrodynamics in explaining variability in fish populations. *J. Sea Res.* 37, 195–212. doi: 10.1016/S1385-1101(97)00024-5
- Yaragina, N. A., Aglen, A., and Sokolov, K. M. (2011). Cod. "The Barents Sea ecosystem, resources, management," in *Half a Century of Russian–Norwegian Cooperation*, eds T. Jakobsen and V. K. Ozhigin (Trondheim: Tapir Academic Press), 225–270.

**Conflict of Interest Statement:** The authors declare that the research was conducted in the absence of any commercial or financial relationships that could be construed as a potential conflict of interest.

Copyright © 2017 Strand, Sundby, Albretsen and Vikebø. This is an open-access article distributed under the terms of the Creative Commons Attribution License (CC BY). The use, distribution or reproduction in other forums is permitted, provided the original author(s) or licensor are credited and that the original publication in this journal is cited, in accordance with accepted academic practice. No use, distribution or reproduction is permitted which does not comply with these terms.



### *Supplementary Material*

## **The northeast Greenland shelf as a potential habitat for the Northeast Arctic cod**

**Kjersti Opstad Strand\*, Svein Sundby, Frode B. Vikebø, Jon Albretsen**

\* **Correspondence:** Corresponding Author: kjersti.opstad.strand@imr.no

### **1 References available on abundance of spawning Northeast Arctic cod (chronological order)**

Jakobsen T. (1978). Skreiinnsiget i Lofoten i 1978 (The spawning migration of Arctic cod in Lofoten in 1978). *Fisken og Havet* 2, 19-28.

Larsen E. (1986). Lofotfisket 1985. *Årsberetning vedkommende Norges Fiskerier 1985 Nr. 5*. Bergen: Fiskeridirektoratet, 1-21.

Larsen E. (1987). Lofotfisket 1986. *Årsberetning vedkommende Norges Fiskerier 1986 Nr. 5*. Bergen: Fiskeridirektoratet, 1-22.

Larsen E. (1988a). Lofotfisket 1987. *Årsberetning vedkommende Norges Fiskerier 1987 Nr. 1*. Bergen: Fiskeridirektoratet, 1-2.

Larsen E. (1988b). Lofotfisket 1988. *Årsberetning vedkommende Norges Fiskerier 1988 Nr. 5*. Bergen: Fiskeridirektoratet, 1-23.

Larsen E. (1989). Lofotfisket 1989. *Årsberetning vedkommende Norges Fiskerier 1989 Nr. 5*. Bergen: Fiskeridirektoratet, 1-23.

Larsen E. (1990). Lofotfisket 1990. *Årsberetning vedkommende Norges Fiskerier 1990 Nr. 6*. Fiskeridirektoratet, 1-23. ISSN 0365-8252

Anon. (1991). Lofotfisket 1991. *Årsberetning vedkommende Norges Fiskerier 1991 Nr. 5*. Fiskeridirektoratet, 1-22. ISSN 0365-8252

Hansen K. O. N. (1992). Lofotfisket 1992. *Årsberetning vedkommende Norges Fiskerier 1992 Nr. 5*. Fiskeridirektoratet, 1-23. ISSN 0365-8252

Hansen K. O. N. (1993). Lofotfisket 1993. *Årsberetning vedkommende Norges Fiskerier 1993 Nr. 5*. Fiskeridirektoratet, 1-13. ISSN 0365-8252

Anon. (1994). Lofotfisket 1994. *Årsberetning vedkommende Norges Fiskerier 1994 Nr. 5*. Fiskeridirektoratet, 1-20. ISSN 0365-8252

Anon. (1995). Lofotfisket 1995. *Årsberetning vedkommende Norges Fiskerier 1995 Nr. 5*.

## Supplementary Material

Fiskeridirektoratet, 1-25. ISSN 0365-8252

Berntzen R. I. (1996). Lofotfisket 1996. *Årsberetning vedkommende Norges Fiskerier 1996 Nr. 5*. Fiskeridirektoratet, 1-25. ISSN 0365-8252

Berntzen R. I. (1997). Lofotfisket 1997. *Årsberetning vedkommende Norges Fiskerier 1997 Nr. 5*. Fiskeridirektoratet, 1-25. ISSN 0365-8252

Berntzen R. I. (1998). Lofotfisket 1998. *Årsberetning vedkommende Norges Fiskerier 1998 Nr. 5*. Fiskeridirektoratet, 1-24. ISSN 0365-8252

Anon. (1999). Lofotfisket 1999. *Årsberetning vedkommende Norges Fiskerier 1999 Nr. 5*. Fiskeridirektoratet, 1-24. ISSN 0365-8252

Berntzen R. I. (2000). Lofotfisket 2000. *Årsberetning vedkommende Norges Fiskerier 2000 Nr. 5*. Fiskeridirektoratet, 1-20. ISSN 0365-8252

Johansen P. O. (2002). Lofotfisket 2001/2002. *Melding fra Utvalgsformannen for Lofotfisket*. Leknes: Fiskeridirektoratet, 1-9.

Anon. (2003). Erratum. "Revidert rapport fra tokt med F/F G.O. Sars, Lofoten 16.03-02.04.02". *Report by Havforskningsinstituttet*. Bergen: Havforskningsinstituttet, 1-18.

Mehl S. and Nedraas K. (2003). Akustisk mengdemåling av gytebestanden av skrei Lofoten mars-april 2003 (Abundance of spawning Northeast Arctic cod spring 2003). *Toktrapport Havforskningsinstituttet*. 13-2003. ISSN 1503-6294

Mehl S. (2004). Akustisk mengdemåling av gytebestanden av skrei Lofoten mars-april 2004 (Abundance of spawning Northeast Arctic cod spring 2004). *Toktrapport Havforskningsinstituttet*. 9-2004. ISSN 1503-6294

# Paper 2

## **5.2 Sub-surface maxima in buoyant fish eggs indicate vertical velocity shear and spatially limited spawning grounds**

Kjersti Opstad Strand, Frode Vikebø, Svein Sundby, Ann Kristin Sperrevik and Øyvind Breivik

*Accepted for publication in Limnology and Oceanography*



## Sub-surface maxima in buoyant fish eggs indicate vertical velocity shear and spatially limited spawning grounds

**Authors:** Kjersti Opstad Strand<sup>1,2,3\*</sup>, Frode Vikebø<sup>1,3</sup>, Svein Sundby<sup>1</sup>, Ann Kristin Sperrevik<sup>3</sup>, Øyvind Breivik<sup>5,2</sup>

<sup>1</sup>Institute of Marine Research, Bergen, Norway

<sup>2</sup>Geophysical Institute, University of Bergen, Norway

<sup>3</sup>Bjerknes Centre of Climate Research, Bergen, Norway

<sup>4</sup>The Norwegian Meteorological Institute, Oslo, Norway

<sup>5</sup>The Norwegian Meteorological Institute, Bergen, Norway

[kjersti.opstad.strand@hi.no](mailto:kjersti.opstad.strand@hi.no), [frode.vikeboe@hi.no](mailto:frode.vikeboe@hi.no), [svein.sundby@hi.no](mailto:svein.sundby@hi.no), [annks@met.no](mailto:annks@met.no), [oyvind@met.no](mailto:oyvind@met.no)

\* Correspondence: Kjersti Opstad Strand, [kjersti.opstad.strand@imr.no](mailto:kjersti.opstad.strand@imr.no).

Sub-surface maxima in buoyant fish eggs

**Key words:** Vertical distributions in plankton, spawning grounds, dispersal, current shear, biophysical, individual-based model, data assimilation

### Abstract

Observed vertical profiles of buoyant particles, in this case pelagic Northeast Arctic cod eggs, occasionally deviate from the vertical diffusion-buoyancy balance by displaying sub-surface maxima. Here we present a mechanism that may explain this phenomenon by combining in situ measurements of Northeast Arctic cod eggs and concurrent environmental conditions with biophysical modeling of Vestfjorden, Norway. Due to limited observational information, we constructed a spawning season by dispersing eggs with an individual-based biophysical model forced by a three-dimensional ocean model including data assimilation improving upper ocean stratification. We show that transient sub-surface maxima in eggs are caused by the combination of vertical velocity shear and spatial limitations of spawning grounds. This demonstrates the need for resolving upper ocean small-scale dynamics in biophysical models to predict horizontal and vertical planktonic dispersal. This is also a precondition for predicting environmental exposure along drift routes, including natural and anthropogenic stressors.

## Introduction

Prediction of particle transport in the upper ocean is needed in a range of applications, from locating accumulation zones of plastic debris (Lebreton et al., 2012), forecasting dispersion of oil spills (e.g. Jones et al., 2016) to predicting distribution patterns of marine planktonic organisms (e.g. Hidalgo et al., 2011). It is useful in survey design for mapping abundances of fish egg, which in turn may be used to estimate the spawning stock biomass as basis for fisheries quotas (Sundby and Bratland, 1987; Checkley et al., 1997; Stratoudakis et al., 2006). In case of oil spills, a correct representation of plankton dispersal may be used for quantifications of plankton exposure to oil (Vikebø et al., 2013). Because ocean currents vary with depth it is necessary to know the dynamical vertical positioning of plankton to obtain correct estimate of dispersal. Hence, simulations of transport and spatial distributions of particles in the ocean must be based on correct representation of physical processes, both horizontal and vertical, from wind-driven currents, fronts and eddies to vertical mixing by wind, tides and convection. In contrast to dissolved substances that do not influence the specific gravity of the solution (such as inorganic nutrients, dissolved organic carbon, and pollutants of water-based liquids), and hence follow the advection and diffusion of the water masses, particulate matter, such as fish eggs, air bubbles, plastics and dispersed oil have distinct vertical velocities determined by their buoyancies. Analytical models for the dynamic vertical distribution of particulate matter have been developed for fish eggs (Sundby 1983), air bubbles (Thorpe 1984) and dispersed oil (Paris et al. 2012). Lagrangian biophysical particle-tracking models advect particles according to the current fields of general circulation models (GCMs), while simultaneously adding vertical movements determined by buoyancy (e.g. Ådlandsvik and Sundby, 1994, Thygesen and Ådlandsvik, 2007) or by vertical behavior in plankton (Vikebø et al. 2007). Variability in ocean currents, horizontal and vertical, caused by atmospheric forcing, tides or eddies result in particle spreading.

Modeling realistic vertical velocity shear is typically challenging for GCMs, as they tend to smooth out vertical gradients in temperatures and salinity due to inaccuracy in representing turbulence and diapycnal mixing in sigma-coordinate models. This causes e.g. erroneous flux of energy from the atmosphere and down through the water column. This reduces the accuracy of dispersal forecasts of particles in the ocean, which is particularly relevant near boundaries where stress is exerted (e.g. surface wind stress). For example, Northeast Arctic cod eggs and larvae drifting close to the ocean surface are shown to spread more than those deeper down due to the stronger influence of variable meteorological forcing near the surface (Vikebø et al., 2005; 2007).

In this study we observed vertical distributions of fish eggs and made concurrent measurements of the environmental conditions. We then employed a numerical particle tracking simulation to assess the influence of combined vertical-horizontal processes affecting the vertical distribution of buoyant, drifting particles. In particular, we investigate observations of sub-surface maxima in vertical profiles of buoyant Northeast Arctic (NEA) cod eggs in the surface mixed layer and show how such a profile structure can be explained.

The choice of NEA cod eggs for this study has several reasons. First, there are sufficiently high concentrations of eggs released in a confined period of time at distinct locations to get excellent observational resolution (Sundby and Bratland, 1987). The majority of spawning occurs from March through April (Ellertsen et al., 1989) along the Norwegian coast (Sundby and Nakken, 2008). Time of spawning is dependent on the integrated temperature from autumn to spawning time (Kjesbu et al. 2010). The main spawning grounds are in Lofoten, with one spawning hotspot near Henningsværstraumen (Sundby and Bratland, 1987). Second, more knowledge of the physical processes affecting early life stages of NEA cod is needed to understand the mechanisms regulating survival during the early life stages (Hjort, 1914, Ottersen

et al., 2014, Strand et al., 2017). Third, the analytical model of vertical distribution of pelagic eggs (Sundby 1983) was based on this species' egg data of physical-biological attributes (i.e. size spectrum and buoyancy) from the present location. Further knowledge about physical-biological attributes throughout egg incubation has been studied in detail by Jung et al. (2014). There are strong vertical and horizontal gradients in egg concentrations at the spawning grounds (Solemdal and Sundby, 1981, Sundby and Bratland, 1987). The patchy horizontal distribution stems from the spawning behavior (Sundby and Bratland, 1987) as well as the presence of physical oceanographic structures. The vertical distribution of NEA cod eggs is determined by the balance between the vertical velocity of the eggs (determined by their buoyancy) and mixed-layer turbulence represented by the vertical eddy diffusivity (e.g. Sundby, 1983; Sundby and Kristiansen, 2015), see eq. 1. For pelagic eggs (i.e. eggs with density lower than the density of the upper mixed layer), such as NEA eggs, concentration declines exponentially with depth from the surface in proportionality to egg ascending speed and in inverse proportion to the eddy diffusion coefficient (Sundby, 1983; 1991).

Still, observed vertical profiles of NEA cod eggs occasionally reveal a transient sub-surface maximum inconsistent with the steady-state vertical analytical formulations by Sundby (1983) (see for example Sundby, 1983, and Röhrs et al., 2014). Here, we investigate potential mechanisms causing these observed deviations from the analytical vertical model for pelagic fish eggs.

Our main hypothesis is that sub-surface maxima in buoyant particles may occur due to horizontal movement in the presence of vertical velocity shear and strong gradients in horizontal egg concentration, conditions that are often observed at spawning hot spots. By designing a numerical experiment based on measured conditions at the main spawning ground of NEA cod we quantify the frequencies by which such events occur, and explore which conditions favor such incidents. We then look at how adding data assimilation in the GCM can improve the representation of vertical and horizontal shear and compare with observations of vertical egg distribution.

### Materials

In our analysis of the main hypothesis, we initiate particles at a well-known spawning site inside Vestfjorden and model their subsequent dispersal with an individual-based biophysical particle-tracking model (Ådlandsvik and Sundby, 1994) forced both by idealized currents and hourly current velocity, hydrography and turbulence from a three-dimensional GCM, constructed by the use of state-of-the-art data assimilation methods (Sperrevik et al., 2017). Particles are initiated at multiple adjacent point locations so that we may analyze the effect of narrow versus wide spawning grounds for the occurrences of sub-surface maxima. An evaluation of the modeled ocean circulation is given in the Supplemental information (Figure S1) where we compare two model realizations, with and without data assimilation, against in situ measurements of NEA cod eggs from observations in 1984 (Sundby and Bratland 1987). By including data assimilation, the NEA cod dispersal is improved compared to the observations (Figure S1). The year 1984 is chosen because of the extensive measurement campaigns providing both physical data for assimilation and evaluation of the GCM, and egg distribution data. As only horizontal (and not vertical) egg observations were available in 1984, we compare our modeled vertical egg profiles with corresponding observations from a scientific cruise during the spawning season from April 4-7<sup>th</sup> 2016 in the same area. Then, only vertical egg profiles were sampled, but no horizontal egg coverage were carried out. However, egg data from 1984 and 2016 may be compared because the

salinity in the area has not changed enough to affect the physical NEA cod egg buoyancy differently. See subsection *NEA cod eggs as oceanographic drifters* below. The horizontal patchiness of the eggs observed in 1984 mirrors the typical traditional spawning areas repeatedly observed during earlier studies (Ellertsen et al. 1981b; Ellertsen et al. 1984; Sundby and Fossum 1990; Sundby et al. 1994), including the specific area sampled in 2016, the Henningsværstraumen. This was studied in detail by Sundby and Fossum (1990), where typically horizontal egg concentration decreases by two orders of magnitude over a 10 km distance from the center of the spawning area (Sundby and Bratland 1987).

#### *NEA cod eggs as oceanographic drifters*

An important characteristic of marine fish eggs is that they are homohaline, implying that they by osmoregulation maintain constant internal salinity independent of the ambient salinity (Sundnes et al. 1965). Furthermore, fish eggs are ectotherms, meaning that their internal temperature equals that of the environment. The thermal expansion coefficient of the eggs is approximately equal to that of the ambient seawater (Sundby and Kristiansen 2015), allowing the in situ buoyancy to be calculated through laboratory experiments based on salinity alone and independent of the ambient temperature. Hence, the buoyancy of NEA cod eggs depends on salinity, but not the temperature. The laboratory-based neutral buoyancy of NEA cod eggs expressed in salinity units ranges between 29.5 and 33.0 PSU, with an average neutral buoyancy of about 31.0 PSU (Solemdal and Sundby, 1981). The stratification in 1984 and 2016 are shown in Figure S2. The CTD data from 1984 are downloaded from <http://ocean.ices.dk/HydChem/>, accessed July 26<sup>th</sup>, 2018, while 2016-data were collected during the cruise described below. The salinity range have changed  $\pm 0.1$  PSU in the upper 30 meters from 1984 to 2016 (while the temperature is 2-3 °C higher in 2016). The lowest salinity observed in 2016 and 1984 was 32.7 PSU and 32.8 PSU, respectively (Figure S2). This means that a small portion of the observed eggs, in both years, could be denser than the ambient water masses. Based on data from Jung et al. (2012a), Jung et al. (2012b) and Stenevik et al. (2008) this amounts to 5.1 (4.1) % of the eggs for 32.7 (32.8) PSU, giving a difference of only 1 % in potentially denser eggs between 1984 and 2016.

A second important characteristic is that the NEA cod at the spawning areas in Lofoten release their eggs in the thermocline, within a temperature range of 4-6 °C, usually at depths varying between 50 and 200 m (Ellertsen et al., 1981a). The thermocline defines the interface between the Norwegian coastal waters (cold and relatively fresh) and inflowing Atlantic waters (warmer and more saline), a typical hydrographic situation for the Lofoten spawning area during spring time (Ellertsen et al., 1981b). While the upper ocean temperature is higher in 2016 than in 1984, the spawning still occurs in the transition zone between Atlantic and Coastal waters.

These characteristics make NEA cod eggs positively buoyant, and newly spawned eggs rise towards the surface and reach their equilibrium vertical distribution in less than 24 hours. The exact time to equilibrium depends on the intensity of wind mixing (Sundby 1991). At the ambient temperatures of upper layers of the Lofoten spawning areas NEA cod eggs typically hatch after about 3 weeks (Strømme 1977), allowing considerable drift distances in the upper ocean from the spawning grounds towards the nursery area before hatching into the larval stages. NEA cod egg develop through six defined stages (Strømme, 1977), enabling quantification of how long individual eggs found at sea have been adrift.

#### *Observations from a scientific cruise, April 4-7<sup>th</sup> 2016*

A scientific cruise was conducted April 4-7<sup>th</sup> 2016 with *R/V Johan Hjort* by the Norwegian Institute of Marine Research in collaboration with the Norwegian Meteorological Institute, the

Nansen Environmental and Remote Sensing Center and the National University of Ireland, Galway. Nine vertical egg profiles (see Figure 1 for locations), including egg-stage determination according to Strømme (1977), are used together with the oceanographic and meteorological observations to evaluate and compare with our modeling study, as explained below.

Eggs were sampled with a Xylem submersible electric pump with a pump capacity of about 100 liters  $\text{min}^{-1}$ . Sea water was pumped on deck through a 75-mm hose and filtered through a T-80 plankton net with mesh size 375  $\mu\text{m}$ . Pump samples were taken at 1 m depth (except for one location at 1.5 m), then every 5 m from 5 to 30 m. Sampling volume from each depth was 200 liters. Egg profiles are presented in numbers  $\text{m}^{-3}$ . The measurement increment is 1 egg per 200 liters, i.e. 5 eggs per  $\text{m}^3$ . The pump technique of sampling vertical egg profiles is therefore sensitive when low numbers of eggs are observed. Given the actual sea state during the cruise, there is an assumed uncertainty of 0.25 m per measurement depth due to the movement of the ship. In addition to the vertical egg samples, 39 net hauls were sampled with the same plankton net. In total, from both vertical egg samples and net hauls, 2991 eggs were counted and staged. For every egg profile, a Conductivity-Temperature-Depth (CTD) profile was taken with a Sea-bird CTD instrument (SBE 911+). The data was post-calibrated against water samples taken with every CTD profile.

Current velocities were measured using an acoustic upward looking Aanderaa Recording Current Doppler Profiler (600 kHz) placed at 40 m depth on a mooring in the center of the survey area (68.09° N, 14.07° E) which is at the assumed center of the Henningsværstraumen spawning area. The bottom depth at the mooring location is 105 m. The instrument was operational from April 4<sup>th</sup> 13:11 UTC until April 7<sup>th</sup> 03:46 UTC. The upper 5 m of the data before April 5<sup>th</sup> 10:00 UTC could not be used due to higher frequency interference with another instrument working at the beginning of the cruise. Processed velocity data are stored in 5-min averages in 1 m depth intervals. The measurements are filtered with a Hanning window to remove variability of time scales less than 1 hour to obtain the same time step as the other observations.

Automatic wind observations were taken from the nearest meteorological station Skrova Lighthouse (WMO st.no. 01160), located on a small island 11 m above sea level (68.15° N, 14.65° E) 25 km from the observational site and operated by the Norwegian Meteorological Institute (<http://eklima.met.no>, accessed April 6<sup>th</sup> 2017). A comparison with the wind mast from the ship shows similar observations, though a time lag of a few hours depending on the situation and location of the ship.

#### *Ocean model setup*

Particles are transported by hourly three-dimensional current fields from a Regional Ocean Modeling System (ROMS, Shchepetkin and McWilliams, 2005; Haidvogel et al., 2008). We used the Generic Length Scale mixing scheme with  $k-\omega$  setup for quantifying spatio-temporal eddy diffusivity (Umlauf and Burchard, 2003; Umlauf et al., 2003). See Warner et al. (2005) for a comprehensive evaluation of the different available mixing schemes. The model application has a horizontal resolution of 2.4 by 2.4 km, 35 vertical terrain-following sigma-coordinates and uses bottom topography taken from the NorKyst-800 archive (Albretsen et al., 2011). The model is forced by atmospheric fields from the Norwegian 10 km hindcast archive (NORA10, Reistad et al., 2011), river runoff from the Norwegian Water Resources and Energy Directorate (NVE, Beldring et al., 2003), and 8 tidal constituents from the TPXO global inverse barotropic model (Egbert and Erofeeva, 2002). Initial and boundary conditions are from the SVIM hindcast archive with a 4 by 4 km horizontal resolution (Lien et al., 2014). A reanalysis of the ocean circulation

was produced by the use of four-dimensional variational (4D-Var) data assimilation (Sperrevik et al., 2017) using hydrographical observations from an extensive field campaign performed by IMR in the main spawning area for NEA cod, the Vestfjorden, in 1984 (Sundby and Bratland, 1987) as well as satellite sea surface temperature.

#### *Individual-based particle tracking*

NEA cod eggs are released continuously at point locations in a regular grid, centered around the main spawning ground at Henningsværstraumen (Sundby and Bratland, 1987). The eggs are advected hourly using a 4<sup>th</sup> order Runge-Kutta advection scheme. The model variables are tri-linearly interpolated to the individual time-varying locations of each egg. The buoyancies of eggs are based on the individual egg sizes and densities (see eq. 1 and Sundby, 1983) and modeled ocean densities. Vertical dynamical positioning of eggs is calculated based on the numerical scheme by Thygesen and Ådlandsvik (2009) utilizing the turbulence from ROMS at the individual time-varying location of each egg (see e.g. Röhrs et al., 2014). The spawning ground is represented by 66 locations (one location per grid cell inside the box, see Figure 1). Particles are released at 50 m depth, with 25 particles per location every 6 hours for 60 days, corresponding to the main spawning period from March 1<sup>st</sup> to April 30<sup>th</sup>, resulting in a total release of 397650 eggs. The individual-based biophysical particle-tracking model is run for 80 days, ending 20<sup>th</sup> of May to ensure that all initialized eggs have hatched. The eggs mature and hatch according to ambient water temperature (Folkvord, 2007). Particle positions are stored every 3 hours, resulting in 8 track positions per day, thus resolving tidal motion.

#### *Sensitivity analysis of sub-surface maxima under idealized currents*

A sensitivity analysis is included where eggs are transported by currents resulting from a two-step reduction of the original modeled currents to an artificial constant depth-independent horizontal current equal to 1  $\text{cm s}^{-1}$ . Also, we have tested the importance of dynamical vertical positioning of eggs due to turbulence and buoyancy for sub-surface maxima by adding simulations with constant egg rise velocities of 1  $\text{mm s}^{-1}$ .

#### *Sampling vertical profiles of cod eggs in the model simulation*

Cod eggs in Lofoten hatch after about 3 weeks. Larvae have different buoyancy than eggs as well as having a vertical behavior. Therefore, the particles are removed from the model once they hatch. Vertical profiles of eggs in the model simulation are then sampled to search for sub-surface maxima, in the upper 20 m where the majority of eggs are located. To identify sub-surface maxima, vertical profiles of particles are sampled at every grid cell where particles were initiated (in the spawning ground set to 66 grid cells). Two methods of sampling vertical profiles of particle distributions were carried out; 1) by only considering the particles initiated at the same grid cell as they are subsequently being sampled, 2) by considering all particles independently of where they are initiated. The latter is expected to better reflect the observations with the egg-pump stations in 2016 as spawning cod is not all gathered in a single point location. The comparison of the two ways of sampling the model enables us to consider the effect of vertical shear and spatial extent of the spawning ground on vertical profiles of buoyant eggs in a turbulent environment, particularly whether situations with sub-surface maxima initiated by vertical shear are obscured by horizontal transport between neighboring spawning locations. Since the biophysical model is computationally demanding there is a limited number of particles representing eggs. We therefore test the robustness of our results by comparing with occurrences

of sub-surface maxima requiring a minimum amount of eggs present. The minimum threshold is tested for values of 30, 40 and 50 % of the mean surface egg concentration.

*Analytical vertical profile of NEA cod eggs*

The mean vertical egg concentration  $C(z)$ , from a balance between turbulent mixing and buoyancy of the NEA cod eggs, is given from equation (5) by Sundby (1983):

$$C(z) = C_a e^{-w(z-a)/K} \quad (\text{eq. 1})$$

where  $z$  is depth,  $C_a$  is the known egg concentration at depth  $a$ ,  $K$  the eddy diffusion coefficient and  $w$  the ascending velocity of the eggs.

Here the following values for the variables have been used to calculate a mean vertical egg profile: Depth  $a=1$  m (the surface layer of the model),  $K=0.02$  m<sup>2</sup> s<sup>-1</sup> according to equation (18) in Sundby (1983) with mean wind speed of 7.4 m s<sup>-1</sup> calculated from NORA10 March-May wind,  $w=1$  mm s<sup>-1</sup> from Figure 1 in Sundby (1983) with mean NEA cod egg diameter of 1.4 mm (from Solemdal and Sundby, 1981) and the density difference ( $\Delta\rho$ ) between the ambient water and NEA cod eggs is 1.8 kg m<sup>-3</sup> ( $\rho_{\text{water}} - \rho_{\text{egg}} = 1026.6 - 1024.8$  kg m<sup>-3</sup>).

**Results**

*Observations April 4-7<sup>th</sup> 2016*

Variations in vertical NEA cod egg profiles, including sub-surface maxima, are observed at Henningsværstraumen, one of the main spawning areas of NEA cod, during the cruise 4-7<sup>th</sup> April 2016 (Figure 2). The concurrent mean water salinity increases almost linearly with depth from 33.0 (range 32.7-33.3) at the surface to 33.3 (range 33.1-33.5) PSU at 30 m (Figure S2). Sub-surface maxima (Figure 2a) occur during periods of enhanced northeasterly wind (Figure 2b and 2c).

The maximum concentration of eggs sampled is about 1000 eggs m<sup>-3</sup>. In total, 2991 eggs were staged, whereof 39.0 % were stage 3 (stage 1: 0.3 %, stage 2: 24.1 %, stage 4: 7.8 %, stage 5: 25.8 % and stage 6: 3.0 %). Of the eggs, 75.6 % were stage 3 or older, i.e. older than 5 days (according to the definition by Sundby and Bratland, 1987).

The mean current during the cruise is 0.15 m s<sup>-1</sup> (Figure 2c) which corresponds to a displacement of about 65 km in 5 days. Observed ocean currents at multiple depths display vertical current shear (Figure 2d and 2e). During the calm wind period succeeding a strong south-westerly wind event (April 4<sup>th</sup> 13:00 UTC to April 5<sup>th</sup> 19:00 UTC, Figure 2) the ocean current speeds are below 0.15 ms<sup>-1</sup> and generally increasing with depth bearing southeast. Subsequently the wind strengthens and veers north-easterly (April 5<sup>th</sup> 19:00 UTC to April 6<sup>th</sup> 16:00 UTC, Figure 2) with stronger ocean currents to the south, particularly near the surface. Finally, the winds weaken while maintaining bearing, though the ocean currents turn northeasterly (April 6<sup>th</sup> 16:00 UTC to April 6<sup>th</sup> 16:00 UTC, Figure 2).

*Numerical model March 1<sup>st</sup> – May 20<sup>th</sup>, 1984*

As particles are being released, they rapidly adjust to the modeled ambient density structure and vertical mixing, resulting in profiles with near exponential decrease from the surface to about 30 m (Figure 3). Figure 3a shows all vertical profiles sampled by method 2 (considering all particles independently of where they are initiated), every three hours, at grid cell 28 (approximately the center grid cell, Figure 1), revealing that while the median profile decreases from just below 100 eggs per m<sup>3</sup> at the surface to almost none at 30 m depth, there are incidents when the surface concentrations are an order of magnitude higher. Figure 3b shows that vertical profiles vary

significantly depending on where, within the modeled spawning ground, they are sampled. Profiles at grid cell 28 of the modeled spawning ground on April 17<sup>th</sup> are distinctively different from those at the southern or northern boundary about 12 km away. The time evolution of vertical egg concentration at grid cell 28 shows a large vertical variability with distinct periods of enhanced mixing and eggs distributed deeper e.g. early in March (Figure S3). The focus in this study, however, is on the occurrence of sub-surface maxima (Figure 3c).

Figure 4a resolves occurrences of sub-surface maxima in the upper 20 m of the vertical egg profiles through time and space. In general, the southern grid cells have the most frequent occurrences of sub-surface maxima in egg concentrations (grey dots), while the northern grid cells have the most frequent occurrences if adding the threshold of 40 % described in Materials (red dots). Summarized across all grid cells per time step (Figure 4b) the time series show periods with increased occurrences of sub-surface maxima, and six shorter periods where none of the grid cells have sub-surface maxima (March 9<sup>th</sup> and 21<sup>st</sup>, April 6-7<sup>th</sup>, April 11-13<sup>th</sup>, May 1<sup>st</sup>-3<sup>rd</sup> and May 18<sup>th</sup>). Only counting the particles spawned locally (method 1), thereby not taking into account import of particles from neighboring grid cells, the occurrence of sub-surface maxima increases substantially (Figure S5, without including the threshold). On average over the whole period (March 1<sup>st</sup> to May 20<sup>th</sup>), 38 % of the area of the spawning ground has sub-surface maxima when not allowing import of particles (Figure S5), while 22 % of the spawning ground has sub-surface maxima when allowing import of particles (grey dots in Figure 4a and 4b). The latter number reduces to 10/8/6 % if adding the threshold of 30/40/50 % while all have similar spatial variability (red dots, Figure 4a and 4b). In order to investigate the causes of this variability, concurrent time series of currents at three depths (the spatial mean across the 66 grid cells) and wind at grid cell 28 are analyzed (Figure 4c and 4d).

The sum of occurrences of sub-surface maxima in vertical profiles of egg concentrations (without including the threshold) is correlated with the wind speed and the surface current, where the Pearson linear correlation coefficient  $r$  is 0.63 ( $p < 0.001$ ,  $t = 20.3$ ,  $df = 639$ ) for wind and 0.46 for surface current ( $p < 0.001$ ,  $t = 13.2$ ,  $df = 639$ ). Correlating wind speed directly with the sea surface current gives  $r = 0.73$  ( $p < 0.001$ ,  $t = 27.4$ ,  $df = 639$ ). Testing for time lags between sub-surface maxima and forcing do not result in significant improvements of the correlations (wind;  $r = 0.65$ , surface current;  $r = 0.47$ ). Replacing surface current with current shear represented as the difference between 20 m and surface, or 7 m and surface, results in about the same correlation with sub-surface maxima as for the surface current (20 m;  $r = 0.44$ , 7m;  $r = 0.47$ ).

Sub-surface maxima do not necessarily occur simultaneously throughout all 66 spawning grounds (Figure 4a). Focusing on March 20-30<sup>th</sup> there are at first no sub-surface maxima (March 21<sup>st</sup>) then sub-surface maxima throughout the spawning ground (grey dots, Figure 4a), with a northward sub-surface maximum signal propagating through the spawning ground (red dots, Figure 4a). A progressive vector diagram for grid cell 28 of the same period displays a strong current shear with a varying direction and decreasing strength with depth (Figure 5a). Red dots (Figure 4a) show that a collection of many eggs is advected across the spawning ground but that the near surface ones are continuously shed off due to the shear resulting in sub-surface maxima. Focusing on a second period, April 15-30<sup>th</sup>, there are two distinct periods of enhanced currents above 0.25 m s<sup>-1</sup>, corresponding to similar peaks in wind forcing and sub-surface maxima. Also, the corresponding progressive vector diagram at grid cell 28 shows a vertical velocity shear of decreasing current strength with increasing depths (Figure 5b). Apparent, in Figure 5b, there is also a two-layer stratification with coastal waters on top (here; upper ~25 meters), and Atlantic water below (also seen in lower left panel, Figure S1). Sub-surface maxima appear first along the southern rim of the spawning ground and later also to the north. This suggest that despite that the

velocity shear may result in sub-surface maxima this is delayed to the north because of continuous supply of eggs near the surface from upstream sources. As the source empties, sub-surface maxima appear successively northwards.

Reducing the current shear or introducing a fixed rise velocity of eggs reduce the number of profiles with sub-surface maxima at grid cell 28 (Figure S4, only considering eggs initialized at the same grid cell, method 1). The left panel shows the original number of total profiles between March 1<sup>st</sup> and May 20<sup>th</sup> with sub-surface maxima (262 profiles). The mid panel shows how this number decreases (237 profiles) if moving particles with reduced current velocity shear. Right panel shows further reduction to about half the number of occurrences if only using the constant current (129 profiles). Removing turbulent dynamical vertical positioning of eggs (not shown) and combining with either the modeled currents or the constant current result in either a strong reduction or a complete removal of sub-surface maxima.

### Discussion

Dispersal of buoyant particles depends on their vertical positions and the vertical current shear. Theoretical considerations of vertical distribution provide a mathematical framework for quantifying vertical profiles under various oceanographic conditions, given their individual densities and sizes of the particles (e.g. Sundby, 1983; Thorpe, 1984). Concentrations of such particles decreases exponentially with depth, where the vertical gradient depends on the buoyancy of the particles and the ambient level of turbulence in the water column. Occasionally, we measure vertical profiles of buoyant particles in the field, in this case Northeast Arctic cod eggs, that differ from the vertical diffusion-buoyancy balance and instead display sub-surface maxima. This is not because theory is proven wrong, but because additional horizontal processes are interacting.

Our main hypothesis is that the deviations in the vertical profiles from the diffusion-buoyancy balance are caused by the combination of vertical velocity shear and strong horizontal gradients in egg concentrations around a spawning ground. Both conditions are observed by extensive measurement campaigns, as reported here and previously (Sundby and Bratland, 1987). From the observations in 2016, about 3/4 of all staged eggs are older than 5 days corresponding to a maximum drift distance of 50 -100 km with currents of  $0.15 \text{ m s}^{-1}$ . Strong horizontal gradients and the presence of older eggs therefore support previous findings that Henningsværstraumen is characteristically a retention area compared to spawning grounds outside Lofoten (Sundby and Bratland, 1987), though older eggs may also originate from spawning grounds elsewhere. Since there is sparse spatial information from observational cruises to analyze, we constructed a spawning season where we perform an extensive egg survey in a numerical model. We demonstrated that there is large variability in the egg profiles, with sub-surface maxima occurring transiently during periods of otherwise exponential decaying concentrations of eggs.

The mean occurrence of sub-surface maxima is 22 % over the whole period when accounting for import of eggs from neighboring spawning grounds. If only accounting for eggs spawned at the site sampled, the mean occurrence increases to 38 % illustrating that spawning grounds with a limited horizontal extent have a higher propensity of exhibiting sub-surface maxima in egg concentration. Including the egg concentration threshold illustrates that a signal of sub-surface maxima should be treated with care if there are low numbers of egg sampled. By investigating periods of increased occurrences of sub-surface maxima against the wind forcing and ocean currents we find that both factors favor sub-surface maxima, in particular periods of persistent forcing or after sudden transitions in the direction. We find a significant correlation

between the time series of wind speed or surface current speed and the occurrence of sub-surface maxima. Considering time lags between wind, currents and sub-surface maxima did not give significant improvement but indicates that wind and currents may lead sub-surface maxima by a few hours. A model study with higher temporal resolution would enable a more decisive answer. There is lower correlation with sub-surface maxima against surface current ( $r=0.46$ ) than sub-surface maxima and wind speed ( $r=0.63$ ), which seems counter-intuitive considering that the ocean current is the direct forcing. However, the wind represents the transient energy exerted on a relatively large area affecting vertical distribution of eggs through several physical processes including ocean currents and turbulence. Contrary, measured and modeled ocean currents represent dispersion and shear on a scale smaller than the size of the spawning ground here represented by 66 grid cells. Hence, even within these spawning cells the currents vary, and the mean current across the spawning ground therefore correlate less with sub-surface maxima than with wind.

A sensitivity test shows that with a constant horizontal flow and no vertical dynamical positioning due to turbulence there will be no sub-surface maxima. However, increasing the strength of the horizontal flow or reducing the width of the sampled water column will eventually result in sub-surface maxima because eggs are moved outside the sampling area before they surface. In reality, turbulence opposes this as it contributes to erase vertical gradients introduced by spawning at depth and join forces with buoyancy moving eggs towards the surface.

#### *Other processes potentially causing sub-surface maxima*

A vertically varying eddy diffusivity coefficient  $K(z)$  may affect the rate at which particles are redistributed vertically if introduced at a certain depth but cannot cause a vertical gradient of particle concentrations unless the particle density is lower than the ambient water density (e.g. Thygesen and Ådlandsvik, 2007). Hence, a high level of turbulence near the sea surface cannot cause egg aggregation immediately below but combined with low numbers of eggs this may happen by chance because of their turbulence-induced dynamical induced distribution. This is supported by the sensitivity analyses quantifying occurrences of sub-surface maxima with and without turbulence. Increased wind forcing results in increased vertical mixing in the ocean causing buoyant particles to be mixed down through the water column. Compared to calm conditions the concentrations of eggs still decrease near exponentially with depth, but to a much lower degree. As the wind forcing dies off and the mixing level ceases, buoyant eggs start to rise towards the surface. For example, NEA cod eggs in Henningsværstraumen mixed down to 10 m depth will rise towards the surface within the next  $\sim 3$  hours, assuming a typical ascending velocity of  $1 \text{ mm s}^{-1}$ . If a strong salinity structure re-establishes before the eggs have reached a new vertical profile, eggs rise faster at depth than near surface because the buoyancy decreases. Altogether, this may cause transient sub-surface maxima in eggs.

Egg densities vary, as mentioned in the section *NEA cod eggs as oceanographic drifters*, where the neutral buoyancy expressed in salinities ranges from 29.5 to 33.0 PSU (Solemdal and Sundby, 1981). From CTD profiles in 2016 (Figure S2), the mean salinity observed in the surface layer is between 32.7 and 33.3 PSU, which is the upper neutral buoyancy range of the NEA cod eggs. This makes 5.1 % of the eggs potentially negatively buoyant (heavier than the ambient water masses) and able to sink creating sub-surface maxima. The two lightest salinity profiles correspond to the egg profiles #304 and #305. Since there is low number of eggs sampled here these measurements may be sensitive to the pump measurement technique. At profile #306, #310 and #315, however, there are higher numbers of eggs sampled experiencing sub-surface maxima.

Since the salinity is above 33.1 PSU for these profiles, the sub-surface maxima signals cannot be explained by buoyancy differences in the eggs, and other physical processes must be responsible.

Newly spawned eggs will attain a vertical equilibrium distribution within about 24 hours, depending on the induced mixing (using eq. 1, see Sundby, 1983 and 1991). Hence, a sub-surface maximum could be observed for newly spawned eggs (Sundby 1991), but only for a short time period in the beginning of the spawning season making it an unlikely process to be observed.

Langmuir cells created by Stokes drift (induced by the presence of surface waves) potentially cause inhomogeneous mixing (Grant and Belcher, 2009, Belcher et al, 2012, Harcourt, 2013), but only in narrow bands of the ocean making it unlikely that they will actually be observed during the time period it takes to measure the vertical egg profiles.

Air bubbles are introduced into the upper ocean when waves break, giving a theoretical possibility, if the air bubbles are small enough and high enough in numbers, to affect the density of the water column. This effect is confined to the upper few meters, on a vertical scale comparable to the significant wave height (Scanlon et al, 2016). However, upper concentration estimations of air bubbles with diameter  $>10 \mu\text{m}$  are  $10^6 \text{ m}^{-3}$  (Zhang et al., 2010). With cod eggs of 1 mm, this gives approximately 1/1000 bubble per egg volume which is too low to change the buoyancy of the individual eggs.

Selective predation on NEA cod eggs in Vestfjorden could be by planktonic predators in the upper water column, with Norwegian Spring-Spawning herring and jellyfish being potential candidates during this time of the year (March-April). The massive numbers of predators needed in the upper 5 m of the water column in order to reduce the egg concentration significantly in a short enough period of time makes this unlikely.

The available turbulence schemes in ROMS are forced by the boundary condition to give turbulent diffusivities that approach zero at the surface (Umlauf and Burchard, 2003; Röhrs et al., 2014). This gives a bias in the upper layer compared to the analytical solution as diffusivity is underestimated. In turn, this causes too many cod eggs at or near the surface counteracting the presence of sub-surface maxima in the model as compared to observations. Sperrevik et al. (2017) found that with data assimilation in the GCM the water column becomes more stratified so that a shallower part of the water column responds to wind forcing exerted at the surface. Again, a higher spatial resolution in the GCM both vertically and horizontally would provide added details on the dynamical manifestations of wind forcing on the upper ocean.

## Conclusion

Observations from a cruise in Lofoten, Norway, in 2016 reveal transient sub-surface maxima in NEA cod egg profiles consistent with previous observations. Our main hypothesis is that this is caused by spatially limited spawning grounds and the presence of vertical current shear. By running a high-resolution model with assimilation of available hydrographic data we were able to reproduce sub-surface maxima and relate this to wind stress and vertical current shear. An idealized sensitivity analysis shows that if vertical current shear is gradually reduced for egg dispersal from a spatially limited spawning ground then the occurrence of sub-surface maxima also decays and eventually disappear, supporting our main hypothesis.

## References

Ådlandsvik, B. and S. Sundby. 1994. Modelling the transport of cod larvae from the Lofoten area. ICES Mar. Sci. Symp. 198: 379-392.

- Albretsen, J., A. K. Sperrevik, A. Staalstrøm, A. D. Sandvik, F. Vikebø, and L. Asplin. 2011. NorKyst-800 report no. 1: User manual and technical descriptions, Tech. Rep. 2. Institute of Marine Research, Bergen, Norway, available at: [http://www.imr.no/filarkiv/2011/07/fh\\_2-2011\\_til\\_web.pdf/nb-no](http://www.imr.no/filarkiv/2011/07/fh_2-2011_til_web.pdf/nb-no)
- Beldring, S., K. Engeland, L. A. Roald, N. R. Sælthun and A. Voksø. 2003. Estimation of parameters in a distributed precipitation-runoff model for Norway. *Hydrol. Earth Syst. Sci.* 7: 304–316, doi:10.5194/hess-7-304-2003
- Belcher, S. E., and others. 2012. A global perspective on Langmuir turbulence in the ocean surface boundary layer. *Geophys. Res. Lett.* 39, doi:10.1029/2012GL052932
- Checkley, Jr, D. M., P. B. Ortner, L. R. Settle, and S. R. Cummings. 1997. A continuous, underway fish egg sampler. *Fish. Oceanogr.* 6(2): 58-73, doi:10.1046/j.1365-2419.1997.00030.x
- Egbert, G. D., and S. Y. Erofeeva. 2002. Efficient Inverse Modeling of Barotropic Ocean Tides. *J. Atmos. Oceanic Tech.* 19(2): 183–204, doi:10.1175/1520-0426(2002)019<0183:EIMOBO>2.0.CO;2
- Ellertsen, B., G. K. Furnes, P. Solemdal, and S. Sundby. 1981a. “Influence of wind-induced currents on the distribution of cod eggs and zooplankton in Vestfjorden”, p. 604-628. In R. Sætre and M. Mork [eds.], *The Norwegian Coastal Current*. University of Bergen.
- Ellertsen, B., P. Solemdal, T. Strømme, S. Sundby, S. Tilseth, T. Westgård and V. Øiestad. 1981b. Spawning period, transport and dispersal of eggs from the spawning area of Arcto-Norwegian cod (*Gadus Morhua* L.). *Rapp. P.-v. Réun. Cons. Int. Explor. Mer.* 178: 260-267.
- Ellertsen, B., P. Fossum, P. Solemdal, S. Sundby, and S. Tilseth. 1984. A case study of the distribution of cod larvae and availability of prey organisms in relation to physical processes in Lofoten, p. 453-477. In E. Dahl, D. S. Danielssen, E. Moksness and P. Solemdal [eds.], *The propagation of cod *Gadus morhua* L.* Flødevigen Rapportser.
- Ellertsen, B., P. Fossum, P. Solemdal, and S. Sundby. 1989. Relation between temperature and survival of eggs and first-feeding larvae of Northeast Arctic cod (*Gadus morhua* L.). *Rapp. P.-v. Réun. Cons. Int. Explor. Mer.* 191: 209-219.
- Folkvord, A. 2007. Erratum: Comparison of size-at-age of larval Atlantic cod (*Gadus morhua*) from different populations based on size- and temperature-dependent growth models. *Can. J. Fish. Aquat. Sci.* 64: 583-585, doi:10.1139/f07-045
- Grant, A. L., and S. E. Belcher. 2009. Characteristics of Langmuir turbulence in the ocean mixed layer. *J. Phys. Oceanogr.*, 39: 1871-1887, doi:10.1175/2009JPO4119.1

- Haidvogel, D. B., and others. 2008. Ocean forecasting in terrain-following coordinates: Formulation and skill assessment of the Regional Ocean Modeling System. *J. Comput. Phys.* 227: 3595-3624, doi:10.1016/j.jcp.2007.06.016
- Harcourt, R. 2013. A Second-Moment Closure Model of Langmuir Turbulence *J. Phys. Oceanogr.* 43: 673-697, doi:10.1175/JPO-D-12-0105.1
- Hidalgo, M., Y. Gusdal, G. E. Dingsør, D. Hjermmann, G. Ottersen, L. C. Stige, A. Melsom, and N. C. Stenseth. 2011. A combination of hydrodynamical and statistical modelling reveals non-stationary climate effects on fish larvae distributions. *Proc. R. Soc. B.* 279: 275-283, doi:10.1098/rspb.2011.0750
- Hjort, J. 1914. Fluctuations in the great fisheries of northern Europe viewed in the light of biological research. *Rapp. P.-v. Réun. Cons. Int. Explor. Mer.* 20: 1-228.
- Jones, C. E., and others. 2016. Measurement and modeling of oil slick transport. *J. Geophys. Res. Oceans* 121: 7759-7775, doi:10.1002/2016JC012113
- Jung, K.-M., A. Folkvord, O. S. Kjesbu, A. L. Agnalt, A. Thorsen, and S. Sundby. 2012a. Egg buoyancy variability in local populations of Atlantic cod (*Gadus morhua* L.). *Mar. Biol.* 159: 1969-1980, doi:10.1007/s00227-012-1984-8.
- Jung, K.-M., A. M. Svardal, T. Eide, A. Thorsen, and O. S. Kjesbu. 2012b. Seasonal trends in adenylate nucleotide content in eggs of recruit and repeat spawning Atlantic cod (*Gadus morhua* L.) and implications for egg quality and buoyancy. *J. Sea Res.* 73: 63-73, doi:10.1016/j.seares.2012.06.007
- Jung, K.-M., A. Folkvord, O. S. Kjesbu, and S. Sundby. 2014. Experimental Parameterisation of Principal Physics in Buoyancy Variations of Marine Teleost Eggs. *PLoS ONE* 9: e104089, doi:10.1371/journal.pone.0104089
- Kjesbu, O. S., D. Righton, M. Krüger-Johnsen, A. Thorsen, K. Michalsen, M. Fonn, and P. R. Witthames. 2010. Thermal dynamics of ovarian maturation in Atlantic cod (*Gadus morhua*). *Can. J. Fish. and Aquat. Sci.* 67: 605-625, doi: 10.1139/F10-011
- Lebreton, L. C.-M., S. D. Greer, and J. C. Borrero. 2012. Numerical modelling of floating debris in the world oceans. *Mar. Pollut. Bull.* 64: 653-661, doi:10.1016/j.marpolbul.2011.10.027
- Lien, V. S., Y. Gusdal, and F. B. Vikebø. 2014. Along-shelf hydrographic anomalies in the Nordic Seas (1960-2011): locally generated or advective signals? *Ocean Dyn.* 64: 1047-1059, doi:10.1007/s10236-014-0736-3
- Ottersen, G., B. Bogstad, N. A. Yaragina, L. C. Stige, F. B. Vikebø, and P. Dalpadado. 2014. A review of early life history dynamics of Barents Sea cod (*Gadus morhua*). *ICES J. Mar. Sci.* 71: 2064-2087, doi:10.1093/icesjms/fsu037

- Paris, C. B., M. Le Hénaff, Z. M. Aman, A. Subramanian, J. Helgers, D.-P. Wang, V. H. Kourafalou, and A. Srinivasan. 2012. Evolution of the Macondo Well Blowout: Simulating the Effects of the Circulation and Synthetic Dispersants on the Subsea Oil Transport. *Environ. Sci. Technol.* 46: 13293-13302, doi:10.1021/es303197h
- Reistad, M., Ø. Breivik, H. Haakenstad, O. J. Aarnes, B. R. Furevik, and J.-R. Bidlot. 2011. A high-resolution hindcast of wind and waves for the North Sea, the Norwegian Sea, and the Barents Sea. *J. Geophys. Res.* 116: C05019, doi:10.1029/2010JC006402
- Röhrs, J., K. H. Christensen, F. Vikebø, S. Sundby, Ø. Sætra, and G. Broström. 2014. Wave-induced transport and vertical mixing of pelagic eggs and larvae. *Limnol. Oceanogr.* 59: 1213-1227, doi:10.4319/lo.2014.59.4.1213
- Scanlon, B., Ø. Breivik, J.-R. Bidlot, P. Janssen, A. H. Callaghan, and B. Ward. 2016. Modelling whitecap fraction with a wave model. *J. Phys. Oceanogr.*, 46: 887-894, doi:10.1175/JPO-D-15-0158.1
- Shchepetkin, A. F., and J. C. McWilliams. 2005. The regional oceanic modeling system (ROMS): a split-explicit, free-surface, topography-following-coordinate oceanic model. *Ocean Model.* 9(4): 347-404, doi:10.1016/j.ocemod.2004.08.002
- Solemdal, P., and S. Sundby. 1981. Vertical distribution of pelagic fish eggs in relation to species, spawning behavior and wind conditions. *ICES C. M./G.* 77: 1-27. (Mimeo)
- Sperrevik, A. K., J. Röhrs, K. H. Christensen. 2017. Impact of data assimilation on Eulerian versus Lagrangian estimates of upper ocean transport. *J. Geophys. Res. Oceans.* 122: 5445-5457, doi:10.1002/2016JC012640
- Stenevik, E. K., S. Sundby, and A.L. Agnalt. 2008 Buoyancy and vertical distribution of Norwegian coastal cod (*Gadus morhua*) eggs from different areas along the coast. *ICES J. Mar. Sci.* 65: 1198-1202, doi:10.1093/icesjms/fsn101
- Strand, K. O., S. Sundby, J. Albretsen, and F. B. Vikebø. 2017. The Northeast Greenland shelf as a potential habitat for the Northeast Arctic cod. *Frontiers Mar. Sci.* 4: 304, doi: 10.3389/fmars.2017.00304
- Stratoudakis, Y., M. Bernal, K. Ganas, and A. Uriarte. 2006. The daily egg production method: recent advances, current applications and future challenges. *Fish and Fisheries.* 6: 35-57, doi:10.1111/j.1467-2979.2006.00206.x
- Strømme, T. 1977. Torskelarvens lengde ved klekking, og virkning av utsulting på larvens egenvekt og kondisjon. En eksperimentell undersøkelse på norsk-arktisk torsk (*Gadus morhua*) [An experimental study on Norwegian-Arctic cod *Gadus morhua*]. Cand.real. thesis. Univ of Bergen.

Sundby, S. 1983. A one-dimensional model for the vertical distribution of pelagic fish eggs in the mixed layer. *Deep-Sea. Res.* 30: 645-661, doi:10.1016/0198-0149(83)90042-0

Sundby, S., and P. Bratland. 1987. Kartlegging av gytefeltene for norsk-arktisk torsk i Nord-Norge og beregning av eggproduksjonen i årene 1983-1985 [spatial distribution and production of eggs from Northeast-arctic cod at the coast of Northern Norway 1983-1985]. Report series Fiskeri og Havet. Institute of Marine Research, Bergen. 1: 1-58.

Sundby, S., and P. Fossum. 1990. Feeding conditions of Arcto-norwegian cod larvae compared with the Rothschild-Osborn theory on small-scale turbulence and plankton contact rates. *J. Plankton Res.* 12: 1153-1162.

Sundby, S. 1991. Factors affecting the vertical distribution of eggs. *ICES Mar. Sci. Symp.* 192: 33-38.

Sundby, S., B. Ellertsen, and P. Fossum. 1994. Encounter rates between first-feeding cod larvae and their prey during moderate to strong turbulent mixing. *ICES. Mar. Sci. Symp.* 198: 393-405.

Sundby, S., and T. Kristiansen. 2015. The Principles of Buoyancy in Marine Fish Eggs and Their Vertical Distributions across the World Oceans. *PLoS ONE* 10: e0138821, doi:10.1371/journal.pone.0138821

Sundby, S., and O. Nakken. 2008. Spatial shifts in spawning habitats of Arcto-Norwegian cod related to multidecadal climate oscillations and climate change. *ICES J. Mar. Sci.* 65: 953-962, doi:10.1093/icesjms/fsn085

Sundnes, G., H. Leivestad, O. Iversen. 1965. Buoyancy determination of eggs from the cod (*Gadus morhua* L.). *J. Cons. Int. Explor. Mer.* 29: 249-252.

Thorpe, S. A. 1984. A Model of the Turbulent Diffusion of Bubbles below the Sea Surface. *J. Phys. Oceanogr.* 14: 841-854.

Thygesen, U. H., and B. Ådlandsvik. 2007. Simulating vertical turbulent dispersal with Finite Volumes and Binned Random Walks. *Mar. Ecol. Prog. Ser.* 347: 145-153, doi:10.3354/meps06975

Umlauf, L., and H. Burchard. 2003. A generic length-scale equation for geophysical turbulence models. *J. Mar. Res.* 61: 235-265, doi: 10.1357/002224003322005087

Umlauf, L., H. Burchard, and K. Hutter. 2003. Extending the  $k-\omega$  turbulence model towards oceanic applications. *Ocean Model.* 5: 195-218, doi: 10.1016/S1463-5003(02)00039-2

Vikebø, F. B., S. Sundby, B. Ådlandsvik, and Ø. Fiksen. 2005. The combined effect of transport and temperature on distribution and growth of larvae and pelagic juveniles of Arcto-Norwegian cod. *ICES J. Mar. Sci.* 62: 1375-1386, doi:10.1016/j.icesjms.2005.05.017

Vikebø, F. B., C. Jørgensen, T. Kristiansen, and Ø. Fiksen. 2007. Drift, growth, and survival of larval Northeast Arctic cod with simple rules of behaviour. *Mar. Ecol. Prog. Ser.* 347: 207-219, doi:10.3354/meps06979

Vikebø, F. B., P. Rønningen, V. S. Lien, S. Meier, M. Reed, B. Ådlandsvik and T. Kristiansen. 2013. Spatio-temporal overlap of oil spills and early life stages of fish. *ICES J. Mar. Sci.* 71: 970-981, doi:10.1093/icesjms/fst131

Warner, J. C., C. R. Sherwood, H. G. Arango, and R. P. Signell. 2005. Performance of four turbulence closure models implemented using a generic length scale method. *Ocean Model.* 8: 81-113, doi:10.1016/j.ocemod.2003.12.003

Zhang, X. E. Boss, and L. Taylor. 2010. Optical Constituents of the Ocean. Air Bubbles. In C. Mobley, E. Boss, and C. Roesler. [eds.], *Ocean Optics Web Book*.

#### **Acknowledgments**

The authors gratefully acknowledge our colleagues and the crew members onboard R/V Johan Hjort for the help collecting the observed data. We also thankfully appreciate the constructive and valuable comments of two anonymous reviewers. K. O. Strand received funding by the Research Council of Norway through the RETROSPECT project (grant 244262).

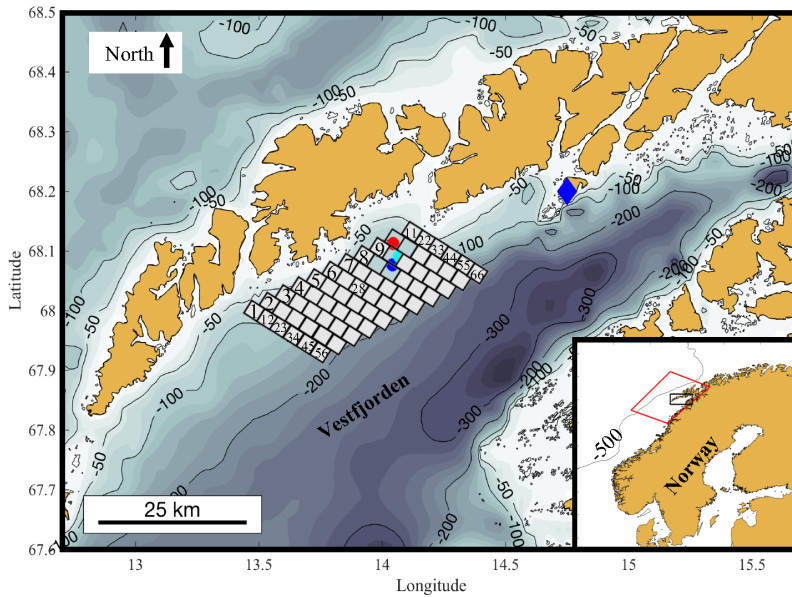


**Figure 1:** Area of interest (black box, lower right corner). The model boundary is indicated as a red box (lower right corner). The modeled spawning ground in the 1984 model run (black squares) represents 66 grid cells where Northeast Arctic cod eggs are initiated (partly numbered). The location for observed wind, the weather station, Skrova Lighthouse, is marked with a blue diamond. Bottom contour lines of -50, -100, -200, -300 and -500 m is in black, while every 20 m between are in shaded blue. The observed vertical egg profiles in 2016 are marked at three different locations (#281 and 287 (blue), #293, 304 and 305 (red), #306, 310, 315 and 316 (cyan)).

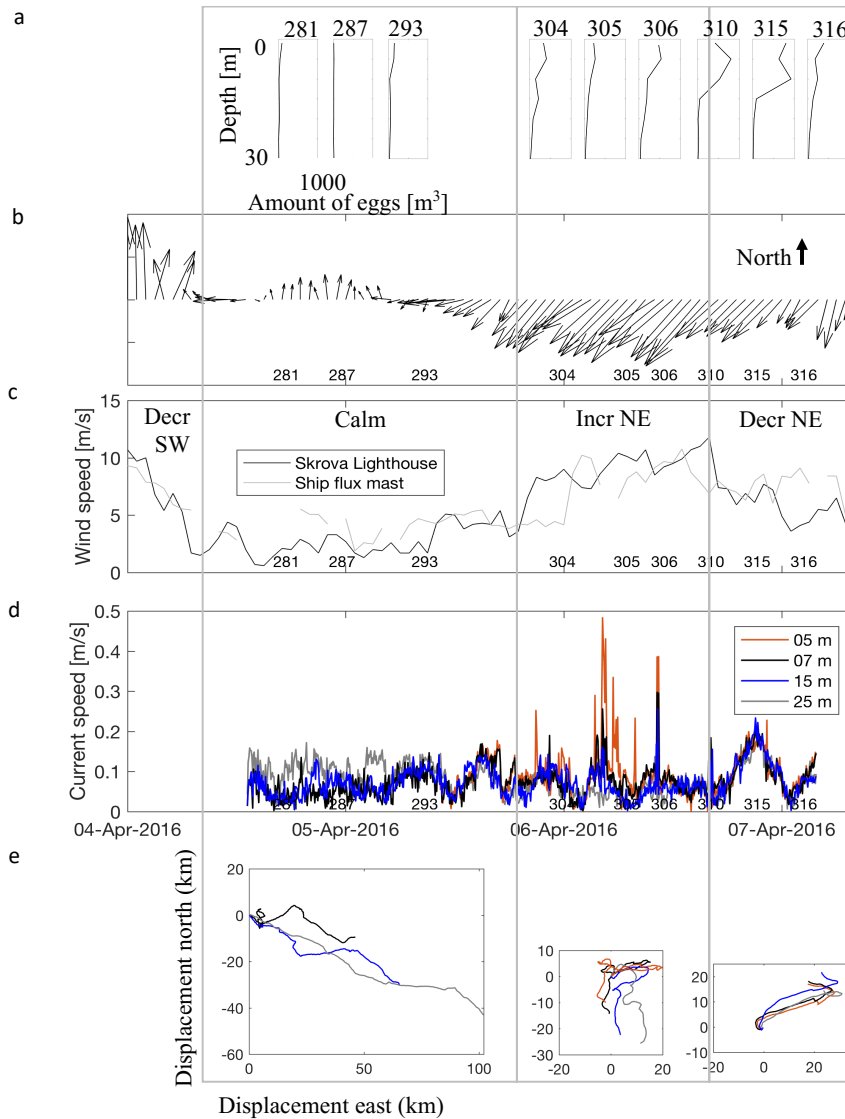


**Figure 2:** Observations from a scientific survey at Henningsværstraumen April 4-7<sup>th</sup> 2016. (a) Observed vertical Northeast Arctic cod pump profiles with stations labeled. Stations are marked at the time-axis in (b-d). (b) Observed wind direction and (c) wind speed from the weather station *Skrova Lighthouse*. Three different wind situations (south-westerly (SW) and north-easterly (NE)) are marked with boxes through the figure; April 4<sup>th</sup> 08:00 - 5<sup>th</sup> 19:00, April 5<sup>th</sup> 19:00 - 6<sup>th</sup> 16:00 and April 6<sup>th</sup> 16:00 - 7<sup>th</sup> 08:00. (d) Observed current speed measurements from the mooring site at different depths (see legend) including (e) progressive vector diagrams separated into the three different wind periods.

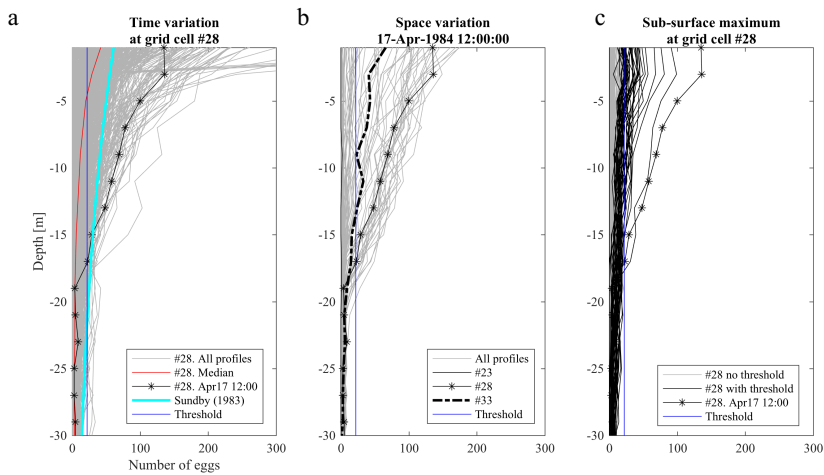


**Figure 3.** Modeled vertical egg profiles. The egg profile at grid cell 28 April 17<sup>th</sup> (black line with dots) and the egg concentration threshold (blue vertical line, see text for explanation) are marked in all panels (a, b and c). (a) All modeled profiles (grey lines) at grid cell 28, with the median profile (red line) and profile according to eq. 1 (cyan line) by Sundby (1983). (b) All profiles April 17<sup>th</sup> (grey lines). Grid cell 33 (black broken line) and 23 (black line) reflect 12 km north and south of grid cell 28, respectively. (c) Profiles at grid cell 28 with sub-surface maxima, above (black lines) and below (grey lines) the egg concentration threshold.

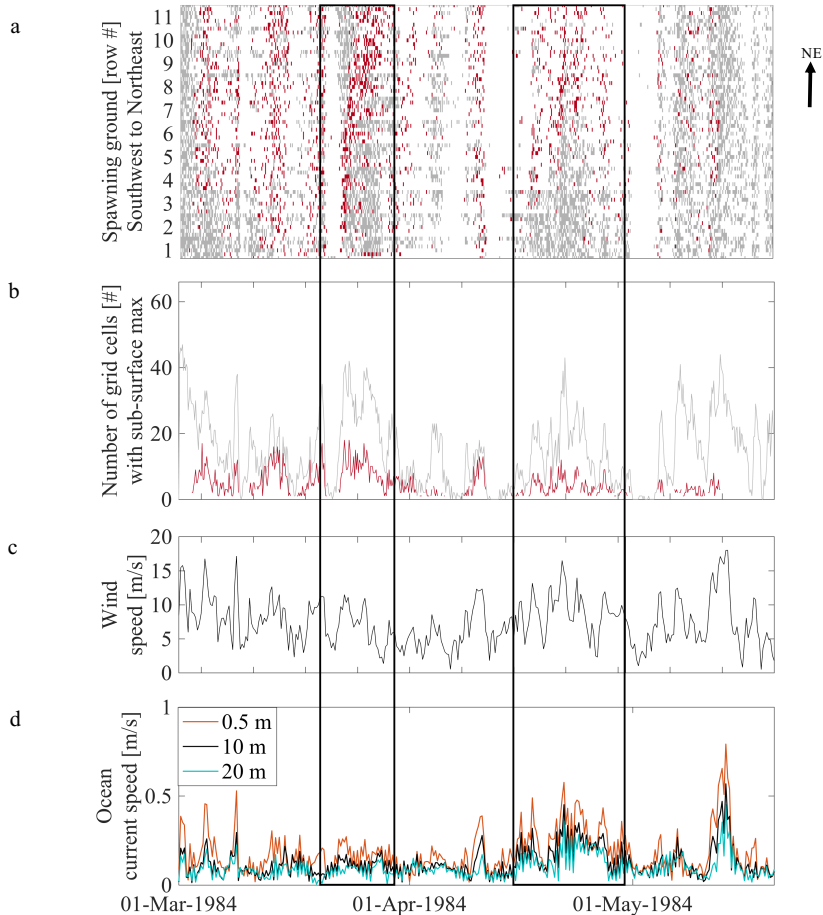


**Figure 4.** Model results March 1<sup>st</sup> to May 20<sup>th</sup>, 1984. Two focus periods (March 20-30<sup>th</sup> and April 15-30<sup>th</sup>) are marked with boxes through the figure. (a) Occurrences of sub-surface maxima in the upper 20 m as a function of the 66 grid cells through time. All particles present within each grid cell (2.4 by 2.4 km) are considered. The grey and red boxes both indicate sub-surface maxima, but the red boxes also have egg concentration above a threshold (see explanation in text). The y-axis is only labeled with grid row numbers sorted northeastward through the spawning ground (Figure 1) with direction indicated with arrow on the right side. In addition, the black bold horizontal line marks the location of grid cell 28. (b) The sum of occurrence of sub-surface maximum through time from panel a) with same color coding. (c) Wind speed (NORA10) every 6 hour at grid cell 28. (d) The spawning ground spatial mean current speed every 6 hour for depths 0.5 m (model surface layer), 10 m and 20 m with colors identified in legend.

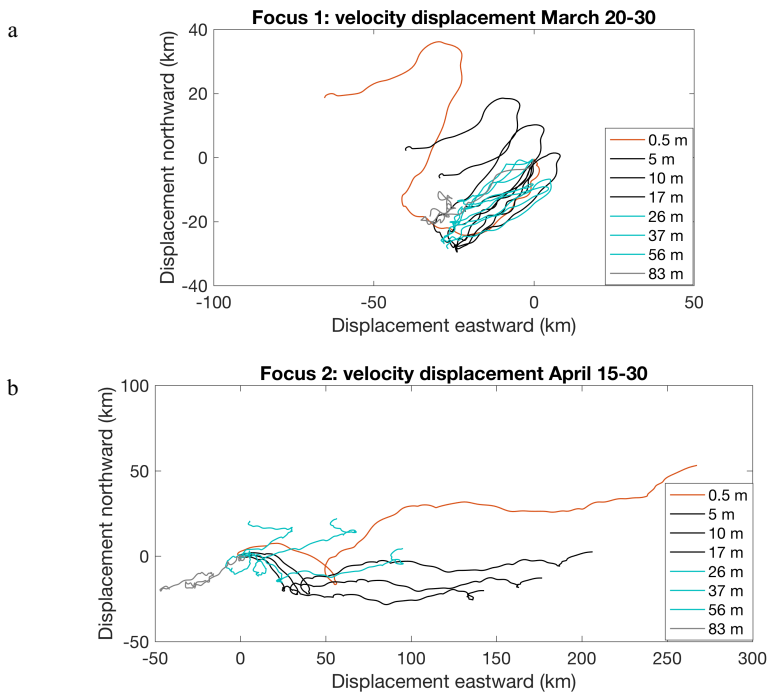


**Figure 5.** Modeled progressive vector diagram at different depths (see legend) at grid cell 28 of the two focus periods marked in Figure 4. (a) Period from March 20-30<sup>th</sup> and (b) from April 15-30<sup>th</sup>.

## Supplemental Information

### *Model evaluation using horizontal cod egg observations in 1984*

An evaluation of the modeled ocean circulation comparing two model realizations, with and without data assimilation, against in situ measurements of Northeast Arctic (NEA) cod eggs from observational cruises in 1984 is presented (Figure S1). As mentioned in the Introduction, both forces in the ocean and the buoyancy of particles depend on the density structure of the water column. As a consequence, it is crucial for the ocean models, used in forecasting transport of planktonic organisms or pollutants, to accurately resolve the vertical structure of temperature and salinity as well as having correct forcing by wind, tides and waves. By assimilating in-situ observations Sperrevik et al. (2017) show that the density structure is much improved in Vestfjorden, particularly for the upper ocean. We ran an individual-based biophysical particle-tracking model with current fields from ROMS integrations with and without data assimilation to compare modeled and observed egg distributions. This allows for an evaluation of the model's ability to realistically represent horizontal egg dispersal, which is essential to our main hypothesis discussed in this manuscript. Note that the modeled spawning ground is based on one main site. In reality, there are also additional sites of spawning in the area (see more details in Sundby and Bratland (1987)). This will affect the horizontal coverage of eggs in the model compared to observations, but the difference between the two model realizations can still be evaluated.

One model realization is simply a down-scaling of the SVIM archive from 4 km to 2.4 km (SVIM-DS), while the other is a realization generated by the use of four-dimensional variational (SVIM-4Dvar) data assimilation (Sperrevik et al., 2017) using hydrographical observations from a particular extensive field campaign performed by IMR in the main spawning area for NEA cod, the Vestfjorden, in 1984 (Sundby and Bratland, 1987) as well as satellite sea surface temperature. The ocean model improves significantly when assimilating observations (Sperrevik et al. 2017) and this is reflected in the ability to reproduce the observed dispersal pattern of NEA cod eggs as shown Figure S1.

The main difference between the two model realizations are the different vertical structure in the hydrography. The hydrography in SVIM-DS is approximately homogenous (one layer) inside Vestfjorden, both in temperature and salinity, compared to the hydrography in SVIM-4Dvar showing a two-layer stratification, with fresher and colder surface water on top of saltier and warmer Atlantic water below (Figure S1, left panels) consistent with observations. The effect can be seen in the different spatial distributions of stage-2 eggs where the eggs are more spread out in a dynamic pattern, including advection by larger eddies, when forced with SVIM-4Dvar compared to when forced with SVIM-DS (Figure S1, middle panels). Observed spatial distribution for stage-2 eggs (Figure S1 right panel; this is Figure 24 in Sundby and Bratland (1987)) resembles the spatial characteristics of the SVIM-4Dvar model realization. This is due to the two-layer stratification, reducing the depth of the wind mixing leading to a shallower layer responding to the wind forcing and consequently an increased response to the wind (also noted by Sperrevik et al., (2017)). The same can be concluded by looking into the difference in vertical distribution of NEA cod eggs (not shown), where there is less eggs mixed down in the SVIM-DS model realization compared to SVIM-4Dvar results.

**References**

Sperrevik, A. K., J. Röhrs, K. H. Christensen. 2017. Impact of data assimilation on Eulerian versus Lagrangian estimates of upper ocean transport. *J. Geophys. Res. Oceans.* 122: 5445-5457, doi:10.1002/2016JC012640

Sundby, S., and P. Bratland. 1987. Kartlegging av gytefeltene for norsk-arktisk torsk i Nord-Norge og beregning av eggproduksjonen i årene 1983-1985 [spatial distribution and production of eggs from Northeast-arctic cod at the coast of Northern Norway 1983-1985]. *Fisken Hav.* 1: 1-58.

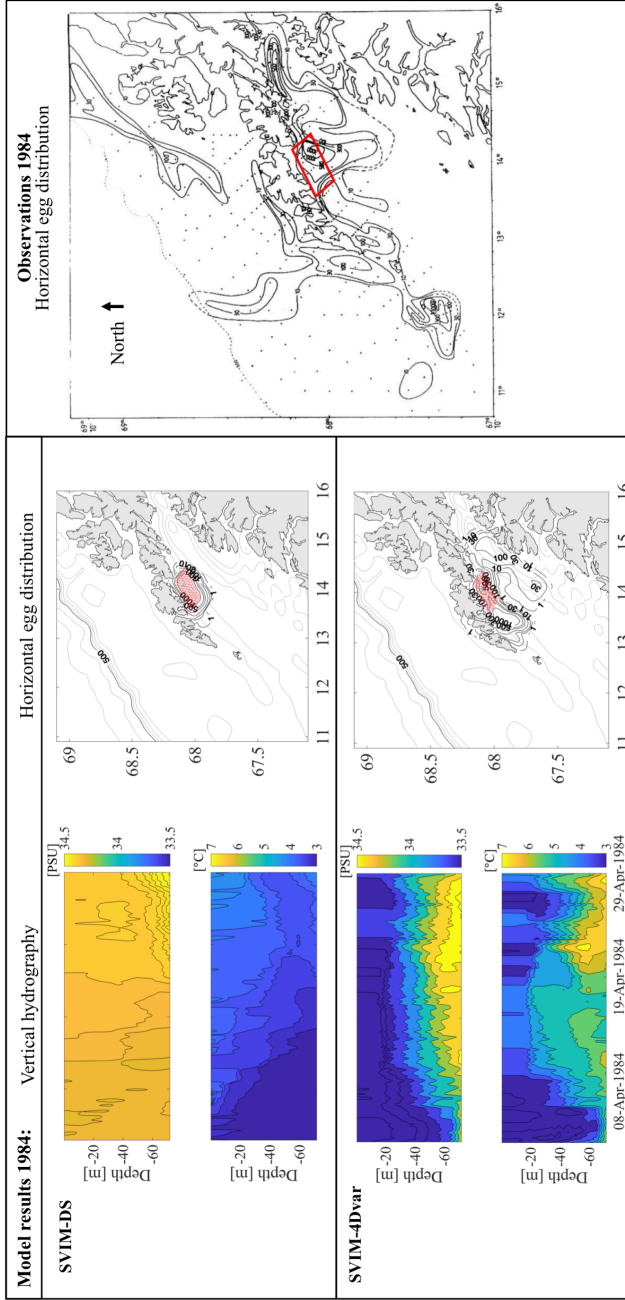


**Figure S1:** Left: Vertical hydrography, both salinity and temperature of two model set-up of ROMS; only down-scaled archive (SVIM-DS) and down-scaled SVIM archive including data assimilation (SVIM-4Dvar). Middle: The resulting difference in horizontal distribution of stage 2 eggs between April 2-9<sup>th</sup> 1984 using the two different model runs. Cyan star marks the location where temperature and salinity are taken (panels on left side). The red boxes are the modeled spawning ground, split into individual grid cells (each 2.4 x 2.4 km). The contour lines 1, 10, 30, 100, 300, 500, and 1000 eggs m<sup>-3</sup> are labeled, to be comparable to the observations from Sundby and Bratland (1987). Right: Distribution of stage 2-eggs observed between April 2-9<sup>th</sup> 1984. The contour lines (10, 30, 100, 300, 500, 1000 and 3000 eggs m<sup>-3</sup>) were drawn by evaluating both observed egg concentrations and hydrography from the same survey. Black dots mark the survey stations of 1984. The figure is taken (with permission) from Sundby and Bratland (1987). The hydrographic observations from this survey are incorporated in the SVIM-4Dvar model run (see lower left figure). The red box plotted on top is to illustrate the modeled spawning area used in the mid panels reproducing the horizontal stage 2-egg distribution.

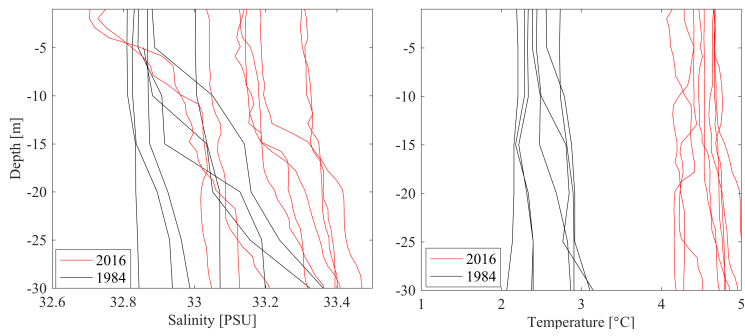


**Figure S2:** Observed temperature and salinity profiles between April 1<sup>st</sup> -7<sup>th</sup> in Vestfjorden, Norway, in 1984 (black lines) and 2016 (red lines). All profiles are taken within the same radius as the three observational dots in Figure 1.

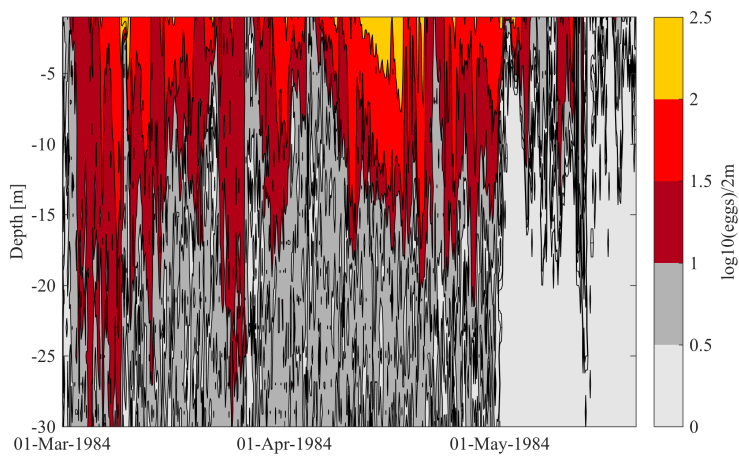


**Figure S3:** The time evolution of the vertical structure of cod eggs (using 2.4 km x 2.4 km ROMS archive including four-dimensional variational data assimilation) at grid cell 28 (approximately the center of spawning area, see Figure 1) allowing advection from the whole spawning ground.

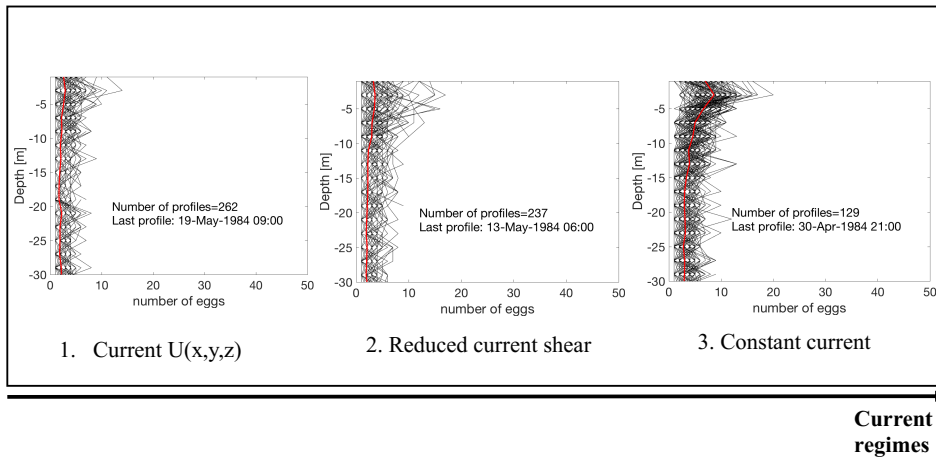


**Figure S4:** Sensitivity study. All vertical egg profiles sampled at grid cell 28 with sub-surface maxima (black lines) including the mean (red line) between March 1<sup>st</sup> and May 20<sup>th</sup>. The total number of profiles are written within the panels, as well as the last date experiencing sub-surface maxima. Particles are moved by three different current regimes; (1) fully resolved current using 2.4 km x 2.4 km ROMS archive including four-dimensional variational data assimilation, (2) reduced current velocity shear, and (3) constant speed of 1 cms<sup>-1</sup>.

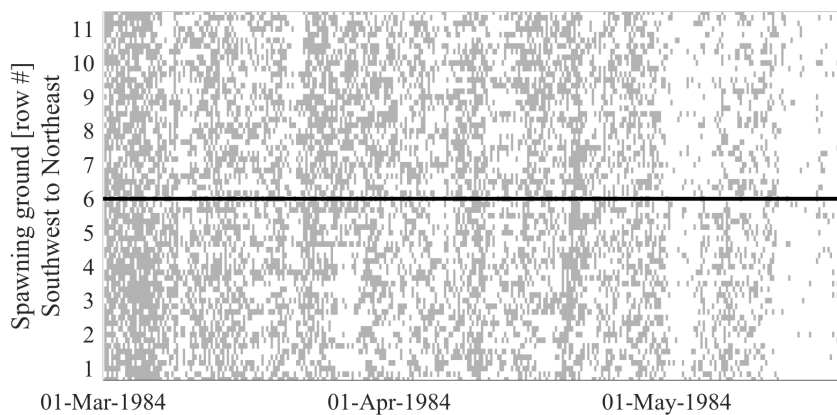


**Figure S5:** Occurrences of sub-surface maxima in the upper 20 m as a function of grid cell and time only considering locally spawned eggs (using 2.4 km x 2.4 km ROMS archive including four-dimensional variational data assimilation). The y-axis is labeled according to row numbers sorted northeastward through the spawning ground (Figure 1).

# Paper 3

## 5.3 Long-term Statistics of Bubble Depth and the Energy Flux from Breaking Waves

Kjersti Opstad Strand, Øyind Breivik, Geir Pedersen, Frode Bendiksen Vikebø, Svein Sundby and Kai Håkon Christensen

*Submitted for publication in Geophysical Research Letters*





Graphic design: Communication Division, UIB / Print: Skjipes Kommunikasjon AS



uib.no

ISBN: 978-82-308-3553-1